

การผลิตแอล-อะลานีนจากกรีคอมบิแนนท์ที่มียีนอะลานีนดีไฮโดรจีเนส
และฟอร์มेटดีไฮโดรจีเนสและการระบุฟอร์มेटดีไฮโดรจีเนสชนิดใหม่



นางสาวรุจิรัตน์ หาดตรงจิตต์

สถาบันวิทยบริการ

วิทยานิพนธ์นี้เป็นส่วนหนึ่งของการศึกษาตามหลักสูตรปริญญาวิทยาศาสตรดุษฎีบัณฑิต

สาขาวิชาชีวเคมี ภาควิชาชีวเคมี

คณะวิทยาศาสตร์ จุฬาลงกรณ์มหาวิทยาลัย

ปีการศึกษา 2551

ลิขสิทธิ์ของจุฬาลงกรณ์มหาวิทยาลัย

**L-ALANINE PRODUCTION FROM THE RECOMBINANT HARBORING
ALANINE DEHYDROGENASE AND FORMATE DEHYDROGENASE GENES
AND IDENTIFICATION OF A NOVEL FORMATE DEHYDROGENASE**



Miss Rujirat Hatrongjit

**A Dissertation Submitted in Partial Fulfillment of the Requirements
for the Degree of Doctor of Philosophy Program in Biochemistry**

Department of Biochemistry

Faculty of Science

Chulalongkorn University

Academic Year 2008

Copyright of Chulalongkorn University

Thesis Title L-alanine production from the recombinant harboring alanine dehydrogenase and formate dehydrogenase genes and identification of a novel formate dehydrogenase

By Miss Rujirat Hatrongjit

Field of Study Biochemistry

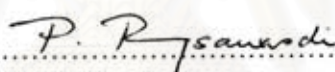
Thesis Advisor Assistant Professor Kanoktip Packdibamrung, Ph.D.

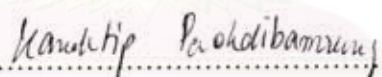
Thesis Co-Advisor Associate Professor Kouhei Ohnishi, Ph.D.

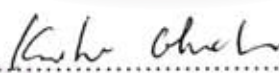
Accepted by the Faculty of Science, Chulalongkorn University in Partial Fulfillment of the Requirements for the Doctoral's Degree

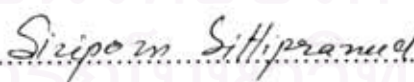

..... Dean of the Faculty of Science
(Professor Supot Hannongbua, Dr.rer.nat)

THESIS COMMITTEE


.....Chairman
(Associate Professor Piamsook Pongsawasdi, Ph.D.)


.....Thesis Advisor
(Assistant Professor Kanoktip Packdibamrung, Ph.D.)


.....Thesis Co-Advisor
(Associate Professor Kouhei Ohnishi, Ph.D.)


.....Examiner
(Associate Professor Siriporn Sittipraneed, Ph.D.)


.....Examiner
(Assistant Professor Teerapong Buaboocha, Ph.D.)


.....External Examiner
(Associate Professor Sunanta Ratanapo, Ph.D.)

รุจิรัตน์ หาดรงจิตต์: การผลิตแอล-อะลานีนจากรีคอมบิแนนท์ที่มียีนอะลานีนดีไฮโดรจีเนสและฟอร์มेटดีไฮโดรจีเนสและการระบุฟอร์มेटดีไฮโดรจีเนสชนิดใหม่ (L-ALANINE PRODUCTION FROM THE RECOMBINANT HARBORING ALANINE DEHYDROGENASE AND FORMATE DEHYDROGENASE GENES AND IDENTIFICATION OF A NOVEL FORMATE DEHYDROGENASE) อ. ที่ปรึกษาวิทยานิพนธ์หลัก: ผศ. ดร. กนกทิพย์ ภักดีบำรุง, อ. ที่ปรึกษาวิทยานิพนธ์ร่วม: ASSOC. PROF. KOUHEI OHNISHI, Ph.D., 160 หน้า

งานวิจัยนี้ได้ทำการปรับปรุงเซลล์เจ้าบ้าน *Escherichia coli* เพื่อเพิ่มการผลิตแอล-อะลานีนและคัดกรองฟอร์มेटดีไฮโดรจีเนสชนิดใหม่ โดยในขั้นตอนแรกทำการแทรกยีน T7 RNA polymerase โดยอาศัย lambda phage ลงในโครโมโซมของ *E. coli* MB2795 ซึ่งเป็นสายพันธุ์ที่ไม่มีการผลิตอะลานีนราซิเมต จากนั้นทรานส์ฟอร์ม pETFA ที่มียีนฟอร์มेटดีไฮโดรจีเนส (FDH) จาก *Mycobacterium vaccae* N10 และอะลานีนดีไฮโดรจีเนสจาก *Aeromonas hydrophila* เข้าสู่ *E. coli* KR ที่สร้างขึ้น อะลานีนที่ผลิตจากรีคอมบิแนนท์โคลนของ *E. coli* KR มีความบริสุทธิ์ของแอล-ไอโซเมอร์มากกว่าร้อยละ 95 สำหรับการคัดกรอง NAD⁺-FDH จากแบคทีเรียชนิดต่างๆ พบ FDH ชนิดใหม่ซึ่งเป็น NADP⁺-FDH ในแบคทีเรีย *Burkholderia cepacia* complex (BCC) ที่สามารถใช้ทั้ง NAD⁺ และ NADP⁺ เป็นโคเอนไซม์โดยสามารถใช้ NADP⁺ ได้ดีกว่า NAD⁺ ซึ่งยังไม่เคยมีรายงานมาก่อน เมื่อศึกษาการแพร่กระจายของยีนฟอร์มेटดีไฮโดรจีเนสใน BCC ทั้งหมด 46 สายพันธุ์จาก 10 สปีชีส์ พบยีนนี้ในหลายสายพันธุ์หรือทุกสายพันธุ์ของ *B. cepacia*, *B. multivorans*, *B. cenocepacia*, *B. stabilis* และ *B. pyrocinia* แต่ไม่พบใน *B. ambifaria*, *B. vietnamiensis*, *B. dolosa*, *B. anthina* และ *B. ubonensis* โดยพบว่ายีนนี้ประกอบด้วยนิวคลีโอไทด์ 1161 คู่เบสที่เข้ารหัสให้กรดอะมิโน 386 เรซิดิวส์ เมื่อเปรียบเทียบลำดับของกรดอะมิโนของ FDH ใน BCC พบว่ามีความคล้ายคลึงกันร้อยละ 91-96 และคิดเป็นร้อยละ 65-71 เมื่อเปรียบเทียบกับแบคทีเรียชนิดอื่น จากการโคลนยีนฟอร์มेटดีไฮโดรจีเนสจาก *B. stabilis* 15516 เข้าสู่ *E. coli* BL21(DE3) แล้วทำเอนไซม์ให้บริสุทธิ์พบว่าเอนไซม์มีน้ำหนักโมเลกุลของหน่วยย่อยประมาณ 42,000 ดาลตัน pH และอุณหภูมิที่เหมาะสมในการเร่งปฏิกิริยาคือ pH 6.0 - 7.5 และ 60 องศาเซลเซียสตามลำดับ เอนไซม์มีความเสถียรที่อุณหภูมิสูงโดยไม่สูญเสียแอกทิวิตีเมื่อบ่มที่ 45, 50, 55 องศาเซลเซียส เป็นเวลา 16, 10 และ 10 ชั่วโมง ตามลำดับ และยังคงมีแอกทิวิตีเหลืออยู่ 50 เปอร์เซ็นต์ เมื่อบ่มเป็นเวลา 36, 36 และ 32 ชั่วโมง ตามลำดับ เอนไซม์มีความเสถียรต่อ pH ในช่วง 4.0-12.0 ค่า K_m ต่อฟอร์มेट NADP⁺ และ NAD⁺ เท่ากับ 62.5, 0.16 และ 1.43 มิลลิโมลาร์ ตามลำดับ เมื่อศึกษาลำดับกรดอะมิโนของเอนไซม์ในกลุ่ม NAD⁺-FDH และ D specific 2-hydroxy acid dehydrogenase ชนิดอื่นๆพบว่ากรดอะมิโนบริเวณ Gly(Ala)XGlyXXGlyX17Asp มีความจำเพาะต่อ NAD⁺ ขณะที่ลำดับกรดอะมิโนของ FDH จาก BCC เป็น GlyXGlyXXGlyX17Gln จึงทำการกลายพันธุ์ฟอร์มेटดีไฮโดรจีเนสจาก *B. stabilis* 15516 ที่กรดอะมิโน Gln223 เป็น Asp พบว่าความชอบของโคเอนไซม์ต่อ NADP⁺ ได้ถูกเปลี่ยนเป็น NAD⁺

ภาควิชา.....ชีวเคมี.....	ลายมือชื่อนิสิต..... <u>รุจิรัตน์ หาดรงจิตต์</u>
สาขาวิชา.....ชีวเคมี.....	ลายมือชื่ออาจารย์ที่ปรึกษาวิทยานิพนธ์หลัก..... <u>Amthue May</u>
ปีการศึกษา.....2551.....	ลายมือชื่ออาจารย์ที่ปรึกษาวิทยานิพนธ์ร่วม..... <u>Kal ohh</u>

4773866023: MAJOR BIOCHEMISTRY

KEYWORDS: alanine dehydrogenase/ formate dehydrogenase/ *Burkholderia cepacia* complex/ alanine production/ NADP⁺-dependent formate dehydrogenase

RUJIRAT HATRONGJIT: L-ALANINE PRODUCTION FROM THE RECOMBINANT HARBORING ALANINE DEHYDROGENASE AND FORMATE DEHYDROGENASE GENES AND IDENTIFICATION OF A NOVEL FORMATE DEHYDROGENASE. THESIS ADVISOR: ASSIST. PROF. KANOKTIP PACKDIBAMRUNG, Ph.D., THESIS CO-ADVISOR: ASSOC. PROF. KOUHEI OHNISHI, Ph.D., 160 pp.

In this research, improvement of *Escherichia coli* host cell for high production of L-alanine and screening of a novel formate dehydrogenase (FDH) were performed. For improvement of host cell, the T7 gene 1 encoding T7 RNA polymerase was introduced into chromosome of *E. coli* MB2795, the racemase-deficiency strain, via transduction of lambda phage. After that, the constructed clone, namely *E. coli* KR, was used as a host cell for transformation of pETF A containing alanine dehydrogenase gene from *Aeromonas hydrophila* and formate dehydrogenase gene from *Mycobacterium vaccae* N10. The optical purity of L-alanine produced by recombinant clone of *E. coli* KR was over 95%. Surprisingly, a novel type of FDH, NADP⁺-FDH, was found in *Burkholderia cepacia* complex (BCC) during the screening of formate dehydrogenase. This FDH was able to use both NAD⁺ and NADP⁺ as coenzyme, however, it preferred NADP⁺ over NAD⁺. The distribution of formate dehydrogenase gene was determined among 46 strains from 10 species of the BCC. The gene was found to be present in several or all tested strains of *B. cepacia*, *B. multivorans*, *B. cenocepacia*, *B. stabilis* and *B. pyrrocinia*, but potentially absent in *B. ambifaria*, *B. vietnamiensis*, *B. dolosa*, *B. anthina* and *B. ubonensis*. The complete coding sequence of all FDH genes from the five species consisted of 1,161 bp encoding for a polypeptide of 386 amino acids. The similarity of amino acid sequences were very high (91-96%) among the five BCC and high 65-70% when compared to other bacterial FDHs. The gene encoding formate dehydrogenase from *B. stabilis* was cloned into *E. coli* BL21 (DE3) and the enzyme was purified to homogeneity. BstFDH had a molecular mass of subunit about 42 kDa. The optimum pH was ranged from 6.0-7.5 and optimum temperature was 60 °C. No loss of the enzyme activity was observed upon incubation at 45, 50 and 55 °C for 16, 10 and 10 hr, respectively and the activity retained 50% after incubation for 36, 36 and 32 hr, respectively. The enzyme was stable over a broad pH ranged from 4.0 to 12.0. The apparent K_m values for formate, NADP⁺ and NAD⁺ were 62.5, 0.16 and 1.43 mM, respectively. Interestingly, all NAD⁺-dependent FDHs and other D specific 2-hydroxy acid dehydrogenases contained the conserved coenzyme binding sequence Gly(Ala)XGlyXXGlyX17Asp for NAD⁺ while the NADP⁺-dependent FDHs from the BCC possessed the sequence GlyXGlyXXGlyX17Gln. Therefore, the Gln223Asp single mutation of BstFDH was performed. Coenzyme preference of the mutant enzyme was completely changed from NADP⁺ to NAD⁺.

DepartmentBiochemistry..... Student's signature..... Rujirat Hatrongjit.....
 Field of study...Biochemistry..... Advisor's signature..... Kanoktip Packdibamrung.....
 Academic year...2008..... Co-Advisor's signature..... Kouhei Ohnishi.....

ACKNOWLEDGEMENTS

I would like to express my deepest gratitude to my advisor, Assist. Prof. Dr. Kanoktip Packdibamrung for her generous advice, skillful assistance, and technical helps guidance, encouragement, supporting, fruitful and stimulating discussions through the period of my study.

Sincere thanks and appreciation are due to Assoc. Prof. Dr. Piamsook Pongsawasdi, Assoc. Prof. Dr. Siriporn Sittipraneed, Assist. Professor Teerapong Buaboocha and Assoc. Professor Sunanta Ratanapo who serve as the members of the Doctor committees, for their helpful suggestions and comments.

I would like to express my sincere thanks to all teachers for their care and encouragement.

My cordial thanks also go to all friends of the Biochemistry department and Biotechnology program for their helps in the laboratory and friendships that make me enjoy and happy throughout my study.

Finally, the warmest gratitude is extended to the patience, understanding, helping, encouragement, constant support and warmhearted love of my family whilst I have spent many hours with this thesis rather than with them. My thanks are also extended to my patience and sedulous too.

The financially support by the 90th anniversary of Chulalongkorn university fund (Ratchadaphiseksomphot Endowment Fund) and Ministry of University affairs (Scholarship under the committee staff development project of commission on higher education) of Kasetsart University, are also gratefully acknowledged.

จุฬาลงกรณ์มหาวิทยาลัย

CONTENTS

	Page
THAI ABSTRACT.....	iv
ENGLISH ABSTRACT.....	v
ACKNOWLEDGEMENTS.....	vi
CONTENTS.....	vii
LIST OF TABLES.....	xiii
LIST OF FIGURES.....	xiv
ABBREVIATIONS.....	xvii
INTRODUCTION.....	1
1.1 L-alanine	1
1.2 Alanine dehydrogenase	4
1.2.1 Source and characteristics.....	4
1.2.2 Application of AlaDH.....	9
1.2.2.1 Analysis of L-alanine.....	9
1.2.2.2 The production of L-alanine and its derivatives.....	9
1.3 Formate dehydrogenase.....	14
1.3.1 Source and characteristics.....	14
1.3.2 Structure and catalytic mechanism.....	19
1.3.3 Application of formate dehydrogenase.....	24
1.3.3.1 Quantitative determination.....	24
1.3.3.2 NADH regeneration system.....	26
1.3.3.3 Bioenergetics.....	28
1.4 Production of L-alanine by co-existence of AlaDH and FDH.....	29
1.5 The outline of this research.....	32

	Page
PART I IMPROVEMENT OF <i>E. coli</i> HOST CELL FOR L-ALANINE PRODUCTION.....	33
CHAPTER I INTRODUCTION.....	34
CHAPTER II MATERIALS AND METHODS.....	39
2.1 Equipments.....	39
2.2 Chemicals.....	40
2.3 Enzymes and restriction enzymes.....	42
2.4 Bacterial strains.....	42
2.5 Plasmids.....	42
2.6 DNA manipulations.....	42
2.6.1 Chromosomal DNA extraction.....	42
2.6.2 Plasmid extraction	43
2.6.3 Agarose gel electrophoresis.....	44
2.6.4 Extraction of DNA fragment from agarose gel.....	44
2.6.5 Transformation of plasmid.....	45
2.6.5.1 Competent cell preparation.....	45
2.6.5.2 Electroporation.....	45
2.7 Construction of T7 expression system in <i>E. coli</i> MB2795 alanine racemase-deficiency mutant (<i>alr⁻ dadX⁻</i>).....	46
2.8 Transformation of pETF _A into <i>E. coli</i> KR	48
2.9 Determination of AlaDH and FDH activities.....	48
2.9.1 Crude extract preparation.....	48
2.9.2 Determination of AlaDH activity.....	49
2.9.3 Determination of FDH activity.....	49
2.9.4 Protein measurement.....	49
2.10 Optimization of AlaDH and FDH production by varying IPTG concentration and induction time.....	50

	Page
2.11 Production of L-alanine	50
2.11.1 Preliminary test of alanine production.....	50
2.11.2 Determination of alanine by TLC.....	51
2.11.3 Optimization of alanine production.....	51
2.11.4 Determination of optical purity of alanine by HPLC.....	52
CHAPTER III RESULTS AND DISCUSSION.....	53
3.1 Construction of T7 expression system into <i>E. coli</i> MB2795 alanine racemase-deficiency mutant (<i>alr</i> ⁻ , <i>dadX</i> ⁻).....	53
3.2 Transformation of pETFFA into <i>E. coli</i> KR.....	53
3.3 Determination of AlaDH and FDH activities in <i>E. coli</i> harboring pETFFA.....	53
3.4 Optimization of AlaDH and FDH production by varying IPTG concentration and induction time.....	57
3.5 Qualitative analysis of alanine production by <i>E. coli</i> KR using TLC technique.....	60
3.6 Optimization of alanine production	60
 PART II SCREENING AND CHARACTERIZATION OF A NOVEL FORMATE DEHYDROGENASE.....	 64
CHAPTER I INTRODUCTION.....	65
CHAPTER II METHODS.....	66
2.1 Equipments.....	66
2.2 Chemicals.....	66
2.3 Enzymes and restriction enzymes.....	67
2.4 Bacterial strains.....	67
2.5 Plasmids.....	67
2.6 Determination of FDH activities.....	67
2.6.1 Crude extract preparation.....	67
2.6.2 FDH activity assay.....	68
2.6.3 Protein determination.....	68

	Page
2.7 Screening of a novel FDH.....	68
2.7.1 Screening of FDH from soil bacteria.....	68
2.7.2 Screening of a novel FDH from bacterial culture collection...	69
2.7.2.1 The reference bacteria.....	69
2.7.2.2 The local strains (isolated from human).....	69
2.7.2.3 The local strains (isolated from environment).....	69
2.8 Oligonucleotide primer design.....	70
2.9 PCR amplification.....	70
2.9.1 PCR amplification of partial FDH gene.....	70
2.9.2 Determination of the partial FDH sequence.....	73
2.9.3 Inverse PCR amplification of the FDH gene.....	73
2.9.4 DNA sequencing and analysis.....	73
2.9.5 PCR amplification of the complete FDH gene.....	75
2.10 Phylogenetic analysis.....	75
2.11 Accession number.....	75
2.12 Cloning of the FDH genes in different BCC isolates into pET-17b..	75
2.13 Optimization of the recombinant FDH production by varying IPTG concentration and induction time.....	77
2.14 Polyacrylamide gel electrophoresis.....	77
2.14.1 SDS-polyacrylamide gel electrophoresis.....	77
2.14.2 Non-denaturing gel electrophoresis.....	78
2.14.3 Protein staining.....	78
2.14.4 Activity staining.....	78
2.15 Site-directed mutagenesis of FDH.....	78
2.16 Purification of formate dehydrogenase.....	80
2.16.1 Preparation of crude extract.....	80
2.16.2 Enzyme purification procedures.....	80
2.16.2.1 DEAE-Toyopearl column chromatography.....	81
2.16.2.2 Butyl-Toyopearl column chromatography.....	81

	Page
2.17 Characterization of formate dehydrogenase.....	82
2.17.1 Coenzyme specificity of formate dehydrogenase.....	82
2.17.2 Effect of pH on formate dehydrogenase activity.....	82
2.17.3 Effect of temperature on formate dehydrogenase activity.....	82
2.17.4 Effect of pH on formate dehydrogenase stability.....	82
2.17.5 Effect of temperature on formate dehydrogenase stability....	83
2.18 Kinetic studies of formate dehydrogenase.....	83
CHAPTER III RESULTS.....	84
3.1 Screening of formate dehydrogenase (FDH) in bacteria.....	84
3.2 Distribution of FDH gene in <i>Burkholderia cepacia</i> complex (BCC).	84
3.3 Determination of flanking region surrounding the FDH gene.....	87
3.4 Cloning of FDH genes.....	90
3.5 Analysis of the nucleotide sequences.....	90
3.6 Comparison of the deduced amino acid sequences from the five FDH genes.....	96
3.7 Optimization of FDH activity by varying IPTG concentration and induction time.....	101
3.8 Determination of recombinant FDH activity from BCC.....	101
3.9 Coenzyme dependence of recombinant FDH.....	101
3.10 Site-directed mutagenesis of FDH.....	104
3.10.1 Cloning of mutant FDH.....	107
3.10.2 Optimization of mutant FDH activity by varying IPTG concentration and induction time.....	107
3.10.3 Determination of mutant FDH activity.....	107
3.10.4 Cofactor dependence of the mutant FDH.....	107
3.11 Purification of formate dehydrogenase.....	112
3.11.1 Preparation of crude extract.....	112
3.11.2 DEAE-Toyopearl column chromatography.....	112
3.11.3 Butyl-Toyopearl column chromatography.....	112
3.11.4 Determination of enzyme purity and protein pattern.....	115

	Page
3.12 Characterization of formate dehydrogenase.....	115
3.12.1 Coenzyme specificity of formate dehydrogenase.....	115
3.12.2 Effect of pH on formate dehydrogenase activity.....	115
3.12.3 Effect of temperature on formate dehydrogenase activity.....	115
3.12.4 Effect of pH on formate dehydrogenase stability.....	120
3.12.3 Effect of temperature on formate dehydrogenase stability....	120
3.13 Kinetic studies of formate dehydrogenase.....	120
3.13.1 Initial velocity studies for oxidative reaction of formate with NADP ⁺ and NAD ⁺	120
CHAPTER IV DISCUSSION.....	127
CONCLUSIONS.....	134
REFERENCES.....	135
APPENDICES.....	147
BIOGRAPHY.....	160

สถาบันวิทยบริการ
จุฬาลงกรณ์มหาวิทยาลัย

LIST OF TABLES

	Page
INTRODUCTION	
1.1 Some properties of AlaDH from various microorganisms.....	8
1.2 Physicochemical properties of NAD ⁺ -dependent FDHs.....	15
PART I IMPROVEMENT OF <i>E. coli</i> HOST CELL FOR L-ALANINE PRODUCTION	
CHAPTER II	
2.1 Nucleotide sequence and T_m of all primers used in PCR amplification.....	47
CHAPTER III	
3.1 AlaDH and FDH activities from crude extract of <i>E. coli</i> KR harboring of pETF A clones.....	56
3.2 AlaDH and FDH activities from crude extract of recombinant clones.....	59
PART II SCREENING AND CHARACTERIZATION OF A NOVEL FORMATE DEHYDROGENASE	
CHAPTER II	
2.1 Primers used in this study.....	71
CHAPTER III	
3.1 The presence of the FDH gene in BCC.....	85
3.2 The percentage of nucleotide sequence identities of FDH genes.....	95
3.3 The percentage of deduced amino acid sequence identities of FDHs	99
3.4 FDH activity from crude extract of recombinant clones.....	103
3.5 Purification of formate dehydrogenase from <i>E. coli</i> BL21 (DE3) cell harboring FDH gene from <i>Burkholderia stabilis</i> 15516.....	116
3.6 The apparent K_m values of substrates of formate dehydrogenase form <i>E. coli</i> BL21 (DE3) harboring pBstFDH 15516.....	126

LIST OF FIGURES

	Page
INTRODUCTION	
1.1 Summary of U.S. amino acids market size.....	2
1.2 Enzymatic synthesis of L-alanine by coupling of enzyme reactions.....	5
1.3 The reaction of L-alanine dehydrogenase.....	6
1.4 The detection system of γ -glutamyl cyclotransferase.....	10
1.5 Production of L-alanine by AlaDH and malic enzyme.....	10
1.6 Conjugated enzyme system of AlaDH and glucose dehydrogenase (GDH) for production of L-alanine.....	11
1.6 Conjugated enzyme system of AlaDH and L-LDH for production of L-alanine.....	11
1.8 Enzymatic reaction system for continuous production of L-alanine with coenzyme regeneration.....	13
1.9 The reaction of formate dehydrogenase.....	17
1.10 Structure of PseFDH.....	20
1.11 Displacement of the active site residues of FDH upon the transition from apo (yellow) to holo state.....	21
1.12 Alignment of FDH sequences with the sequences of D-specific 2 hydroxydehydrogenases.....	23
1.13 The main steps of the FDH molecular mechanism.....	25
1.14 Conjugated enzyme system of AlaDH and FDH for production of L-alanine.....	30
1.15 Map of recombinant plasmid pETAlaDH and pETFAs.....	31

PART I IMPROVEMENT OF *E. coli* HOST CELL FOR L-ALANINE
PRODUCTION

CHAPTER I

1.1 Control element of the pET system.....	37
1.2 Diagram of λ DE3	38

CHAPTER III

3.1 PCR amplification of T7 RNA polymerase gene on chromosome of <i>E. coli</i> KR.....	54
3.2 Colony PCR amplification of <i>E. coli</i> KR harboring pETFA.....	55
3.3 AlaDH and FDH productions of <i>E. coli</i> KR harboring pETFA transformant No. 2 at various final concentrations of IPTG.....	58
3.4 Separation of optical isomers of FDAA alanine on reversed phase TLC plates.....	61
3.5 Alanine production of various recombinant clones.....	62

PART II SCREENING AND CHARACTERIZATION OF A NOVEL
FORMATE DEHYDROGENASE

CHAPTER II

2.1 Deduced amino acid sequence alignment of FDHs.....	72
2.2 Diagram of inverse PCR.....	74
2.3 Construction of the representative BstFDH.....	76
2.4 Megaprimer PCR mutagenesis strategy.....	79

CHAPTER III

3.1 PCR amplification of the partial FDH gene.....	86
3.2 Chromosomal DNA digestion of a representative of BCC.....	88
3.3 The inverse PCR products of 5 BCC species.....	89
3.4 Alignment of the coding nucleotide sequence of FDH gene from five BCC.....	91
3.5 Amino acid sequence alignment of 5 FDHs from BCC.....	93
3.6 Restriction pattern of pBstFDH	94

	Page
3.7 The flanking genes at upstream and downstream of the FDH genes.....	97
3.8 Deduced amino acid sequence alignment of FDHs.....	98
3.9 Neighbor-joining based dendogram of FDH gene.....	100
3.10 Protein pattern of <i>E. coli</i> BL21 (DE3) harboring pBstFDH clone at various induction times detected by SDS-PAGE.....	102
3.11 Coenzyme specificity of the crude recombinant FDH enzyme from <i>Mycobacterium vaccae</i> N10, BcnFDH 11197 and BstFDH 15516.....	105
3.12 Structure of the <i>B. stabilis</i> 15516 wild-type and mutant enzymes.....	106
3.13 PCR amplification of FDH gene using megaprimer-based mutagenesis strategies.....	108
3.14 Restriction pattern of mutant BstFDH	109
3.15 Protein pattern of cell harboring mutant pBstFDH at various induction times detected by SDS-PAGE.....	110
3.16 Coenzyme preference of the crude FDH from pBstFDH 15516 and the mutant clones.....	111
3.17 Purification of formate dehydrogenase from pBstFDH 15516 clone by DEAE-Toyopearl column.....	114
3.18 Purification of formate dehydrogenase from recombinant pBstFDH 15516 clone by Butyl-Toyopearl column.....	115
3.19 Protein pattern from each step of purification investigated by SDS-PAGE and the purified FDH at last step examined by native PAGE.....	117
3.20 Effect of pH on formate dehydrogenase activity.....	118
3.21 Effect of temperature on formate dehydrogenase activity.....	119
3.22 Effect of pH on formate dehydrogenase stability.....	121
3.23 Effect of temperature on formate dehydrogenase stability.....	122
3.24 Initial velocity patterns.....	123

ABBREVIATIONS

A	absorbance, 2'-deoxyadenosine (in a DNA sequence)
ADPR	adenosine diphosphoribose
AlaDH	alanine dehydrogenase
bp	base pairs
BLAST	Basic Local Alignment Search Tool
BSA	bovine serum albumin
C	2'-deoxycytidine (in a DNA sequence)
°C	degree Celsius
CarAlaDH	alanine dehydrigenase of <i>Carnobacterium</i> strain St2
cm	centrimeter
d	day
Da	Dalton
DEAE	diethylaminoethyl
DNA	deoxyribonucleic acid
dNTP	2'-deoxynucleoside 5'-triphosphate
DTT	dithiothreitol
EC	Enzyme Commission
EDTA	ethylene diamine tetraacetic acid
g	gram
FDA	1-fluoro-2, 4-dinitrophenyl-5-L-alanine amide
FDH	formate dehydrogenase
G	2'-deoxyguanosine (in a DNA sequence)
GCT	γ -glutamyl cyclotransferase
GDH	glucose dehydrogenase
hr	hour
HCl	hydrochloric acid
HPLC	high-performance liquid chromatography
IPTG	isopropyl β -D-1-thiogalactopyranoside
kb	kilobase pairs in duplex nucleic acid, kilobases in single-standed nucleic acid

KCl	potassium chloride
kDa	kiloDalton
K_m	Michaelis constant
KOH	potassium hydroxide
KPB	potassium phosphate buffer
L	liter
LB	Luria-Bertani
LeuDH	leucine dehydrogenase
L-LDH	lactate dehydrogenase
LysDH	lysine dehydrogenase
μg	microgram
μl	microliter
μmol	micromole
μM	micromolar
M	mole per liter (molar)
mA	milliampere
mg	milligram
min	minute
ml	milliliter
mM	millimolar
MW	molecular weight
N	normal
NAD^+	nicotinamide adenine dinucleotide (oxidized)
NADH	nicotinamide adenine dinucleotide (reduced)
NADP^+	nicotinamide adenine dinucleotide phosphate (oxidized)
NADPH	nicotinamide adenine dinucleotide phosphate (reduced)
ng	nanogram
NH_4Cl	ammonium chloride
$(\text{NH}_4)_2\text{SO}_4$	ammonium sulfate
nm	nanometer
nt	nucleotide
OD	optical density

ORF	open reading frame
PAGE	polyacrylamide gel electrophoresis
PCR	polymerase chain reaction
PEG	polyethylene glycol
pI	isoelectric point
pmol	picomole
PMSF	phenyl methyl sulfonyl fluoride
PseFDH	formate dehydrogenase of <i>Pseudomonas</i> sp. 101
RNase	ribonuclease
SDS	sodium dodecyl sulfate
sec	second
SheAlaDH	<i>Shewanella</i> sp. strain Ac10
T	2'-deoxythymidine (in a DNA sequence)
TB	Tris-borate buffer
TE	Tris-EDTA buffer
TEMED	<i>N, N, N', N'</i> -tetramethyl ethylene diamine
TLC	thin-layer chromatography
T_m	melting temperature, melting point
UV	ultraviolet
V	voltage
v/v	volume by volume
w/w	weight by weight

INTRODUCTION

Commercial interest in amino acids is an outgrowth of an understanding of the many functions that these life-giving substances perform in humans and animals. As understanding of these functions and properties increases, current usage is likely to expand rapidly. L-amino acids are widely used in feed additives, food ingredients, cosmetics, medicines and pharmaceutical industries. The commercial amino acids in the U.S. was represented a billion-dollar market for the first time in 1999. Figure 1.1 displays an increasing of U.S. amino acid marketing size during 2005-2013. The prospect focuses on three commercial amino acid markets: animal feed supplements, flavoring and nutritional additives for human food, and special uses including medical, therapeutic, research and industrial applications (<http://www.bccresearch.com/report/BIO007H.html>). Therefore, the global amino acids market is projected to grow at 6.8% annually through 2013 (<http://www.researchandmarkets.com/reports/c90591>).

1.1 L-alanine

L-alanine is a non-essential amino acid which was first isolated in 1879. With the chemical formula $\text{CH}_3\text{CH}(\text{NH}_2)\text{COOH}$, it is one of the simplest structure. L-alanine plays a role in proper function of the central nervous system and also the metabolism of several substances, including glucose, tryptophan, pyridoxine and vitamin B6 (Eisenberg and Star, 1968). Alanine can be manufactured in the body from pyruvate and branch chain amino acids such as valine, leucine, and isoleucine. Alanine is most commonly produced by reductive amination of pyruvate. Because transamination reactions are readily reversible and pyruvate pervasive, alanine can be easily formed and thus has close links to metabolic pathways such as glycolysis, gluconeogenesis, and the citric acid cycle. It also arises together with lactate and generates glucose from protein via the alanine cycle. For alanine cycle, it is crucial for preserving balanced levels of nitrogen and glucose in the body. Alanine is also produced when muscles produce lactate during times of decreased oxygen. This alanine is shuttled to the liver where it is used to make glucose. Alanine plays a key role in glucose-alanine cycle between tissues and the liver.

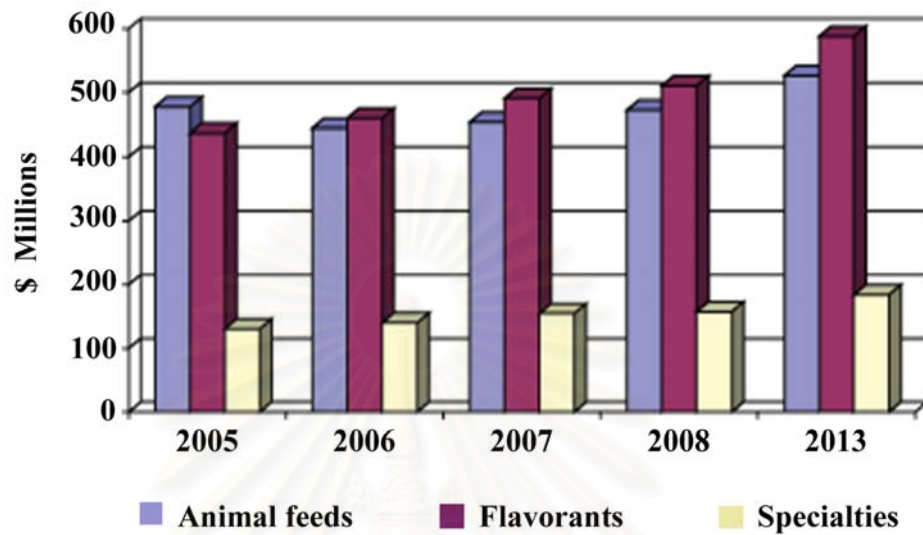


Figure 1.1 Summary of U.S. amino acids market size

Source: BCC research (<http://www.bccresearch.com/report/BIO007H.html>)

สถาบันวิทยบริการ
จุฬาลงกรณ์มหาวิทยาลัย

In muscle and other tissues that degrade amino acids for fuel, amino groups of amino acid are collected in the form of glutamate by transamination. Glutamate can then transfer its amino group through the action of alanine aminotransferase to pyruvate, a product of muscle glycolysis, forming alanine and alpha-ketoglutarate. The alanine formed is passed into the blood and transported to the liver. A reverse of the alanine aminotransferase reaction takes place in liver. Pyruvate regenerated forms glucose through gluconeogenesis, which returns to muscle through the circulation system. Glutamate in the liver enters mitochondria and degrades into ammonium ion through the action of glutamate dehydrogenase, which in turn participate in the urea cycle to form urea (<http://en.wikipedia.org/wiki/Alanine>).

In prokaryote, alanine plays many important roles in the growth and physiology of enteric bacteria. It is one of the major amino acids present in proteins and can be used in the biosynthesis of the amino acid valine (Whalen and Berg, 1982), and the vitamin biotin (Eisenberg and Star, 1968). Both the L- and D-stereoisomers of alanine are major constituents of the peptidoglycan layer of bacteria (Matsushashi, 1994).

Application of L-alanine is widely used in dairy products and food additive as sweetener because of its sweet taste, which is about 70% of sugar. It is also used for pharmacy and medicine in which it is incorporated together with several other L-amino acids in standard infusions for parental administration in clinical preoperative and postoperative nutrition therapy such as to treat benign prostatic hyperplasia, or hypertrophy of the prostate gland, and hypoglycemia (Feinblatt, *et al.*, 1958; Damrau, 1962; Zello, *et al.*, 1995). L-alanine is also applied in animal feed supplement. Moreover, alanine derivatives such as 3-fluoro-L-alanine is used as antibacterial and antiviral agents (Ohshima, 1989) which L- β -chloroalanine is used as pesticide (Kato, *et al.*, 1993).

A various method has been used for the production of L-alanine. (i) Chemical synthesis used of the Strecker reaction in which acetaldehyde, prussic acid and ammonium are used as starting material. However, this process is not desirable when the L-alanine product is applied as a food additive because the toxic cyanogens are used in the Strecker reaction. (ii) Direct fermentation of sugars by using bacteria such as *Corynebacterium gelinosium*, *Zymomonas mobilis*, *Arthrobacter oxydans*, *Brevibacterium lactofermentum*, *Clostridium* sp. and *Pyrococcus furiosus*. By this method, D- and L-alanine can be produced with a maximum conversion rate of 50 to

60% (Holes, *et al.*, 2003). (iii) Enzymatic processes such as production of L-alanine from decarboxylation of L-aspartic acid catalyzed by L-aspartate- β -decarboxylase of immobilized cells or cell suspension of *Pseudomonas dacunhae* (Yamamoto, *et al.*, 1980; Takamatsu, *et al.*, 1981). This method, however, has a high substrate cost. Lastly, the reductive amination of pyruvate catalyzed by L-alanine dehydrogenase (L-AlaDH) can be an alternative way to produce L-alanine (Suye, *et al.*, 1992). This method is used to produce various L-amino acids such as L-leucine (Ohshima, *et al.*, 1985), L-valine, L-isoleucine (Gu and Chang, 1990) and L-phenylalanine (Matsunaga, *et al.*, 1987) from their corresponding keto-acids.

To produce L-alanine and other L-amino acid with low cost, the coenzyme regenerating system by coupling between alanine and formate dehydrogenase (FDH) has been applied (Figure 1.2) (Galkin, *et al.*, 1997; Hatrongjitt, 2004).

1.2 Alanine dehydrogenase

1.2.1 Source and characteristics

Alanine dehydrogenase (L-alanine; NAD⁺ oxidoreductase, deaminating, EC 1.4.1.1, AlaDH) is a cytoplasmic enzyme that catalyzes the reversible pyridine nucleotide-dependent oxidative deamination of L-alanine to ammonia, pyruvate and NADH as shown in Figure 1.3. The substrate specificity of the enzyme for oxidative deamination is high since L-alanine is exclusively deaminated. However, the specificity for keto acids in the reverse reaction is quite low. Not only pyruvate, α -ketobutyrate, α -ketovalerate and 3-hydroxypyruvate can be aminated. Therefore, AlaDH is applied in the industrial production of L-alanine and its related amino acids (Popov and Lamzin, 1994).

AlaDH has been found in vegetative cells (Hong, *et al.*, 1959) and endospores (Nitta, *et al.*, 1974) of various bacilli and some other bacteria (Germano and Anderson, 1968; Holmes, *et al.*, 1961). Wiame and Pierard firstly identified AlaDH from *Bacillus subtilis* in 1955. Then this enzyme was purified by Yoshida and Freese in 1964. It showed molecular mass of 228 kDa. Sakamoto, *et al.* (1990) cloned the gene encoding thermostable AlaDH from *Bacillus stearothermophilus* into vector pKK223-3 and expressed in *E. coli* 600. The enzyme was purified 30-fold with 46% yield.

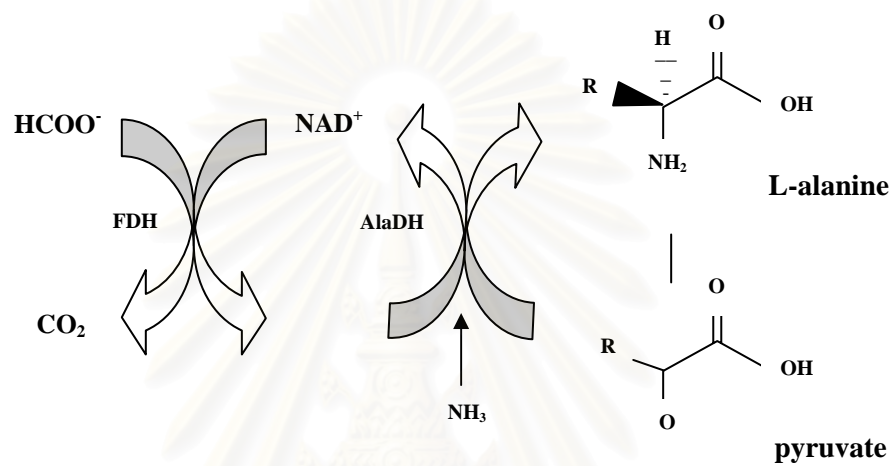


Figure 1.2 Enzymatic synthesis of L-alanine by coupling of enzyme reactions

AlaDH: alanine dehydrogenase

FDH: formate dehydrogenase

Source : Galkin, *et al.*, 1997

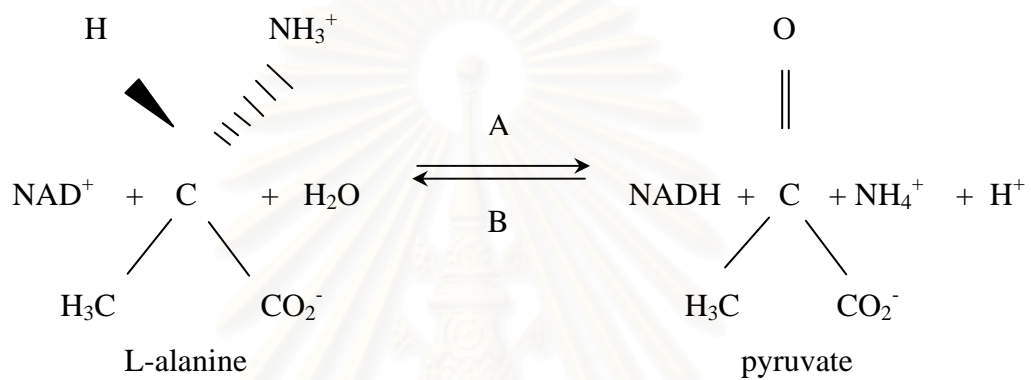


Figure 1.3 The reaction of L-alanine dehydrogenase

(A) oxidative deamination (B) reductive amination

สถาบันวิทยบริการ
จุฬาลงกรณ์มหาวิทยาลัย

It consisted of six subunits (40 kDa) with molecular mass about 240 kDa. In 1990, Kuroda, *et al.* reported gene cloning of AlaDHs from *B. sphaericus* and *B. stearothermophilus* into *E. coli* 600 with pICD322 vector. The AlaDH genes from *B. sphaericus* and *B. stearothermophilus* consisted of 1116 bp open reading frame which encoded 372 amino acid residues corresponding to subunits of the hexameric enzyme. The similarity of amino acid sequence between these two AlaDHs is more than 70 %. Chowdhury, *et al.* (1998) purified AlaDH from *Enterobacter aerogenes* ICR0220 and the gene was cloned into *E. coli* JM109 cells using pUC18. The deduced amino acid sequence was very similar to that of the AlaDH from *B. subtilis* about 76%.

AlaDHs differ with respect to their subunit structures. Up to the present, the majority of purified L-AlaDHs exist as homohexamers. This form includes those from a wide range of Gram positive and Gram negative bacteria such as *Geobacillus stearothermophilus*, *Aeromonas hydrophila*, *Anabaena cylindrica*, *Enterobacter aerogenes*, *Phormidium lapideum*, *Rhodobacter capsulatus*, *Streptomyces phaeochromogenes* and *Thermus thermophilus*. Tetramer form of the L-AlaDH has been reported from Gram negative bacteria, *Pseudomonas* sp., *Rhizobium japonicum*, and actinomycetes *Streptomyces fradiae*. The octameric enzyme form was reported in *Streptomyces aureofaciens* while the enzyme of halophilic bacteria and *Streptomyces clavuligerus* are monomer. The properties of various microbial AlaDHs are summarized in Table 1.1.

Galkin, *et al.* in 1999 studied the AlaDH from *Shewanella* sp. strain Ac10 (SheAlaDH) and *Carnobacterium* strain St2 (CarAlaDH). The genes were cloned to plasmid pUC18 and expressed in *E. coli* TG1. Their deduce amino acid sequences were compared with the sequences of AlaDH from other bacteria. CarAlaDH exhibited the highest overall levels of identity in range 58.5 to 62.8 % with the enzymes from members of the same group of the low-G+C-content Gram-positive bacteria, such as *B. stearothermophilus*, while SheAlaDH was most similar in level of 76.5 % identity to *Vibrio proteolyticus*. SheAlaDH showed more stable than CarAlaDH but less stable than all of the AlaDHs from mesophilic *B. subtilis* and thermophilic *B. stearothermophilus*.

Table 1.1 Some properties of AlaDH from various microorganisms

Source	M_r (x10 ³) (subunit structure)	Optimum pH	Optimum temperature	K_m values (mM)					Reference
				L-ala	NAD ⁺	pyr	NH ₃	NADH	
<i>Aeromonas hydrophila</i>	230 (6x40,000)	10.5	37	20.0	0.17	1.33	77	0.25	Phungsangtham, 1997
<i>Anabaena cylindrica</i>	270 (6x43,000)	9.6	-	0.4	0.01	0.11	8-133	-	Rowell and Stewart, 1976
<i>Bacillus cereus</i>	255 (6x 42,000)	10.5	-	11.3	0.18-1.18	0.48	22-30	0.03-0.32	Porumb, <i>et al.</i> , 1987
<i>Bacillus japonicum</i>	190	10	-	1	0.2	0.49	8.9	0.08	Brunhuber, <i>et al.</i> , 1994
<i>Bacillus sphaericus</i>	230 (6x38,000)	10	70	0.01	0.01	1.7	3.8	0.01	Ohshima and Soda, 1979
<i>Bacillus subtilis</i>	228 (6x38,000)	10.1	-	1.73	0.18-0.36	0.54	38	0.02	Yoshida and Freese, 1965
<i>Desulfovibrio desulfuricans</i>	-	9.8	-	2	-	5	24	0.05	Germano, <i>et al.</i> , 1968
<i>Enterobacter aerogenes</i>	245 (6x41,000)	10.9	-	0.47	0.16	0.22	66.7	-	Chowdhury, <i>et al.</i> , 1998
<i>Geobacillus stearothermophilus</i>	240 (6x40,000)	10.7	-	13.3	1.67	5	0.07	-	Sakamoto, <i>et al.</i> , 1990
<i>Halobacterium cultirubrum</i>	72.5 (monomer)	9	-	7	0.5	0.8	0.82	0.2	Kim and Fitt, 1977
<i>Halobacterium salinarum</i>	60 (monomer)	9	-	-	-	-	-	-	Keradjopoulos and Holldorf, 1979
<i>Mycobacterium tuberculosis</i>	-	7-10	-	13.8	0.31	1.45	35.4	0.09	Hutter and Singh,
<i>Phormidium lapideum</i>	240 (6x41,000)	9.2	60	5	0.04	0.33	111	0.02	Sawa, <i>et al.</i> , 1994
<i>Pseudomonas sp.</i>	217 (4x53,000)	9	-	-	-	4.3	26	0.05	Bellion and Tan, 1987
<i>Rhizobium japonicum</i>	168 (4x42,000)	8.6-10	-	-	-	0.68	-	0.04	Mueller and Werner, 1982
<i>Rhizobium sp.</i>	-	-	-	0.37	-	0.43	5.5	0.02-0.09	Smith, <i>et al.</i> , 1993
<i>Rhodobacter capsulatus</i>	246 (6x42,000)	10.5	30	1.25	0.15	0.13	16	0.25	Caballero, <i>et al.</i> , 1989
<i>Rhodospseudomonas capsulata</i>	-	9.8	-	0.45	0.14	0.37	28	0.06	Tolxdorff-Neutzling, <i>et al.</i> , 1982
<i>Shewanella sp.</i>	-	-	-	7.6	0.24	-	-	-	Irwin, <i>et al.</i> , 200; Galkin, <i>et al.</i> , 1999
<i>Streptomyces aureofaciens</i>	395 (8x48,000)	10	75	5	0.11	0.56	6.67	0.02	Vancurova, <i>et al.</i> , 1988
<i>Streptomyces clavuligerus</i>	92(monomer)	8.4	-	9.1	0.5	1.1	20	0.14	Aharonowitz, <i>et al.</i> , 1980
<i>Streptomyces fradiae</i>	210 (4x51,000)	10	60	10	0.18	0.23	11.6	0.05	Vancura, <i>et al.</i> , 1989
<i>Streptomyces phaeochromogenes</i>	240 (6x39,000)	8	60	1.9	0.03	0.29	61	0.04	Itoh, <i>et al.</i> , 1983
<i>Thermus thermophilus</i>	290 (6x48,000)	10.5	-	0.18-4.2	0.12	0.75	59	0.03	Vali, <i>et al.</i> , 1980

1.2.2 Application of AlaDH

1.2.2.1 Analysis of L-alanine

Alanine dehydrogenase is applied for quantitative analysis of L-alanine in sample. It is useful in medical application for detection of γ -glutamyl cyclotransferase, which is the marker enzyme of malignant hematopoietic disease. This disease is caused by the serious defect in the production of red blood cell. The patients have abnormal level of this enzyme which can be detected by using AlaDH as shown in Figure 1.4 (Ohshima and Soda, 1990).

To develop the determination of alanine, Kwan, *et al.* (2004) reported an enzyme Clark electrode containing three different enzymes. This sensor is based on specific dehydrogenation of L-alanine dehydrogenase in combination with salicylate hydroxylase and pyruvate oxidase. The enzymes are entrapped by a poly (carbamoyl) sulfonate hydrogel on a Teflon membrane. The sensor has a fast response (2 sec) and short recovery times (2 min) with a linear range between 10 and 800 μM alanine and a detection limit of 7.2 μM . A good agreement with spectrophotometric method was obtained in beverage sample measurements.

1.2.2.2 The production of L-alanine and its derivatives

AlaDH is mainly useful in an industry of L-alanine and its derivatives production. There are various methods to produce of alanine and its derivatives. Suye, *et al.*, (1992) reported the production of L-alanine by AlaDH from *Corynebacterium flaccumfaciens* AHU-1622 coupling with NAD(P)^+ -linked malic enzyme from *Pseudomonas diminuta* IFO - 13182 for NADH regeneration as shown in Figure 1.5. After 72 hr, the conversion of L-malic acid to L-alanine reached 95 % of incubation at 30 °C. One hundred and six mol/m^3 of L-alanine produced was purified in crystal form with 99.4 % purity based on HPLC analysis.

Lin, *et al.* (1997) studied the co-immobilized enzyme system in a nanofiltration membrane bioreactor for the production of L-alanine from pyruvate by AlaDH from *Bacillus subtilis* with regeneration of NADH with glucose dehydrogenase (GDH) of *Bacillus* sp. as shown in Figure 1.6. The maximum conversion, reactor productivity and NAD regeneration number were 100%, 320 g/liter/d and 20,000, respectively.

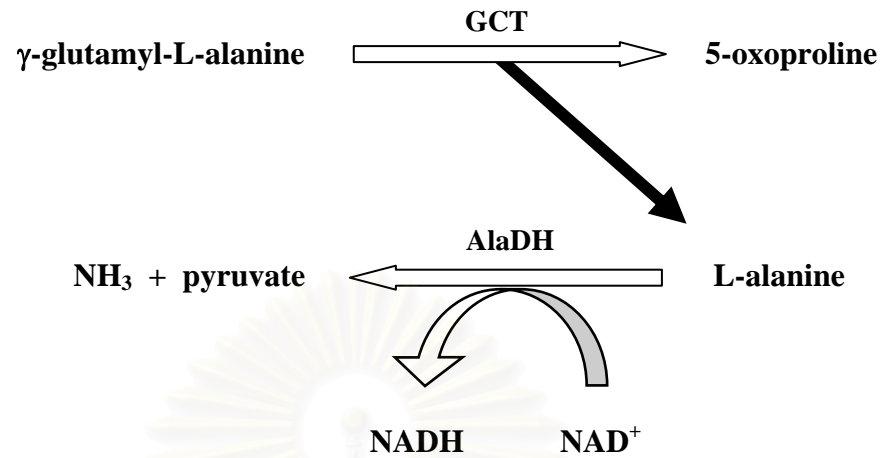


Figure 1.4 The detection system of γ -glutamyl cyclotransferase

GCT: γ -glutamyl cyclotransferase

AlaDH: alanine dehydrogenase

Source: Ohshima and Soda, 1990

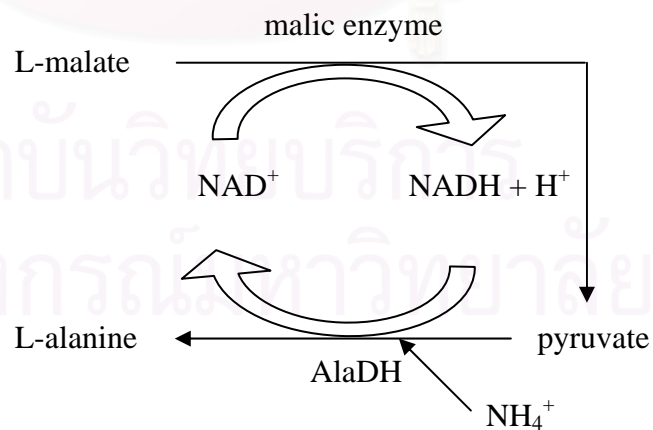


Figure 1.5 Production of L-alanine by AlaDH and malic enzyme

Source: Suye, *et al.*, 1992

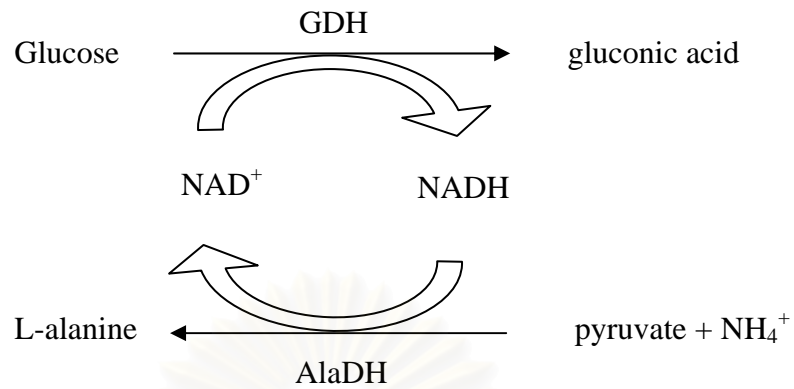


Figure 1.6 Conjugated enzyme system of AlaDH and glucose dehydrogenase (GDH) for production of L-alanine

Source: Lin, *et al.*, 1997

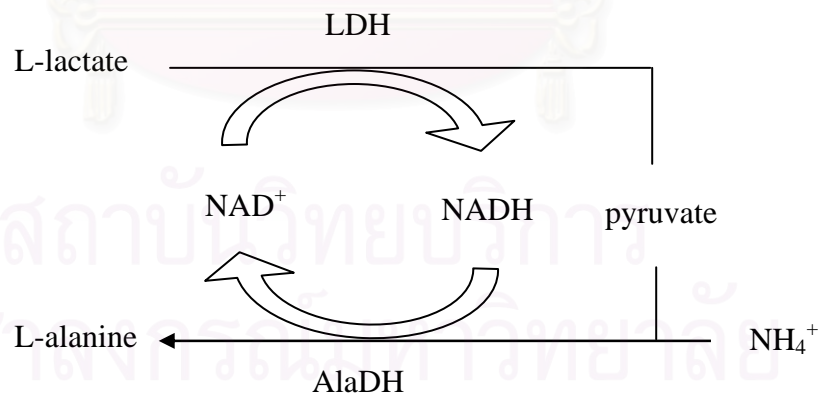


Figure 1.7 Conjugated enzyme system of AlaDH and L-LDH for production of L-alanine

Source: Lin, *et al.*, 1997

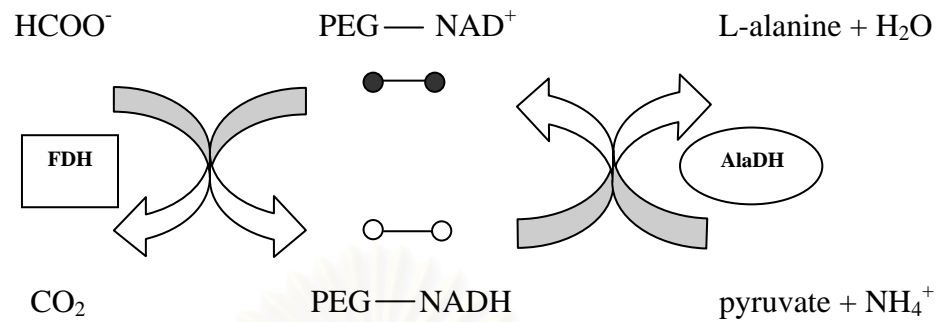
A consecutive reaction system containing lactate dehydrogenase (L-LDH) from bovine heart and AlaDH was used to avoid the effect of pyruvate instability. In this system, L-LDH provides pyruvate for the AlaDH reaction, so the pyruvate could be consumed as soon as it was produced as shown in Figure 1.7. The maximum conversion, reactor productivity, and the NAD regeneration number were 100%, 160 g/liter/d, and 20,000, respectively. However, the starting material of this system, L-lactate, is very expensive and not suitable in economic reason (Lin, *et al.*, 1997).

A coupled enzymatic system for the simultaneous synthesis of (*S*)-3-fluoroalanine and (*R*)-3-fluorolactic acid with L-alanine dehydrogenase from *Bacillus subtilis* and rabbit muscle L-lactate dehydrogenase using *rac*-1 fluoroalanine and NAD⁺ was described (Goncalves, *et al.*, 2000). Analysis of isolated products of the laboratory preparative scale process revealed (*S*)-3-fluoroalanine in 60% yield and 88% enantiomeric excess and (*R*)-3-fluorolactic acid in 80% yield and over 99% enantiomeric excess. The compounds (*S*)-3-fluoroalanine and (*R*)-3-fluorolactic acid represent chiral building blocks for the synthesis of several products with pharmacological activity.

The production of L-alanine and other aliphatic L-amino acids from their corresponding keto acid analogs and ammonium formate was investigated with an ultrafiltration membrane reactor (molecular cut-off at MW 5,000) containing AlaDH, yeast formate dehydrogenase (FDH, MW 80,000) and NADH or NAD bound covalently to polyethylene glycol (PEG, MW 20,000) (Fiolitaktis and Wandrey, 1983). Due to PEG-NADH can not penetrate through the membrane while FDH catalyzes regeneration of the PEG-NADH with formate. It is considerably stable and cheaply available and its reaction is irreversible. Pyruvate and ammonium formate are continuously pumped into the reactor following by production of L-alanine together with CO₂ (Figure 1.8).

Concerning the enzymatic regeneration, the use of glucose-(6-P)-dehydrogenase (Wong and Whitesides, 1981), alcohol dehydrogenase (Wong and Whitesides, 1982), lactate dehydrogenase (Davies, *et al.*, 1974; Wandrey, *et al.*, 1984), glucose dehydrogenase and formate dehydrogenase are well known. The latter allows an economic regeneration of NADH from NAD⁺ with formate.

a)



b)

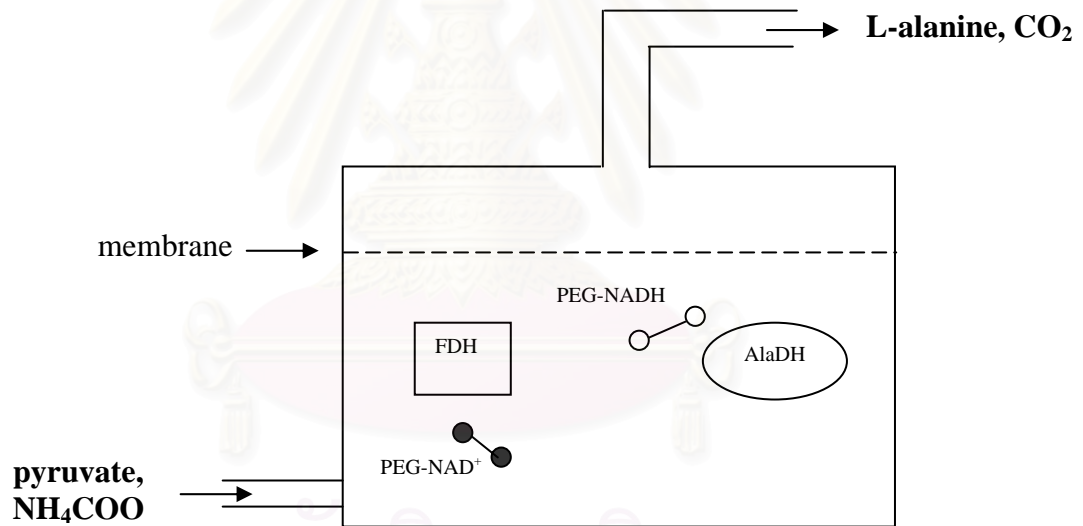


Figure 1.8. Enzymatic reaction system for continuous production of L-alanine with coenzyme regeneration

(a) Enzyme reaction scheme (b) Enzyme membrane reactor scheme

AlaDH: alanine dehydrogenase

FDH: formate dehydrogenase

PEG: polyethyleneglycol

Source: Hummel, *et al.*, 1987

1.3 Formate dehydrogenase

1.3.1 Source and characteristics

Formate dehydrogenases (FDH) are a large set of enzymes which catalyze the oxidation of formate to carbon dioxide (bicarbonate). This enzyme belongs to the class of D-specific 2-hydroxy acid dehydrogenases acting on D-stereoisomers of the respective substrates (Vinals, *et al.*, 1993). FDH may be classified into two major families. The first family includes a diverse group of conjugated iron-sulphur metal containing proteins of microbial origin differing in physiological role, cellular location and substrate specificity, content and type of prosthetic groups, nature of the physiological electron acceptor. These enzymes are distinguished by their high molecular mass, complex quaternary structure, the present of various prosthetic groups and their labile towards oxygen. The second family comprises NAD^+ -dependent FDHs with few exceptions represented by proteins devoid of any prosthetic group as summarized in Table 1.2 (Popov and Lamzin, 1994).

However, they can be broadly split into well distinct groups based upon the electron acceptor, as those that interact with cytochromes, the formate ferricytochrome-b1 oxidoreductases (EC 1.2.2.1). The cytochrome-dependent enzymes are more important in anaerobic metabolism in prokaryotes (Jormakka, *et al.*, 2003). For example, in *E. coli*, the formate: ferricytochrome-b1 oxidoreductase is an intrinsic membrane protein with two subunits and is involved in anaerobic nitrate respiration (Graham and Boxer, 1981). The second group uses NAD^+ (or NADP^+ but currently unreported) as the electron acceptor, the formate NAD^+ oxidoreductases (EC 1.2.1.2, FDHs). Only the later class, known as NAD^+ -dependent formate dehydrogenases will be described in this research.

NAD^+ -dependent formate dehydrogenases catalyze the oxidation of formate to CO_2 coupled to the reduction of NAD^+ to NADH as shown in Figure 1.9. They are essential enzymes to methylotrophic yeasts and bacteria that catabolise in the final step of C1 compounds such as methanol and supplying these organisms with energy and reducing equivalents (Kato, *et al.*, 1974; Schutte, *et al.*, 1976; Van Dijken, *et al.*, 1976; Izumi, *et al.*, 1989; Avilova, *et al.*, 1985; Allen and Holbrook, 1995). The enzyme was first discovered in pea seeds over 60 years ago (Mathews and Vennesland, 1950;

Table 1.2 Physicochemical properties of NAD⁺-dependent FDHs

Source ^a	Subunits (kDa) [pI]	Activity (units/mg) ^b	Temp. stability (°C)	pH optimum	K _m ^{NAD} (μM)	K _m ^{formate} (mM)	inhibitor	Comments	References
Bacteria									
<i>Pseudomonas oxalaticus</i>	2x100, 2x59			7.5	105	0.14	N ₃ ⁻ , CN ⁻ , NO ₃ ⁻ , Hg ₂ ⁺ , PCMB	Light- and oxygen-labile; contains Fe, S ₂ ⁻ and FMN	Muller, <i>et al.</i> , 1978
<i>Methylomonas methylica</i> (x32)		3.1 (37 °C)		7.7-8.0	160	0.40			Babel and Mothes, 1980
<i>Methylomonas extorquens</i> AM1 (x3)		0.42 (22 °C)		8.4	90	0.25	CN ⁻ , Cu ₂ ⁺ , Fe ₃ ⁺ , iodoacetamide	Temperature-labile	Johnson and Quayle, 1964
<i>Pseudomonas</i> sp. 101 ^{c, d}	2x44 [4.6-5.2]	16.0 (37 °C)	55	6.0-9.0	110	15	N ₃ ⁻ , CN ⁻ , NO ₃ ⁻ , Hg ₂ ⁺ , PCMB, DTNB	Active with NADP ⁺ ; uses GSF; random BI- BI kinetic scheme	Egorov, <i>et al.</i> , 1979; Tishkov, <i>et al.</i> , 1991; Egorov, <i>et al.</i> , 1980
<i>Moraxella</i> sp. C-1	2x48 [3.9]	6.0 2(5 °C)	55	6.0-9.0	68	13	N ₃ ⁻ , CN ⁻ , Ag ⁺ , Hg ₂ ⁺ , DTNB, hydroxylamine		Asano, <i>et al.</i> , 1988
<i>Paracoccus</i> sp. 12-A	2x49 [5.4]	11.6	50-55	6.5-7.5	36	5	N ₃ ⁻ , CN ⁻ , Ag ⁺ , Hg ₂ ⁺ , PCMB		Iida, <i>et al.</i> , 1993
<i>Mycobacterium vaccae</i> 10	2x44 [4.6]	6.0 (37 °C)	57	6.0-9.0	200	20	N ₃ ⁻ , SCN ⁻ , Cu ₂ ⁺ , Hg ₂ ⁺ , DTNB		Tishkov, 1993
<i>Thiobacillus</i> sp.		7.53	55	5-10	0.048	1.6	Hg ₂ ⁺ , PCMB, 1-chloro-2- oxopropane 2-chloro-1- (3-pyridyl)-ethanone		Nanba, <i>et al.</i> , 2003
<i>Ancylobacter aquaticus</i>	2x44	9.47	50	5-10.5	0.057	2.4	Cu ₂ ⁺ , Hg ₂ ⁺ , PCMB		Nanba, <i>et al.</i> , 2003
Yeasts									
<i>Candida boidinii</i>	2x36 [5.4]	2.4 (30 °C)	55	6.5-8.5	90	13	N ₃ ⁻ , CN ⁻ , SCN ⁻ , NO ₃ ⁻ , Ag ⁺ , Hg ₂ ⁺ , PCMB	Order Bi-Bi kinetic scheme	Schutte, <i>et al.</i> , 1976; Kato, <i>et al.</i> , 1979
<i>Candida methylica</i>	2x43 [4.6-4.8]	10.0 (37 °C)	50	6.0-9.0	100	13	N ₃ ⁻ , CN ⁻ , Hg ₂ ⁺ , DTNB	Order Bi-Bi kinetic scheme	Avilova, <i>et al.</i> , 1985; Zars, <i>et al.</i> , 1982
<i>Candida methanolica</i>	2x43 [5.5]	7.5 (30 °C)	50	6.5-9.5	110	3	N ₃ ⁻ , CN ⁻ , Hg ₂ ⁺ , Ni ₂ ⁺ , PCMB	Order Bi-Bi kinetic scheme	Izumi, <i>et al.</i> , 1987
<i>Kloeckera</i> sp. 2201		0.14 (30 °C)	50	7.0-8.0	100	22	CN ⁻ , Hg ₂ ⁺ , Cu ²⁺ , PCMB, DTNB		Kato, <i>et al.</i> , 1974

Table 1.2 Physico-chemical properties of NAD⁺-dependent FDHs (continued)

Source ^a	Subunits (kDa) [pI]	Activity (units/mg) ^b	Temp. stability (°C)	pH optimum	K_m^{NAD} (μM)	K_m^{formate} (mM)	inhibitor	Comments	References
Yeasts									
<i>Pichia pastoris</i> NRRL-Y-7556	2x47	8.2	20-25	6.5-7.5	140	16	N ₃ ⁻ , CN ⁻ , Hg ₂ ⁺ , Cu ²⁺ , PCMB		Hou, <i>et al.</i> , 1982
<i>Pichia pastoris</i> IFP 206	2x34	2.8 (37°C)	47	7.5	270	15			Allais, <i>et al.</i> , 1983
<i>Hansenula polymorpha</i> ^c (x6)	2x40	2.8 (37°C)	60	7.0	70	40		uses GSF	Dijken, <i>et al.</i> , 1976; Hollenberg and Janowicz, 1989
Plants									
<i>Phasoleus aureus</i>	2x46				7.2	1.6		Order Bi-Bi kinetic scheme	Peacock and Boulter, 1970
<i>Pisum sativum</i>	2x42	3.7 (25°C)		6.0-8.0	43	1.7	DTNB, PCMB		Ohyama and Yamazaki, 1974
<i>Pisum sativum</i> sp. Onwards	2x42	4.1 (25°C)			23	2.1		uses GSF	Uotila and Koivusalo 1979
<i>Glycine soja</i> var. Beeson	2x47	1.4 (25°C)		6.0	5.7	0.6		uses GSF; Order Bi-Bi kinetic scheme	Farinelli, <i>et al.</i> , 1983
<i>Solanum tuberosum</i> ^f	2x42 [6.8]								Colas des Francs-Small, <i>et al.</i> , 1993

^a For partially purified preparations, purification (fold) is shown in parentheses.

^b Units/mg are mol/min per mg of protein; the temperature at which the activity was measured is given in parenthesis.

^c Gene sequenced and expressed.

^d Three-dimensional structure available.

^e Date on subunit composition not available; the molecular mass of the whole protein was divided by two.

^f Gene sequenced.

Source: Popov and Lamzin, 1994.



Figure 1.9 The reaction of formate dehydrogenase

สถาบันวิทยบริการ
จุฬาลงกรณ์มหาวิทยาลัย

Davidson, 1951) and has been found in various organisms such as plants (Ohyama and Yamazaki, 1974; Colas des Francs-Small, *et al.*, 1993; Olson, *et al.*, 2000), fungi (Chow and Raj Bhandary, 1993; Saleeba, *et al.*, 1992) and bacteria (Galkin, *et al.*, 1995; Nanba *et al.*, 2003; Popov and Lamzin, 1994; Ferry, 1990). However, these enzymes are not so widely distributed in bacteria. Of the naturally occurring NAD⁺-FDHs currently known, only the FDHs from bacteria show a high activity and stability (Tiskov and Popov, 2004) making them of greater interest in potential biotechnological applications.

Genes encoding FDH were found on genome of various organisms such as bacteria: *Pseudomonas* sp. 101, *Moraxella* C-1 (EMBL Y13245), *Paracoccus* sp. 12A, *Mycobacterium vaccae* N10 and *Hyphomicrobium* sp. JC1, methylotrophic yeast: *Pichia angusta*, *Candida methylica* and *Candida boidinii*; baker's yeast: *Saccharomyces cerevisiae* (EMBL Accession Z75296); fungi: *Aspergillus nidulans*, *Neurospora crassa* and *Magnaporthe grisea* (EMBL AA415108) and higher plants: potato *Solanum tuberosum*, barley *Hordeum vulgare*, rice *Oryza sativa* (EMBL AB019533), *Arabidopsis thaliana* (EMBL AB023897) and even mammals: mouse *Mus musculus* (EMBL AI505623) (Popov and Tishkov, 2004).

Up to the present, a few FDHs have been cloned and characterized. In bacteria, they were from *Pseudomonas* sp.101 (Tishkov, *et al.*, 1993), *Moraxella* sp. C-2 (EMBL Accession O08375), *Mycobacterium vaccae* N10 (Galkin, *et al.*, 1995), *Hyphomicrobium* strain JT-17 (FERM P-16973), *Paracoccus* sp. 12-A (Shinoda, *et al.*, 2002), *Ancylobacter aquaticus* (Nanba, *et al.*, 2003a) and *Thiobacillus* sp. KNK65MA (Nanba, *et al.*, 2003b). During the same period, the FDH genes of yeasts were cloned from *Hansenula polymorpha* (Hollenberg and Janowicz, 1989), *Candida methylica* (Allen and Holbrook, 1995), *Candida boidinii* (Sakai, *et al.*, 1997) and *Pichia pastoris* (Goldberg, *et al.*, 2002). Those from fungi were *Aspergillus nidulans* (Saleeba, *et al.*, 1992) and *Neurospora crassa* (Chow and RajBhandarg, 1993).

The majority of characterized NAD^+ -dependent FDHs do not contain any prosthetic groups or metal ions. The enzymes from eukaryotes, as well as from some methylotrophic bacteria, have molecular masses ranging from 70 to 100 kDa. The enzymes display a relatively low specific activity, a low affinity for formate ion and a broad pH optimum for catalytic activity at neutral pH (Table 1.2). FDH from *Pseudomonas* sp. 101 (PseFDH) transfers hydrogen to the pro-R position of the nicotinamide moiety of NAD^+ and thus belongs to the family of A-specific dehydrogenases. The majority of NAD^+ -dependent FDHs are highly specific towards NAD^+ and do not utilize NADP^+ as a coenzyme. However, at least one of them, PseFDH, displays dual coenzyme specificity. Under optimal reaction conditions, the activity of PseFDH towards NADP^+ reaches nearly 30 % of that with NAD^+ (Popov and Lamzin, 1994).

All NAD^+ -dependent FDHs, except the enzyme from *P. oxalaticus*, are stable in oxygen (Table 1.2). Many NAD^+ -dependent FDHs have closely similar thermostabilities and are rapidly inactivated at 55-60 °C. They are labile on storage in the absence of activity stabilizers such as SH-containing compound, EDTA, polyethylene glycol and glycerol (Table 1.2). Heat treatment at 50 °C is widely used as a purification step in the course of FDH isolation.

1.3.2 Structure and catalytic mechanism

FDH is a typical NAD^+ -dependent dehydrogenase composed of two identical subunits each comprising two domains: a coenzyme binding domain and a substrate binding domain based on Rossmann folds. The structure of FDH from *Pseudomonas* sp. 101 is shown in Figure 1.10 (Popov and Lamzin, 1994). The two domains are connected via two long α -helices, αA and $\alpha 8$. The active center is situated at the domain interface and is formed by residues from only one subunit. FDH undergoes considerable conformational change on cofactor binding, as revealed by a structure of the FDH- NAD^+ -azide ternary complex (Figure 1.11). The conformational transition is accomplished via a rotation of peripheral catalytic domains at an angle of 7.5° around hinges connecting residues 146-147 and 340-341 located in the αA and $\alpha 8$ helices respectively. The FDH-ADPR (adenosine diphosphoribose) binary complex reveals the

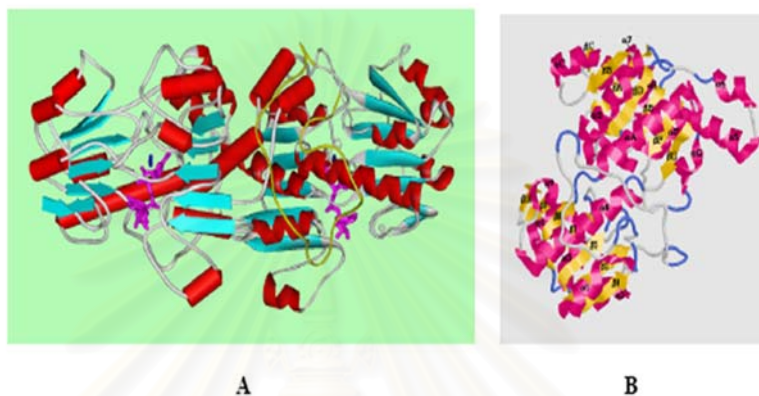


Figure 1.10 Structure of PseFDH A) FDH ternary complex with NAD⁺ (magenta) and formate (blue) occupying azide binding site. α -helices are depicted as red cylinders (left subunit) or helices (right subunit) while β -strands as cyan arrows (left) or strips (right). A long loop comprising α/α residues 12-47 present in bacterial FDHs but absent in the enzymes from other species is shown in yellow. B) Representation of the structure of the FDH subunit.

Source: Popov and Lamzin, 1994

สถาบันวิทยบริการ
จุฬาลงกรณ์มหาวิทยาลัย

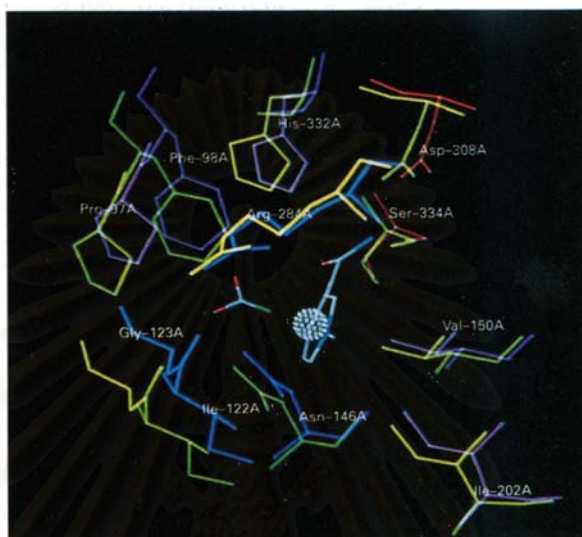


Figure 1.11 Displacement of the active site residues of FDH upon the transition from apo (yellow) to holo state Residues in the holo state are colored according to their charge: magenta – hydrophobic walls and His332; red – negatively charged; blue – positively charged and Ile122.

Source: Popov and Lamzin, 1994

same overall conformation as the apo FDH (r.m.s. 0.2 Å) with only one minor difference in the region of a short loop Ile122-Asp125, where the atoms move more than 1 Å. The loop advances towards the enzyme active site in the transition state enabling Ile122 to be implicated in the substrate binding. Thus revealed flexibility of the loop forms an important structural foundation for FDH catalysis. However ADPR does not induce gross structural changes comparable to those found in PseFDH-NAD⁺-azide ternary complex. This suggests that the nicotinamide moiety of NAD⁺ is the main driving force of the conformational change giving rise to apo-holo transition and essential for transition state formation.

Alignment of FDHs with other D-specific-2-hydroxydehydrogenases revealed a significant relationship between FDHs and D-specific 2-hydroxydehydrogenases acting on D-isomers of hydroxyacids, which have been shown to constitute a related family of proteins, evolutionarily distinct from L-specific 2-hydroxyacid dehydrogenases (Kochhar, *et al.*, 1992). FDH and D-specific dehydrogenases may have similar folds (Popov and Lamzin, 1994). As shown in Figure 1.12, homologous regions were found in the interdomain contact region, where some catalytically important residues are located. A high degree of conservation of the nicotinamide subsite (β D- β F) and a β A- α B structural element comprising the characteristic nucleotide binding template G(A)XGXXG17XD was also observed (Wierenga, *et al.*, 1986). The alignment did not extend to the catalytic domain. A number of residues, i.e. Gly-200, Gly-203, Gly-304, Ala-151, Ala-340, Val-142, Ile-202, Phe-213, Pro-256, Asp-128, Asp-249, Asn-281, Arg-162, Arg-284, Lys-274 and His-332, are essentially conserved in the alignment. Among the FDH active site residues, Ile-202, Arg-284, Asp-308 and His-332 appear to be essentially conserved in the alignment, whereas some areas are conserved in terms of hydrophobicity and some regions (Pro-97-Phe-98, Asn-146, Gln-313, Ser-334) are specific to FDHs (Figure 1.12) (Popov and Lamzin, 1994).

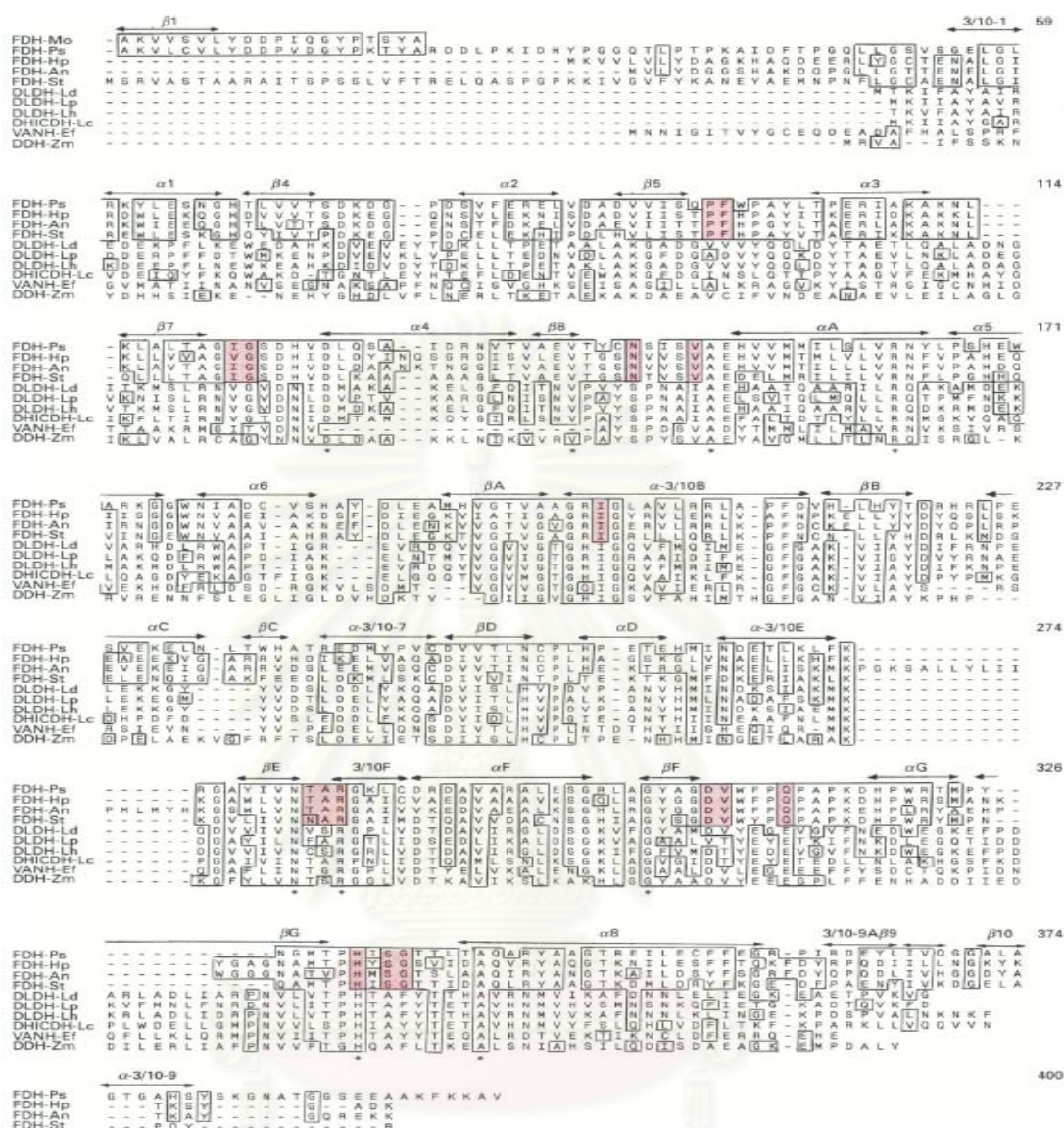


Figure 1.12 Alignment of FDH sequences with the sequences of D-specific 2 hydroxydehydrogenases Sequences are FDH from *Moraxella* sp. C-1 (FDH-Mo), FDH from *Pseudomonas* sp. 101 (FDH-Ps), FDH from *Hansenula polymorpha* (FDH-Hp), a polypeptide from *Aspergillus nidulans* (FDH-An), FDH from potato *Solanum tuberosum* (FDH-St), D-lactate dehydrogenases from *Lactobacillus deibruueckii* (DLDH-Ld), from *Lactobacillus plantarum* (DLDH-Lp) and from *Lactobacillus helveticus* (DLDH-Lh), D-2-hydroxyisocaproate dehydrogenase from *Lactobacillus casei* (DHICDH-Lc), vancomycin-resistant protein from *Enterococcus faecium* (VANH-Ef) and D-dehydrogenase homologue from *Zymomonas mobilis* (DDH-Zm). The residues are numbered according to the sequence of FDH-Ps. Asterisks mark the invariant residues. The residues essential for FDH catalysis and substrate binding are highlighted in light red. The secondary structure of FDH from *Pseudomonas* sp.101 is shown by the arrows. Boxes delineate the matching region. The following residues were considered to be similar: non-aromatic non-polar (L, I, V, M); aromatic polar (F, Y, W); small with near-neutral polarity (C, S, T); small and breaking the folding pattern (G, A, P); acid and uncharged polar (D, E, N, Q); basic polar (H, R, K).

Source: Popov and Lamzin, 1994

The kinetic mechanism of FDH is an order Bi-Bi two-substrate kinetic scheme (or its variants), with NAD^+ being the first substrate (Popov and Lamzin, 1994). While the molecular catalytic mechanism follows two tasks: stabilize the transition state of the reaction and/or destabilize the initial states of the reactants. The net result is lowering of the reaction barrier and enhancement of the rate. In the transition state of the reaction catalysed by FDH, a hydride anion leaves formate and attacks the electrophilic C4N of the positively charged nicotinamide moiety of NAD^+ . As a result two neutral species, CO_2 and NADH , are produced, while NAD^+ C4N changes its hybridization from sp^2 to sp^3 and the nicotinamide moiety becomes uncharged. The mechanism of hydrogen transfer in the FDH-catalysed reaction is mainly governed by electrostatic effects. The positively charged nicotinamide unit of NAD^+ is properly oriented in the active center by multiple interactions with a negatively charged cluster and hydrophobic side chains, whereas formate is bound and oriented by multiple H-bonds with a positive charged cluster. Several stabilizing and destabilizing interactions take place in the active center in the course of catalysis (Figure 1.13). An important factor for catalysis by all NAD^+ -dependent dehydrogenases, including FDH, is enhancement of the electrophilic properties of C4N of the nicotinamide moiety of the coenzyme. This might be achieved through sufficient polarization of the NAD^+ carboxamide group via interactions with negatively charged ligands and perturbation of its ground state due to the twist of the carboxamide with respect to the pyridine plane.

1.3.3 Application of formate dehydrogenase

1.3.3.1 Quantitative determination

NAD^+ -FDHs are currently used as a diagnostic tool for the quantitative determination of oxalic and formic acids in biological samples such as foods and physiological fluids (Schaller and Triebig, 1994; Hatch, *et al.*, 1977), and are one potential reporter system under investigation for nanosensors for the same compounds.

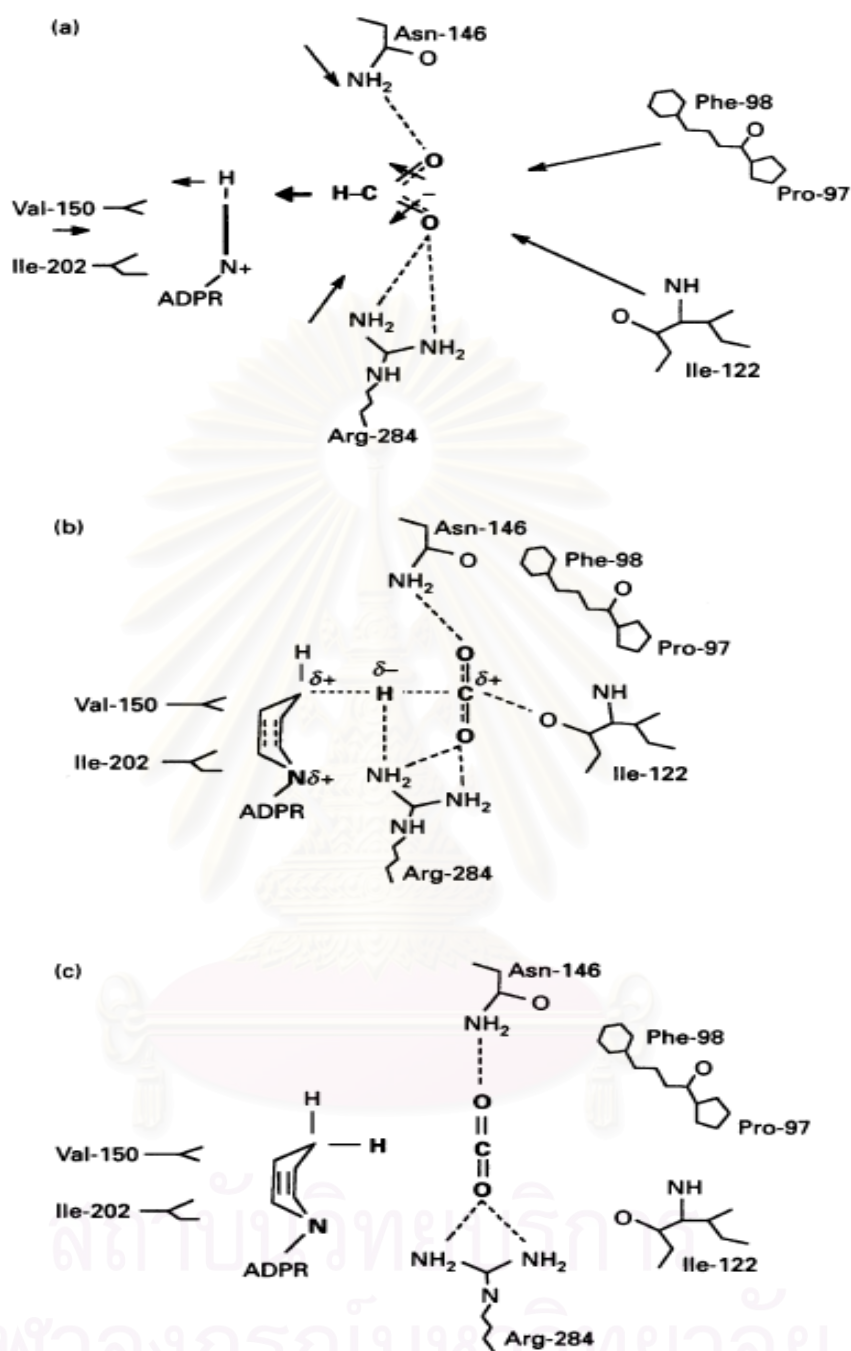


Figure 1.13 The main steps of the FDH molecular mechanism Pre-transition (a), transition (b) and states of the reaction (c). Arrows indicate the movements of parts of the enzyme active center and the reactants during the course of the catalytic transformation. The size of the arrows represents the relative displacement of the respective amino acid residues on the transition of FDH from the apo to the holo state.

Source: Popov and Lamzin, 1994

1.3.3.2 NADH regeneration system

Perhaps of greater economic size importance, FDH is one of the most enzymes extensively studied as a candidate for developing industrial NAD(P)H regeneration with oxidoreductases in the multi-enzymatic systems for synthesis of optically active compounds such as drug, chiral hydroxy acids and esters, amino acids and other fine chemicals using NAD⁺-dependent dehydrogenase that used in many food and pharmaceutical industries (Wichmann, *et al.*, 1981; Hummel and Kula, 1989; Drauz and Waldmann, 1995; Peters, 1998; Bommarius, *et al.*, 1995; Ernst, *et al.*, 2005). For example, the strict Food and Drug Administration (FDA) requirements of > 99% chiral purity of such drugs is technically difficult and expensive to meet by many otherwise cheap chemical synthesis systems but not by the enzymic dehydrogenases due to their extremely high stereospecificity yielding an optical purity of products in excess of 99.9% (Bentley, 1970). However, the limiting drawback of such systems is the economically prohibitive high price of the required coenzyme NADH and NADPH.

The current bulk price (more than 1 kg) for 1 mol NADH (709 g) and NADPH (833 g) is \$5,000 and \$39,000, respectively (Popov and Tishkov, 2003). Accounting for a low molecular mass of an optically active product (usually 200-350 Da), the synthesis of 1 kg of the target product will require 3-4 kg of the reduced cofactor. Thus, the production cost of 1 kg of the target product will reach dozens thousand of US \$.

The problem solution is thought to be in the introduction of an additional enzyme, such as FDH responsible for NAD(P)⁺ regeneration *in situ* (Popov and Tishkov, 2003). Coenzyme regeneration systems are thus of central interest since they can overcome the high price of coenzyme reagents for the economical viability of the process (Hummel, 1999; Wichmann and Vasic-Racki, 2005). Chemical, photochemical and electrochemical regeneration systems are all inferior to enzymatic regeneration systems (Nakamura, *et al.*, 1988). Additional advantages of FDHs are the practically irreversible and 100% conversion of products is possible in coupled reactions. Formate, as substrate for the FDH, is one of the cheapest hydrogen sources and does not inhibit most other dehydrogenases. The oxidation product CO₂ can be easily removed from the reaction mixture. The enzyme has a broad pH optimum of activity so that it can be easily implemented in coupled enzymatic synthesis. The disadvantages of FDH reside

in its relatively low specific activity and limited coenzyme specificity (towards NAD⁺ only).

The company in Germany has developed for production of *tert*-L-leucine in an industrial scale process with FDH as a catalyst of NADH regeneration, and this is one of the largest enzymatic processes in pharmaceutical chemistry (Bommarius, *et al.*, 1995)

Co-immobilized preparations of D-LDH and FDH were employed for production of D-lactate from pyruvate (Shaked and Whitesides, 1980). The optical purity of the product was above 92%, the yield was about 80% and the NAD⁺ cycling number was about 1500.

Carrea and co-workers (1984) used FDH to regenerate NADH for production of 12-oxochenodeoxycholic acid from dehydrocholic acid in a system comprising two hydroxysteroid dehydrogenases. The concentration of the final product reached 0.9% (w/v), with 100% conversion of the starting material. The coenzyme was recycled 1200 times.

Izumi, *et al.*, 1983 reported that cells of *Arthrobacter* sp. KM62 containing a high level of FDH activity in freeze-thawed, air-dried or acetone-dried form or entrapped in various supports (Nath, *et al.*, 1990) were used to produce NADH. The result showed 90-100% conversion was obtained and the isolated NADH was 83% pure.

Cyclohexanone mono-oxygenase from *Acinetobacter* NCIMB 9871 and a protein-engineered formate dehydrogenase from *Pseudomonas* sp. 101 for regeneration of NADPH were used in the synthesis of chiral ϵ -lactones (Rissom, *et al.*, 1997). Syntheses were carried out in a repetitive-bath reactor with integrate bubble-free aeration by means of a thin-walled. 4-Methylcyclohexanone was used as the model substrate yielding (*S*)-(-)-5-methyl-oxepane-2-one with high chemical and enantiomeric purity.

However, the catch lies in that whilst the enzymatic synthesis of many desirable compounds, such as chiral alcohols, ϵ -lactones (Seelbach, *et al.*, 1996; Rissom, *et al.*, 1997; Schwarz-Linek, *et al.*, 2001) and (*S*)-ethyl 4-chloro-3-hydroxybutanoate (Rozzell, *et al.*, 2004), are obtained by using NADP⁺-specific oxidoreductases (Drauz and Waldmann, 1995). The currently known FDHs show a high preference for NAD⁺ over NADP⁺ as the electron acceptor (Tiskov and Popov, 2004),

leading to an absence of natural NADPH regenerating systems. One approach to solve this dilemma has been protein engineering of NAD⁺-FDHs by mutagenesis to change the coenzyme specificity from NAD⁺ to NADP⁺. Single point mutations targeting the conserved Asp195 residue in the NAD-FDHs from *Candida methylica* (Gul-Karaguler, *et al.*, 2001), *Saccharomyces cerevisiae*, *Pseudomonas* sp. 101 (Serov, *et al.*, 2002) and *Candida boidinii* (Rozzell, *et al.*, 2004) have looked promising, whilst the recent double mutation targeting both Asp195 and Tyr196 residues in *C. boidinii* is particularly promising, yielding a recombinant enzyme with a 2×10^7 fold improvement in catalytic activity in the presence of NADP⁺ for only a 700 fold loss in that with NAD⁺ (Andreadeli, *et al.*, 2008). However, besides these obvious target sites for protein engineering the negatively charged aspartic/glutamic acid residue requirement at the conserved fingerprint region for NAD⁺ binding, plus the positively charged amino acids for binding of the NADP⁺ 2-phosphate group (Carugo and Argos, 1997a, 1997b), other conserved regions of importance that may affect the conformation, pH tolerance and so on are poorly understood. It thus remains of great interest to characterize natural (i.e. evolutionary selected and optimized) NADP⁺-FDHs either to supply directly suitable recombinant enzymes, or to provide additional comparative sequence information to guide further protein engineering studies towards optimal enzymes for biotechnology.

1.3.3.3 Bioenergetics

Sukhno and co-workers (1978) demonstrated that formate can be easily oxidized on a pyrographite electrode in the presence of FDH, diaphorase and methyl viologen as a mediator. A current density of 12 mA/cm² was obtained. Prospects for formic acid as a convenient energy carrier were investigated. Storage of the hydrogen gas obtained, e.g. through biophotolysis of water in the form of formic acid, were discussed (Egorov, *et al.*, 1981).

1.4 Production of L-alanine by co-existence of AlaDH and FDH

Our research group screened L-alanine dehydrogenase-producing bacteria from soil in Bangkok and *Aeromonas hydrophila* was found to produce the highest activity of AlaDH among many isolates (Phungsangtham, 1997). AlaDH from this bacterium has molecular mass of about 230 kDa and consists of 6 identical subunits which highly specific to L-alanine and NAD^+ . Optimum temperature for reductive amination and oxidative deamination are 45 and 55 °C, respectively. Enzyme remained full activity upon the incubation at 55 °C for 16 hr. The optimum pH for reductive amination is 8.0 while the reverse reaction rate is highest at pH 10.5. The oxidative deamination proceeds through a sequential ordered binary-ternary mechanism in which NAD^+ binds first to the enzyme followed by L-alanine and products are released in the order of pyruvate, ammonia and NADH, respectively. The K_m values for NAD^+ , L-alanine, pyruvate, ammonia and NADH are 0.17, 20, 1.33, 77 and 0.24 mM, respectively.

The AlaDH gene was cloned in pUC18 and expressed into *E. coli* JM109 cells (Poomipark, 2000). This gene has an open reading frame of 1,113 bp which encodes for 371 amino acids residues and has GC content about 65 %. Comparison of deduced amino acid sequence with AlaDHs from other bacteria shows over 50 % similarity. The transformant had specific activity 50 folds higher than that of the enzyme from wild type. To obtain the high expression recombinant, the gene was cloned into vector pET-17b and expressed into *E. coli* BL21 (DE3) under T7 expression system. The specific activity of crude recombinant enzyme was 6.2 and 310 fold higher those from pUC18 clone and wild type, respectively (Hatrongjitt, 2004).

The efficiency of alanine production was improved using NADH regenerating system by formate dehydrogenase from *Mycobacterium vaccae* N10 which was constructed in *E. coli* BL21 (DE3) host cell (Figure 1.14). Co-existence of AlaDH and FDH genes was performed by two methods (Hatrongjitt, 2004) (I) cloning of heterologous gene of AlaDH and FDH genes under T7 promoter of pET-17b (pETAF and pETFa, Figure 1.15) and (II) co-transformation of plasmids containing AlaDH and FDH genes under T7 promoter of plasmid vector pMPM-K3 and pET-17b, respectively (pMPMAlaDH/pETFDH). However, the production of alanine from pyruvate and ammonium formate by resting cells of various recombinant clones were not

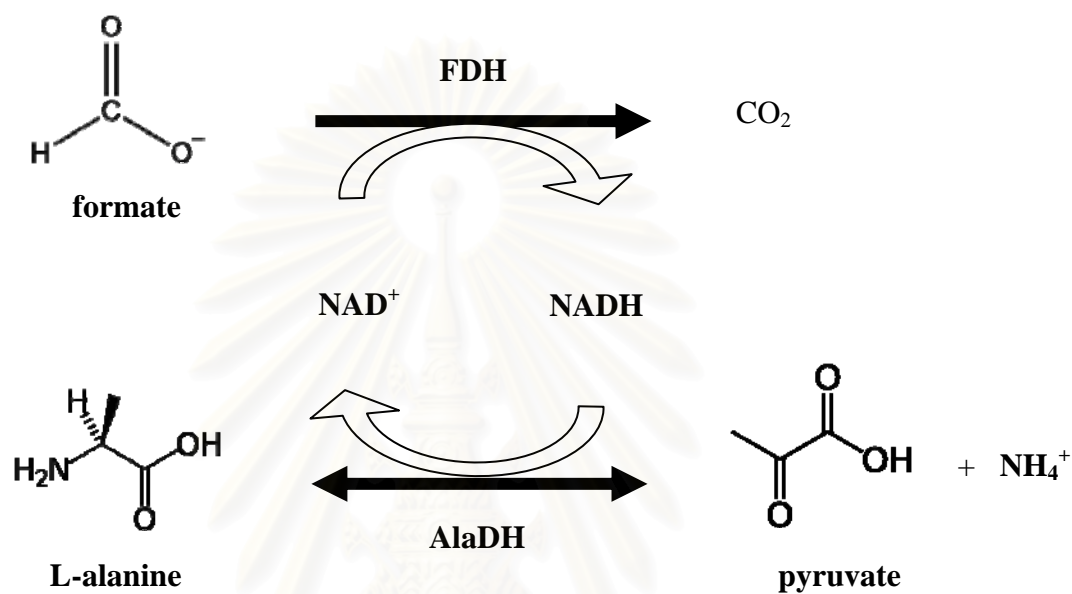
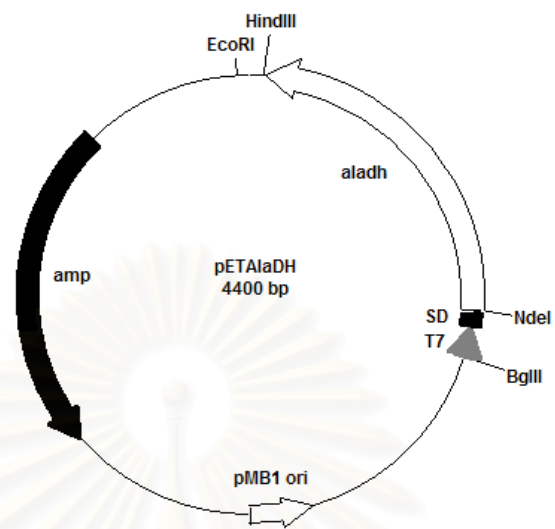


Figure 1.14 Conjugated enzyme system of AlaDH and FDH for production of L-alanine

สถาบันวิทยบริการ
จุฬาลงกรณ์มหาวิทยาลัย

pETAlaDH



pETFa

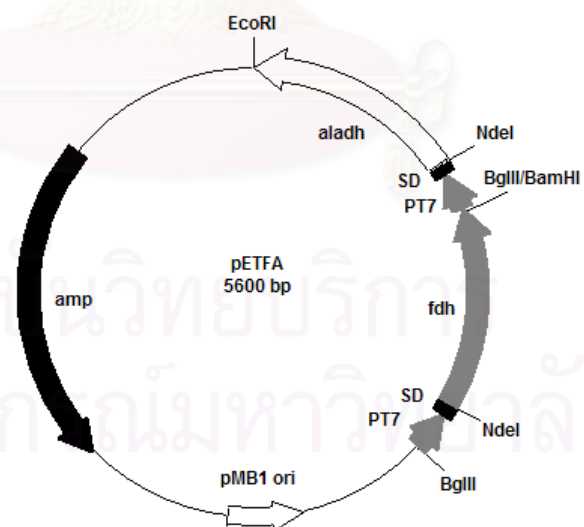


Figure 1.15 Map of recombinant plasmid pETAlaDH and pETFa

significantly different with ratio of D:L form about 1.6:1. This was probably due to the action of the alanine racemase produced by the host cells.

To improve the production of high optical purity and high yield of L-alanine, the strategy of this study was divided into 2 parts; (I) Construction of alanine racemase-deficiency *E. coli* host which supports the expression of pET system and (II) Screening for a novel bacterial FDH.

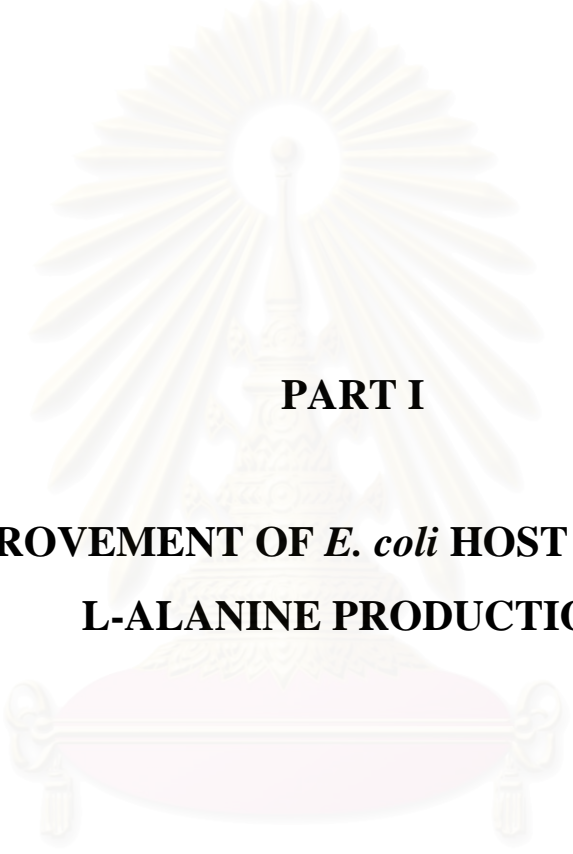
1.5 The outline of this research

Part I: Improvement of *E. coli* host cell for L-alanine production

1. Construction of bacterial host cells for pET series by insertion of T7 RNA polymerase gene into chromosome of *E. coli* MB 2975 alanine racemase-deficiency mutant (*alr*⁻, *dadX*⁻) by using λ DE3 lysogenization kit
2. Transformation of pETFAs into the constructed *E. coli* KR
3. Optimization of AlaDH and FDH genes expression in *E. coli* KR harboring pETFAs
4. Production of alanine by the recombinant clone

Part II: Screening and characterization of a novel FDH

1. Screening of FDH producing bacteria
2. Identification of bacteria containing FDH
3. Cloning and expression of the FDH gene into *E. coli* BL21 (DE3) using vector pET-17b
4. Determination of the recombinant FDH activity
5. Optimization of the recombinant FDH production by varying IPTG concentration and induction time
6. Site-directed mutagenesis of the formate dehydrogenase gene
7. Purification and characterization of the novel formate dehydrogenase



PART I

**IMPROVEMENT OF *E. coli* HOST CELL FOR
L-ALANINE PRODUCTION**

สถาบันวิทยบริการ
จุฬาลงกรณ์มหาวิทยาลัย

CHAPTER I

INTRODUCTION

The alanine production from pyruvate and ammonium formate by resting cells of various recombinant clones in the previous research was not significantly different with the ratio of D: L form about 1.6:1 after incubation for 12 hr (Hatrongjitt, 2004). This was probably due to the action of the alanine racemase produced by the bacteria host cells. Galkin, *et al.*, (1997) also studied L-alanine production by *E. coli* TG1 which expressed heterologous genes of AlaDH and FDH under the tandem *lac-tac* promoter using vector pUC119 (pFDHAlaDH). They inserted AlaDH gene from *B. stearothermophilus* at downstream of FDH gene from *Mycobacterium vaccae* N10 and found that the amount specific activities in the clone cell extract were 1.2 U/mg for FDH and 7.3 U/mg for AlaDH. The resting cells of transformed *E. coli* TG1 were used as the catalyst for L-alanine production from pyruvate and ammonium formate. The amount of L-alanine produced increased as the concentration of pyruvate increased. Moreover, the optical purity of L-alanine decreased with prolonged incubation. The enantiomeric excess of L-alanine was 88% after 3 hr, while it was only 80% after 10 hr. Their result supports our hypothesis that alanine racemase produced by the host cells should influence on the existence of D-alanine in the reaction product.

Gram-positive and gram-negative bacteria require the D-isomer of alanine as an essential building block in the synthesis of the peptidoglycan layer of cell walls. The D-isomer of alanine is converted from L-alanine by alanine racemase. In *E. coli*, two genes of alanine racemase are reported (Strych, *et al.*, 2002). The *alr* gene encodes the constitutively expressed biosynthetic enzyme, sufficient to provide enough D-alanine for cell wall biosynthesis. The catabolic *dadX* gene encodes a second alanine racemase isozyme whose expression is subjected to induction by L-alanine and thus is most active when L-alanine is used as a carbon and energy source.

To express recombinant proteins in *E. coli*, the pET system is usually used since it is one of the most powerful systems for cloning and expression. The pET plasmids contain an expression cassette in which the gene of interest is inserted behind an extremely strong promoter from the *E. coli* bacteriophage T7. In the absence of the specific T7 RNA polymerase, this promoter is completely shut off. For expression, the

pET plasmids are transformed into bacteria strains that typically contain a single copy of the T7 RNA polymerase on the chromosome in a lambda lysogen (the most commonly used lysogen is known as DE3). The T7 RNA polymerase is under the control of the *lacUV5* promoter. When cells are grown in media without lactose, the *lac* repressor (*lacI*) binds to the *lac* operator and prevents transcription from the *lac* promoter. When lactose is the sole carbon source, or when the lactose analog IPTG is added to the media, lactose (or IPTG) binds to the repressor and induces its dissociation from the operator, permitting transcription from the promoter. Finally, addition of glucose to the culture media contributes to repression of the T7 RNA polymerase via the mechanism of catabolite repression, as shown in Figure 1.1.

In this part, the *E. coli* host cell was improved to produce the high purity of L-alanine. *E. coli* MB2795, a kindly gift from Dr. Michael J. Benedik, University of Houston, U.S.A., which is alanine racemase-deficiency (*alr⁻*, *dadX*) mutant of the *E. coli* K12 was used as a host cell for L-alanine production. However, this strain does not contain the T7 RNA polymerase which is necessary for expression of pETF A containing FDH and AlaDH genes. Therefore, T7 gene 1 encoding T7 RNA polymerase was integrated into chromosome of *E. coli* MB2795 by using λ DE3 lysogenization kit (Novagen, USA).

The λ DE3 lysogenization kit is designed for site-specific integration of λ DE3 prophage into an *E. coli* host chromosome. Lysogenization is accomplished in a three-way infection with λ DE3, a helper phage and a selection phage. The kit also contains a tester phage for verification of λ DE3 lysogeny on most host strains, and a positive control lysogen. λ DE3 is a recombinant phage carrying the cloned gene for T7 RNA polymerase under *lacUV5* control. λ DE3 (*imm²¹ Δnin5 Sam7*) is created by inserting the T7 RNA polymerase gene behind the *lacUV5* promoter using the *Bam*HI cloning site of λ D69 (Figure 1.2). Cloning into the *Bam*HI site of λ D69 interrupts the *int* gene. Therefore, λ DE3 cannot integrate into (or be excised from) the chromosome by itself. The helper phage provides the *int* function that λ DE3 lack, but cannot form a lysogen by itself because it is *cI⁻* (had any repressor). The selection phage can neither kill λ DE3 lysogens, because they has the same immunity, nor integrate into susceptible cells (*cI⁻*), but does kill a major class of λ DE3 host range mutant that otherwise will be among the surviving cells. The tester phage, a T7 RNA polymerase deletion mutant, is unable to

make a plaque on cells that lack T7 RNA polymerase, but make normal plaques on λ DE3 lysogens in the presence of IPTG.



สถาบันวิทยบริการ
จุฬาลงกรณ์มหาวิทยาลัย

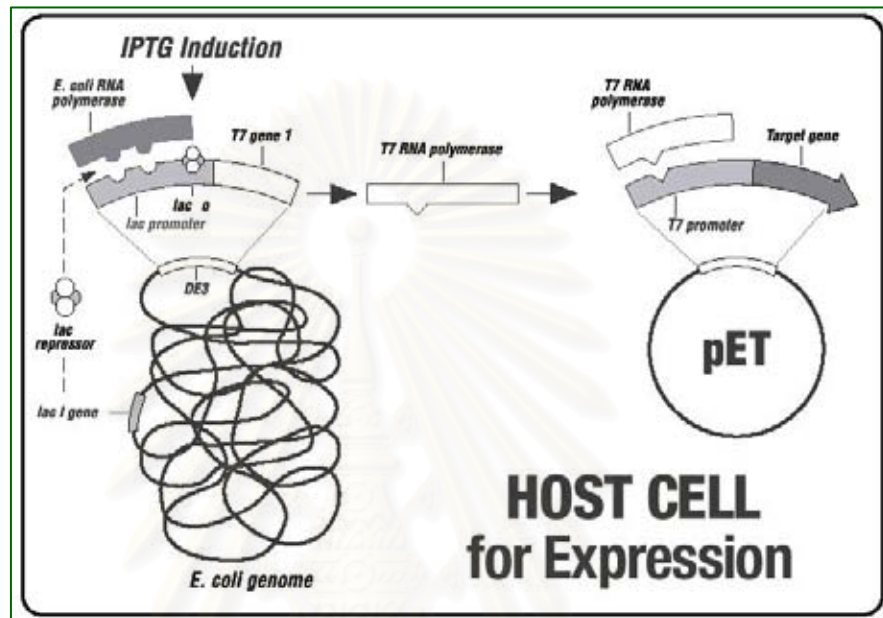


Figure 1.1 Control element of the pET system

Source: Novagen, U.S.A.

สถาบันวิทยบริการ
จุฬาลงกรณ์มหาวิทยาลัย

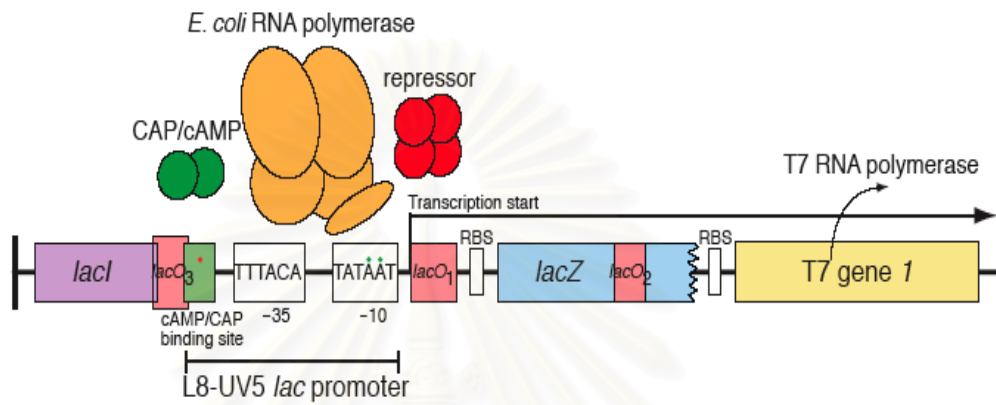


Figure 1.2 Diagram of λ DE3 λ DE3 is created by insertion of T7 RNA polymerase gene behind the *lacUV5* promoter using the *Bam*HI cloning site of λ D69

Source: Novagen, U.S.A.

สถาบันวิทยบริการ
จุฬาลงกรณ์มหาวิทยาลัย

CHAPTER II

MATERIALS AND METHODS

2.1 Equipments

Autoclave: Model LS-20, REXALL industries Co., Ltd., Taiwan

Autoclave: MLS-3020, SANYO Electric Co., Ltd., Japan

Autopipette: Pipetman, Gilson, France

Centrifuge, refrigerated centrifuge: Model J-301, Beckman Instrument Inc., U.S.A.

Centrifuge, microcentrifuge: Model 22R, Beckman Coulter, Inc., Germany

Centrifuge tube: Nalgene, USA.

Gel Doc: BioDoc-ItTM Imaging system, Model M20, Cambridge, UK

Gene Pulser^R/*E. coli* PulserTM Cuvettes: Bio-Rad, U.S.A.

Heating box: Model RS232 Dry bath incubator, Taiwan

High Performance Liquid Chromatography (HPLC): SHIMADZU, Japan

Incubator, waterbath: Model M20S, Lauda, Germany; BioChiller 2000;

FOTODYNE Inc., U.S.A.

Incubator shaker: InnovaTM 4080, New Brunswick Scientific, U.S.A.

Incubator shaker: Model Excella E24R, New Brunswick Scientific, U.S.A.

Lamina flow: HT123, ISSCO, U.S.A.

Magnetic stirrer: Model Clifton Cerastir, Nickel-Electro, Ltd, UK.

Membrane filter: cellulose nitrate, pore size 0.45 μm , Whatman, England

Microcentrifuge tubes 0.5 and 1.5 ml, Axygen Hayward, U.S.A.

Microwave oven: Model Galaxy GX2021M, Asian electric. Industries Co., Ltd, Thailand

pH meter: Model S20-K, Schwerzenbach, Switzerland

Power supply: Model POWER PAC 300, Bio-Rad, U.S.A.

Rotary shaker: Model LD-427, Labinco BV, Netherlands

Shaking waterbath: Model G-76, New Brunswick Scientific Co., Inc., U.S.A.

Sonicator: Vibra cellTM, SONICS & MATERIALS, Inc., USA

Spectrophotometer: DU Series 650, Beckman, U.S.A.

Spin microtubes: Model microONE, Tomy Digital Biology Co., Ltd., Japan

Thermal cycler: Mastercycler gradient, Eppendorf, Germany

Thermolyne dri-bath, Branstead International, U.S.A.

Thin-wall microcentrifuge tubes 0.2 ml, Axygen Hayward, U.S.A.

TLC plate (RP-18 F_{254s}, 5 cm x 10 cm) Merck, Germany

Ultrafilter: Suprec^{Tm-01, Tm-02}, pore size 0.20 and 0.22 μm , Takara Shuzo Co, Ltd., Japan

UV transilluminator: Model 2011 Macrovue, San Gabriel California, U.S.A.

Vortex: Model K-550-GE, Scientific Industries, Inc, U.S.A.

Vortex: TopMix FP15024, Fisher Scientific, U.S.A.

2.2 Chemicals

Acetonitrile: (HPLC grade) Labscan, Ireland

Acetone: Labscan, Ireland

Agar: Merck, Germany

Agarose: SEKEM LE Agarose, FMC Bioproducts, U.S.A.

D-alanine: Sigma, USA

DL-alanine: Sigma, U.S.A.

L-Alanine: Sigma, U.S.A.

Ammonium formate: Wako, Japan

Ampicillin: Sigma, U.S.A.

Boric acid: Merck, Germany

Bovine serum albumin: Sigma, U.S.A.

Bromphenol blue: Merck, Germany

Chloroform: BDH, England

DNA marker: Lamda (λ) DNA digested with *Hind*III, BioLabs, Inc., U.S.A.

100 base pair DNA ladder, Promega Co., U.S.A.

λ DE3 lysogenization kit: Novagen, U.S.A.

Ethidium bromide: Sigma, U.S.A.

Ethyl alcohol absolute: Carlo Erba Reagenti, Italy

Ethylene diamine tetraacetic acid (EDTA): Merck, Germany

1-Fluoro-2,4-dinitrophenyl-5-L-alanine amide (FDAA or Marfey's reagent), Sigma, U.S.A.

Glacial acetic acid: Carlo Erba Reagenti, Italy

Glycerol: Merck, Germany

Glycine: Sigma, U.S.A.

Glucose: BDH, England
Hydrochloric acid: Carlo Erba Reagenti, Italy
Isoamyl alcohol: Merck, Germany
Isopropanol: Merck, Germany
Isopropylthio- β -D-galactosidase (IPTG): Sigma, U.S.A.
Magnesium sulphate 7-hydrate: BDH, England
Maltose: Sigma, U.S.A.
 β - Mercaptoethanol: Fluka, Switzerland
Methanol: Lab-Scan, Thailand
 β -Nicotinamide adenine dinucleotide (oxidized form) (NAD⁺): Sigma, U.S.A.
N-*tert*-butyloxycarbonyl-L-cysteine: Sigma, U.S.A.
Peptone from casein pancreatically digested: Merck, Germany
Phenazine methosulfate: Nacalai Tesque, Inc., Japan
Phenol: BDH, England
O-phthaldialdehyde: Sigma, U.S.A.
Potassium acetate: Merck, Germany
Potassium chloride: Merck, Germany
Potassium di-hydrogen phosphate: Carlo Erba Reagenti, Italy
di-Potassium hydrogen phosphate: Carlo Erba Reagenti, Italy
Potassium hydroxide: Carlo Erba Reagenti, Italy
Pyruvic acid (sodium salt): Sigma, USA
QIA quick Gel Extraction Kit: QIAGEN, Germany
Sodium acetate: Merck, Germany
Sodium carbonate anhydrous: Carlo Erba Reagenti, Italy
Sodium chloride: Carlo Erba Reagenti, Italy
Sodium dodecyl sulfate: Sigma, U.S.A.
Sodium hydroxide: Merck, Germany
Triethylamine: Merck, Germany
Trifluoroacetic acid: BDH, England
Tris (hydroxymethyl)-aminomethane: Carlo Erba Reagenti, Italy
Yeast extract: Scharlau microbiology, European Union

2.3 Enzymes and restriction enzymes

Lysozyme: Sigma, USA

Proteinase K: Sigma, USA

Restriction enzymes: New England BioLabs, Inc., U.S.A.; Zibenzyme, Sweden, and Fermentas, Lithuania.

RNaseA: Sigma, U.S.A.

Pfu DNA polymerase: Promega, U.S.A.

Taq DNA polymerase: Promega, U.S.A.

2.4 Bacterial strains

Escherichia coli BL21 (DE3), genotype: $F^- ompT hsdS_B (r_B m_B) gal dem$ (DE3) was used as a host for expression.

Escherichia coli MB2795, genotype: $F- \lambda- ilvG- rfb-50 rph-1 alr::frrt dadX::frrt$ was used as a host for expression.

2.5 Plasmids

pET-17b, a vector for cloning and expression (Appendix A).

pETA_{Ala}DH, a pET-17b plasmid containing alanine dehydrogenase gene from *Aeromonas hydrophila*.

pETF_A, a pET-17b plasmid containing formate dehydrogenase gene from *Mycobacterium vaccae* N10 and alanine dehydrogenase gene from *Aeromonas hydrophila*.

2.6 DNA manipulations

2.6.1 Chromosomal DNA extraction

Chromosomal DNA was isolated by the method of Frederick, *et al.*, (1995). The cell pellet was resuspended in 550 μ l of TE buffer (10 mM Tris-HCl and 1 mM EDTA, pH 8.0) by repeated pipetting. The cell solution was then treated with 3 μ l of 5 mg/ml lysozyme, 2 μ l of 10 mg/ml RNaseA, 30 μ l of 10 % SDS followed by the addition of 3 μ l of 20 mg/ml proteinase K and incubated for 1 hr at 37 °C. After incubation, the DNA was extracted with an equal volume of phenol-chloroform (1:1 V/V). A viscous fluid formed at the aqueous layers obtained by centrifugation at

12,000xg for 10 min was then carefully transferred to a new microcentrifuge tube. DNA was precipitated by the addition of 5 M NaCl to the final concentration of 1 M and 2 volume of absolute ethanol. The solution was stood at -20 °C at least 30 min to complete the precipitation. Afterwards, the DNA solution was centrifuged at 12,000 xg for 10 min. DNA pellet was collected and washed with 70% ethanol. After drying, the pellet was dissolved in an appropriate volume of TE buffer. Finally, DNA concentration was estimated by submarine agarose gel electrophoresis compared with known amount of λ /HindIII standard DNA marker.

2.6.2 Plasmid extraction (Sambrook, *et al.*, 1992)

Bacteria which harboring recombinant plasmid was grown in LB-medium (1% peptone, 0.5% NaCl and 0.5% yeast extract, pH 7.2) containing an appropriate concentration of antibiotic drug overnight at 37 °C with rotary shaking. The cell culture was collected by centrifugation at 10,000 xg for 5 min in each 1.5 ml microfuge tube. Then 100 μ l of ice-cold Solution I (50 mM glucose, 25 mM Tris-HCl and 10 mM EDTA, pH 8.0) was added and the cell pellet was resuspended by repeated pipetting and left at room temperature for 10 min. After that, the 200 μ l of freshly prepared Solution II (0.2 N NaOH and 1% SDS) was added, gently mixed by inverting the tube for five times and placed on ice for 10 min. Then the 150 μ l of cold Solution III (3 M sodium acetate, pH 4.8) was added and the tube was placed on ice for 10 min. The mixture was centrifuged at 10,000 xg for 10 min and then the supernatant was transferred to a new tube. An equal volume of phenol-chloroform-isoamyl alcohol (25: 24: 1) was added, mixed and centrifuged at 12,000 xg for 10 min. The upper-phased liquid was transferred to a new tube. The plasmid DNA was precipitated with 2 volume of cool absolute ethanol, mixed and placed at -20 °C at least 30 min. The mixture was centrifuged at 12,000 xg for 10 min. The supernatant was discarded and the pellet was washed with 70% ethanol. After drying, the pellet was finally dissolved in an appropriate volume of TE buffer, pH 8.0 containing 20 μ g/ml DNase-free pancreatic RNase.

2.6.3 Agarose gel electrophoresis

Electrophoresis through agarose is the standard method used to separate, identify, and purify DNA fragments. The 1.0 g of agarose powder was added to 100 ml electrophoresis buffer (89 mM Tris-HCl, 8.9 mM boric acid and 2.5 mM EDTA, pH 8.0) in an Erlenmeyer flask and heat until complete solubilization in a microwave oven. The agarose solution was cooled down to 60 °C until all air bubbles were completely eliminated. The solution was then left at room temperature to 50 °C before pouring into an electrophoresis mould. After the gel was completely set, the comb and seal of the mould was carefully removed. When ready, the DNA samples were mixed with one-fifth volume of the desired gel-loading buffer (0.025% bromphenol blue, 40% ficoll 400 and 0.5% SDS) and slowly loaded the mixture into the agarose gel. Electrophoresis had been performed at constant voltage of 10 volt/cm until dye migrated to approximately distance through the gel. The gel was stained with 2.5 µg/ml ethidium bromide solution for 1 min and destained to remove unbound ethidium bromide in distilled water for 5 min. DNA fragments on agarose gel were visualized under a long wavelength UV light and photographed. The concentration or molecular weight of DNA sample was compared with the intensity or relative mobility of the standard DNA fragment.

2.6.4 Extraction of DNA fragment from agarose gel

Extraction of DNA fragment from agarose gel was performed according to QIAquick gel extraction kit protocol. Briefly, DNA fragment was excised from an agarose gel and transferred to an eppendorf tube. Three volume of buffer QG was then added and incubated for 10 min at 50 °C. After the gel slice had been dissolved completely, the sample was applied to the QIAquick column and centrifuged for 1 min. The flow-through was discarded. Buffer QG was added and centrifuged for 1 min. The column was washed twice with buffer PE and centrifuged for 1 min. Finally, the elution buffer was added to the center of the QIAquick membrane to elute the DNA, the column was left stand for 1 min, and then centrifuged for 1 min. The DNA solution was used in the next experiment.

2.6.5 Transformation of plasmid

2.6.5.1 Competent cell preparation (Dower, 1988)

A single colony of *E. coli* host cell was cultured as a starter in 10 ml of LB-broth and incubated at 37 °C with 250 rpm shaking for 24 hr. The starter was inoculated to 1 liter of LB-broth and was then incubated at 37 °C with 250 rpm shaking until the optical density at 600 nm of the cells reached 0.5 - 0.8 (~3 - 4 hr). After that, the culture was chilled on ice for 15 to 30 min and the cells were harvested by centrifugation at 6,000 xg for 15 min at 4 °C. The supernatant was removed. The cell pellet was washed twice with 1 volume and 0.5 volume of cold sterile water, respectively. The cells were resuspended and centrifuged at 6,000 xg for 15 min at 4 °C. The supernatant was discarded. The pellet was washed with 10 ml of 10% (v/v) ice cold sterile glycerol and finally resuspended in a final volume of 2 - 3 ml of 10% ice cold sterile glycerol. The cell suspension was divided into 40 µl aliquots and stored at -80 °C until used.

2.6.5.2 Electroporation

In the electroporation step, 0.2 cm cuvette and sliding cuvette holder were chilled on ice. The Gene Pulser apparatus was set to 25 µF capacitor, 2.50 kV and the pulse controller unit was set to 200 Ω. Competent cells were gently thawed on ice. One to two µl of DNA solution was mixed with 40 µl of the competent cells and then placed on ice for 1 min. This mixture was transferred to a cold cuvette. The cuvette was applied one pulse at the above setting. Subsequently, one ml of LB medium was added immediately to the cuvette. The cells were quickly resuspended with a pasteur pipette. The cell suspension was transferred to new tube and incubated at 37 °C for 1 hr with shaking at 250 rpm. Finally, this suspension was spread onto the LB agar plate containing selective antibiotic drug for the selection of recombinant plasmid.

2.7 Construction of T7 expression system in *E. coli* MB2795 alanine racemase-deficiency mutant (*alr*⁻, *dadX*⁻)

E. coli MB2795 was grown in LB broth supplemented with 0.2% maltose, 10 mM MgSO₄ and 0.5 mM D-alanine at 37 °C with shaking at 250 rpm to an OD₆₀₀ of 0.5. Then, the cells were collected and kept at 4 °C until used.

T7 RNA polymerase (T7 gene 1) gene was inserted into chromosome of *E. coli* MB2795 using λDE3 lysogenization kit (Novagen, USA). Various amounts of host cell were mixed with 10⁸ pfu λDE3, 10⁸ pfu helper phage, and 10⁸ pfu selection phage to produce plates containing 50–200 candidate lysogens as isolated colonies. Host/phage mixtures were incubated at 37 °C for 20 min to allow phage to adsorb to host. After that, the mixtures were pipetted and spread onto LB plate and then incubated at 37 °C overnight. Most surviving colonies should be λDE3 lysogens. Then chromosomal DNA of this *E. coli* was extracted and purified as described in section 2.6.1. The insertion of T7 gene 1 gene into chromosome of *E. coli* MB2795 was confirmed again by PCR technique using primer T7RNAPF and T7RNAPR (Table 2.1), in a total volume 25 µl consisting of 20 mM Tris-HCl (pH 8.4), 50 mM KCl, 1.5 mM MgCl₂, 0.5 µM of each primer, 0.2 mM dNTPs, 1 U of *Taq* DNA polymerase (Fermentas, Lithuania) and 0.7 µg of chromosomal DNA template. The PCR thermal profile consisted of an initial denaturation at 95 °C for 3 min followed by 30 cycles of 95 °C for 1 min, 56 °C for 30 sec and 72 °C for 1 min after, followed by a final extension at 72 °C for 7 min. Then the PCR product was checked by electrophoresis on 1% agarose gel with ethidium bromide (2.5 µg/µl) and analyzed by a gel documentation system.

The *E. coli* MB2795 mutant containing T7 RNA polymerase system was named *E. coli* KR.

Table 2.1 Nucleotide sequence and T_m of all primers used in PCR amplification

No.	Primers	Sequence (5' - 3')	T_m (°C)
1	T7RNAPF	AGGAAACAGACCATGAACACGATTAACGCTAA GAAC	60
2	T7RNAPR	TTACGCGAACGCGAAGTCC	60
3	AlaDHF <i>Nde</i> I	GGAATTC <u>CATATG</u> ATTATCGGTGTACCTAAGG	62
4	AlaDHR <i>Hind</i> III	CCCA <u>AAGCTT</u> CAGTTCAGCAGGGTCAGGG	62
5	FDHF <i>Nde</i> I	GGAATTC <u>CATATG</u> GCAAAGGTCCTGTG	60
6	FDHR <i>Bam</i> HI	CGG <u>GATCCT</u> CAGACCGCCTTCTTGAAGTTG	60

Restriction sites are underlined.

2.8 Transformation of pETFA into *E. coli* KR

The pETFA was transformed into *E. coli* KR host cells by electroporation as described in section 2.6.5. The transformed cell was grown on LB agar plates containing 100 µg/ml ampicillin and 0.5% D-alanine at 37 °C for 16 hr. Cell containing pETFA was screened by colony PCR using primer AlaDHF*Nde*I and AlaDHR*Hind*III for AlaDH gene as well as FDHF*Nde*I and FDHR*Bam*HI for FDH gene (Table 2.1). The PCR amplification was performed as described in 2.7 except using annealing temperature at 60 °C and single fresh colony as a source of chromosomal DNA.

2.9 Determination of AlaDH and FDH activities

The transformants were grown in 5 ml of LB-medium supplemented with 100 µg/ml ampicillin and 0.5 mM D-alanine at 37 °C overnight. After that, 1% of the cell cultures were inoculated into 200 ml LB-medium containing 100 µg/ml ampicillin and 0.5 mM D-alanine and shaken at 37 °C, 250 rpm. When the turbidity of the cultures at 600 nm had reached 0.6, the final concentration of 0.4 mM IPTG was added to induce the enzyme production. The cultivation was continued at 37 °C for 8 hr before cell harvesting. Finally, crude extracts were prepared and assayed for the enzyme activity of AlaDH and FDH and protein determination.

2.9.1 Crude extract preparation

Bacterial cells were grown at appropriated conditions. The cells were harvested by centrifugation at 8,000 xg for 15 min, then washed twice with cold 0.85% NaCl and centrifuged at 8,000 xg for 15 min. After that, the cell pellets were washed once with cold extraction buffer (0.1 M potassium phosphate buffer, pH 7.4 containing 0.1 mM PMSF, 0.01 β-mercaptoethanol and 1.0 mM EDTA) and centrifuged again. The cell pellets were stored at -80 °C until the next step. For enzyme extraction, the cell pellets were resuspended in 5 ml of cold extraction buffer and then broken by discontinuously sonication on ice with 5 sec pulse and 2 sec stop interval for 15 min by sonic dismembrator. Unbroken cell and cell debris were removed by centrifugation at 12,000 xg for 30 min. The supernatants were stored at 4 °C for enzyme and protein assays.

2.9.2 Determination of AlaDH activity

The activity of AlaDH for oxidative deamination of alanine was spectrophotometrically assayed. Reaction mixture 1 ml comprised of 200 μmol of glycine-potassium chloride-potassium hydroxide buffer, pH 10.5, 20 μmol of L-alanine, 1 μmol of NAD^+ , and enzyme. In a blank tube, L-alanine was replaced by water. Incubation was carried out at 30 °C in a cuvette of 1-cm light path. The reaction was started by addition of NAD^+ and was monitored by measuring the initial change in absorbance of NADH at 340 nm.

One unit of the enzyme is defined as the amount of enzyme that catalyzes the formation of 1 μmol of NADH in 1 min. Specific activity is expressed as units per milligram of protein.

2.9.3 Determination of FDH activity

The activity of FDH was spectrophotometrically assayed. Reaction mixture 1 ml comprised of 200 μmol of potassium phosphate buffer, pH 7.5, 20 μmol of ammonium formate, 1 μmol of NAD^+ , and enzyme. In a blank tube, ammonium formate was replaced by water. Incubation was carried out at 30 °C in a cuvette of 1-cm light path. The reaction was started by addition of NAD^+ and was monitored by measuring the initial change in absorbance of NADH at 340 nm.

One unit of the enzyme is defined as the amount of enzyme that catalyzes the formation of 1 μmol of NADH in 1 min. Specific activity is expressed as units per milligram of protein.

2.9.4 Protein measurement

Protein concentration was determined by the method of Lowry, *et al.* (1951) using bovine serum albumin (BSA) as the protein standard (Appendix B and C). The reaction mixture 5 ml containing 20-300 μg of protein, 100 μl of solution A (0.5% copper sulfate, 1% potassium tartate, pH 7.0) and 5 ml of solution B (2% sodium carbonate, 1 N sodium hydroxide) was mixed and incubated at 30 °C for 10 min. After that, the solution mixture was incubated with 0.5 ml of solution C (phenol reagent) at

room temperature for 20 min. The protein concentration was derived from the absorbance at 610 nm and calculated from the curve of protein standard (BSA).

2.10 Optimization of AlaDH and FDH production by varying IPTG concentration and induction time

The *E. coli* transformants were grown in 5 ml of LB-medium supplemented with 100 µg/ml ampicillin and 0.5 mM D-alanine at 37 °C overnight. After that, 1% of each cell culture was inoculated into 200 ml LB-medium containing 100 µg/ml ampicillin and 0.5 mM D-alanine, shaken at 37 °C, 250 rpm. When the turbidity of the cultures at 600 nm had reached 0.6, various final concentration of IPTG (0, 0.1, 0.2, 0.4 and 0.8 mM) was added to induce enzyme production, and the cultivations were continued at 37 °C for various times (0, 2, 4, 6, 8, 12, 16, 20 and 24 hr) before cell harvesting. Finally, crude extracts were prepared and assayed for the enzyme activity of AlaDH and FDH and protein determination as described above.

2.11 Production of L-alanine

2.11.1 Preliminary test of alanine production

The *E. coli* KR containing pETFA was cultured at its optimum condition by growing the seed culture in 5 ml of LB-medium supplemented with 100 µg/ml ampicillin and 0.5 mM D-alanine at 37 °C overnight. After that, 1% of the cell culture was inoculated into 200 ml LB-medium containing 100 µg/ml ampicillin and 0.5 mM D-alanine, shaken at 37 °C, 250 rpm. When the turbidity of the cultures at 600 nm had reached 0.6, the cultivation was continued without induction at 37 °C for 8 hr before cell harvesting. Cell was harvested by centrifugation at 8,000 xg for 20 min. The cell pellet was washed twice with cold 0.85% NaCl and centrifuged at 8,000 xg for 15 min. After that, the cell pellet was washed once with cold 10 mM phosphate buffer pH 7.4 and centrifuged again. For alanine production, the 2 ml of cell suspension containing 0.1 g wet weight of washed cell, 0.5 M ammonium formate (pH 7.5) and 0.3 M pyruvate was made. The reaction was performed at 37 °C, 250 rpm with reciprocal shaking for 12 hr. The supernatant was separated from the cell for analysis of alanine production by TLC technique.

2.11.2 Determination of alanine by TLC

The supernatant obtained 2.11.1 above was derivatized with 1-fluoro-2, 4-dinitrophenyl-5-L-alanine amide (FDAA or Marfey's reagent) according to Marfey's methods (cited in Nagata, *et al.*, 2001). One hundred μg of standard D- or L- alanine in 20 μl of H_2O or sample 20 μl and 8 μl of 1 M NaHCO_3 was mixed with 400 μg FDAA in 40 μl acetone and incubated at 40 $^\circ\text{C}$ for 1 hr with occasional shaking. The reaction was terminated by adding 4 μl of 2 M HCl. The acetone, water and HCl were removed by evaporation under reduced pressure in a centrifugal evaporator. After evaporation, 20 μl of methanol was added to dissolve the FDAA amino acid. FDAA amino acid solution (2 μl) was spotted on a reversed phase pre-coated TLC plate (RP-18 F_{254S}, 5 cm x 10 cm) and developed with acetonitrile: 50 mM triethylamine-phosphate buffer, pH 5.0 at ratio 35:65 in a pre-equilibrated glass chamber at 25 $^\circ\text{C}$. The FDAA amino acid spots were yellow. When the ascending solvent front nearly reached the top margin, the plate was removed from the chamber and dried with a hot air. Since FDAA is light sensitive, the FDAA amino acids were protected from exposure to light during all procedures.

2.11.3 Optimization of alanine production

The *E. coli* BL21 (DE3) and *E. coli* KR containing pETAlaDH or pETFAla were cultured at their optimum condition for the enzyme induction. For *E. coli* BL21 (DE3) harboring pETAlaDH and pETFAla were grown in LB medium containing 100 $\mu\text{g}/\text{ml}$ ampicillin and shaken at 37 $^\circ\text{C}$, 250 rpm. When turbidity of the cell cultures at 600 nm had reached 0.6, the final concentration of 0.4 mM IPTG was added to induce enzyme production and the cultivation were continued for 4 and 8 hr, respectively. Cells were harvested by centrifugation at 8,000 xg for 10 min. The cell pellets were washed twice with cold 0.85% NaCl and centrifuged at 8,000 xg for 10 min. After that, the cell pellets were washed once with cold 10 mM phosphate buffer, pH 7.4 and centrifuged again. For alanine production, the 5 ml of reaction mixture 0.2 g wet weight of washed cell, 0.5 M ammonium formate (pH 7.5) and various concentration of pyruvate (0.2, 0.4, 0.6, 0.8 M) were made. The reactions were performed at 37 $^\circ\text{C}$, 250 rpm with reciprocal shaking for various times (0, 2, 4, 6, 8, 10, 12, 16, 20 and 24 hr). Aliquots of the supernatants were separated from the cells for analysis of the amounts of D- and L- alanine production by HPLC.

2.11.4 Determination of optical purity of alanine by HPLC

For quantitative determination of alanine enantiomers, alanine derivatization was performed. The 100 μ l of standard D- and L-alanine or sample were incubated in 0.28 M borate buffer, pH 9.0 containing 0.2% *O*-phthalaldehyde (OPA) and 0.2% *N*-*tert*-butyloxycarbonyl-L-cysteine (Boc-L-Cys) for 2 min at 25 °C. Then 10 μ l aliquot of the product mixture was analyzed by HPLC using a Nova-Pack C18 column (4 μ m, 3.9 x 300 mm, Waters, Tokyo, Japan) connecting with spectrofluorometer detector. Excitation and emission wavelengths were 344 and 443. The column was operated at a constant flow-rate of 0.7 ml/min. The mobile phase A was the 0.1 M acetate buffer, pH 6.0 with 7% acetonitrile and 3% tetrahydrofuran (THF) and mobile phase B was 0.1 M acetate buffer, pH 6.0 with 47% acetonitrile and 3% THF. The separation of amino acids accomplished with a linear gradient from mobile phase A to B in 40 min (Hashimoto, *et al.*, 1992).

CHAPTER III

RESULTS AND DISCUSSION

3.1 Construction of T7 expression system into *E. coli* MB2795 alanine racemase-deficiency mutant (*alr*⁻, *dadX*⁻)

To produce optically pure L-alanine, *E. coli* MB2795 alanine racemase-deficiency mutant was selected to use in this research, however, this *E. coli* cannot act as the host cell for expression of pET series because it lacks T7 RNA polymerase. Therefore, T7 RNA polymerase gene (T7 gene 1) was integrated into chromosome of the *E. coli* MB2795 (*alr*⁻, *dadX*⁻) using λ DE3 lysogenization kit to complete T7 promoter system in the alanine racemases deficiency *E. coli* host cell.

The insertion of 2.7 kb T7 RNA polymerase gene on the chromosome of *E. coli* MB2795 was proven by PCR amplification as shown in Figure 3.1. The constructed *E. coli* clone containing T7 RNA polymerase system was named *E. coli* KR.

3.2 Transformation of pETFFA into *E. coli* KR

The pETFFA, which is containing the alanine dehydrogenase and formate dehydrogenase genes under the T7 promoter, was transformed into *E. coli* KR host cells by electroporation. The transformed cells were grown on LB agar plates containing 100 μ g/ml ampicillin and 0.5% D-alanine at 37 °C for 16 hr. Cell containing pETFFA was screened by colony PCR as described in section 2.8. A 1.1 kb PCR product of AlaDH gene and a 1.2 kb PCR product of FDH gene were shown in Figure 3.2.

3.3 Determination of AlaDH and FDH activities in *E. coli* KR harboring pETFFA

Ten transformant colonies were randomly picked up for determination of AlaDH and FDH activities as described in section 2.9. The transformants showed various levels of the total activity and specific activity of AlaDH from 975.9-2205.5 U and 7.5-21.5 U/mg protein, respectively as well as total activity and specific activity of FDH from 8.5-17.2 U and 0.1-0.2 U/mg protein, respectively, as shown in Table 3.1. The transformant No.2 which had the highest total activities and specific activities of both AlaDH and FDH: 2205.5 U and 21.5 U/mg protein and 17.2 U, 0.2 U/mg protein, respectively, was chosen for the next experiment.

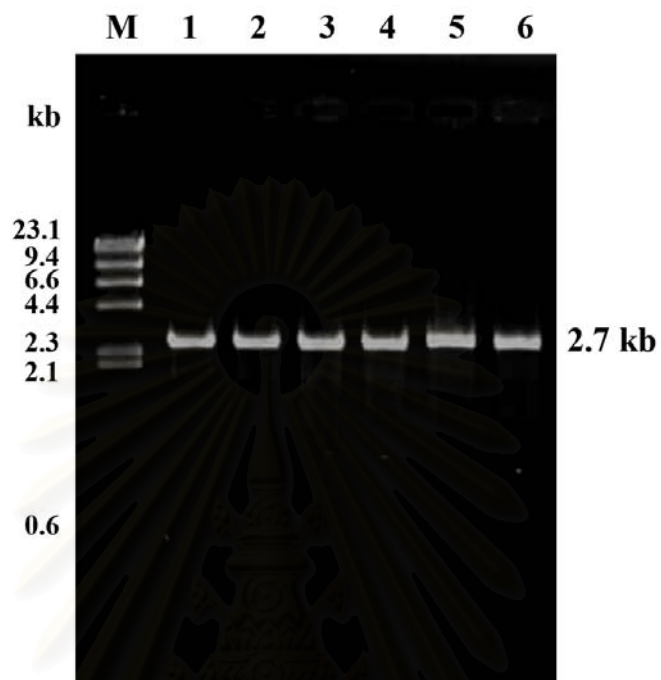


Figure 3.1 PCR amplification of T7 RNA polymerase gene on chromosome of *E. coli* KR.

Lane M = λ /HindIII standard DNA marker

Lane 1-6 = 2.7 kb PCR product of T7 RNA polymerase gene (T7 gene 1)

สถาบันวิทยบริการ
จุฬาลงกรณ์มหาวิทยาลัย

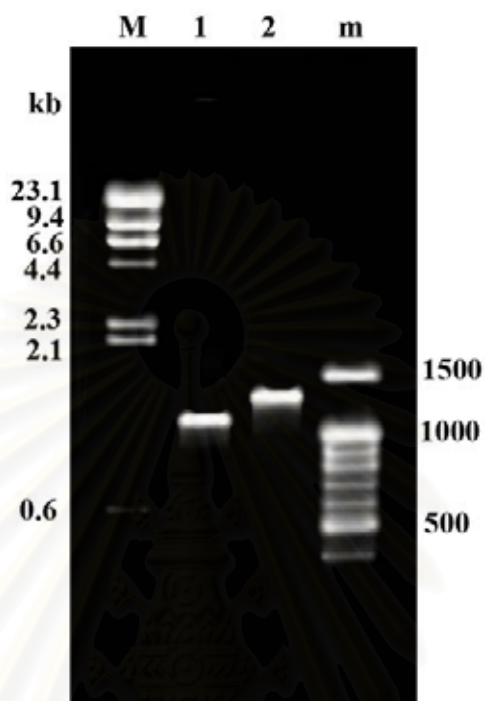


Figure 3.2 Colony PCR amplification of *E. coli* KR harboring pETFA.

Lane M = λ /HindIII standard DNA marker

Lane 1 = 1.1 kb PCR product of alanine dehydrogenase gene

Lane 2 = 1.2 kb PCR product of formate dehydrogenase gene

Lane m = 100 bp DNA ladder

จุฬาลงกรณ์มหาวิทยาลัย

Table 3.1 AlaDH and FDH activities from crude extract of *E. coli* KR harboring pETFA clones

Clone number	Cell wet weight (g)	Total activity (U) ^a		Total protein (mg)	Specific activity (U/mg protein)	
		AlaDH	FDH		AlaDH	FDH
1	0.75	1035.4	12.4	98.3	10.5	0.1
2	0.83	2205.5	17.2	102.5	21.5	0.2
3	0.85	1439.9	15.5	130.9	11.0	0.1
4	0.86	975.9	14.3	129.7	7.5	0.1
5	0.84	1689.3	11.3	118.0	14.3	0.1
6	0.79	1365.3	13.8	104.5	13.1	0.1
7	0.85	2067.9	16.4	143.7	14.4	0.1
8	0.91	1849.7	15.4	157.3	11.8	0.1
9	0.79	1980.6	12.3	134.3	14.8	0.1
10	0.93	2139.9	8.5	138.4	15.5	0.1

^a Total activity from 200 ml culture.

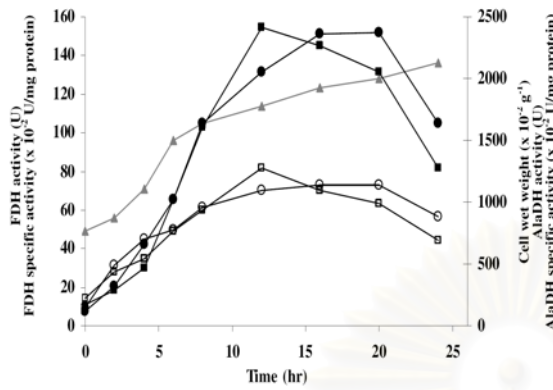
สถาบันวิทยบริการ
จุฬาลงกรณ์มหาวิทยาลัย

3.4 Optimization of AlaDH and FDH production by varying IPTG concentration and induction time

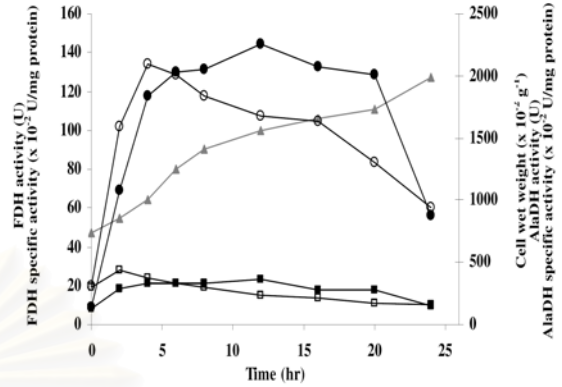
For IPTG concentration and induction time course studies, the transformant No. 2 had been grown and induced by IPTG at various final concentrations of 0, 0.1, 0.2, 0.4 and 0.8 mM, respectively before cells were harvested at various times: 0, 1, 2, 4, 8, 12, 16, 20 and 24 hr, respectively, as described in section 2.10. The result showed that upon the induction with IPTG at 0.1-0.8 mM, FDH activities were dramatically decreased when compared with that activity obtained when the transformant No. 2 was cultured without IPTG. Without induction of IPTG, the cell wet weight increased rapidly in the first 6 hr. After that cell wet weight increased slowly until 24 hr. The highest AlaDH total activity and specific activity were 2368.9 U and 13.1 U/mg protein, respectively when the cells were induced for 20 hr and after that the AlaDH activity and specific activity were decreased. The highest total activity and specific activity of FDH were 154.5 U and 0.8 U/mg protein at 12 hr. After that the activity was decreased. At 12 hr, the activity and specificity of AlaDH were 2055.5 U and 11.0 U/mg protein, respectively. Therefore, the optimal condition for AlaDH and FDH production of *E. coli* KR harboring pETFA was cultivation without IPTG for at 12 hr after OD₆₀₀ nm reached 0.6 (Figure 3.3).

Hatrongjitt (2004) reported that when *E. coli* BL21 (DE3) containing pETFA was cultured at its optimum condition; induction with 0.4 mM IPTG for 8 hr, AlaDH and FDH with total activity of 1747.1 U and 32.5 U, respectively were obtained (Table 3.2). The result indicated that *E. coli* KR seemed to be a good host for expression of FDH gene since FDH produced by *E. coli* KR harboring pETFA was about 5 fold of that produced by *E. coli* BL21 (DE3) containing pETF.

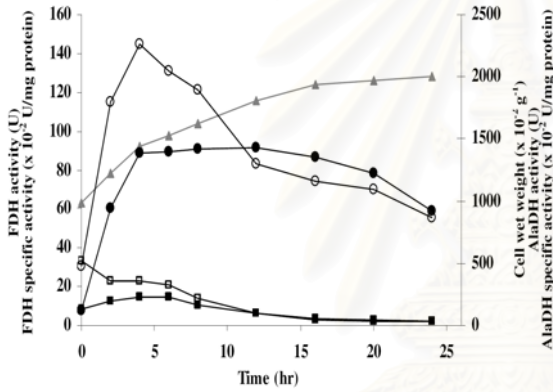
0 mM IPTG



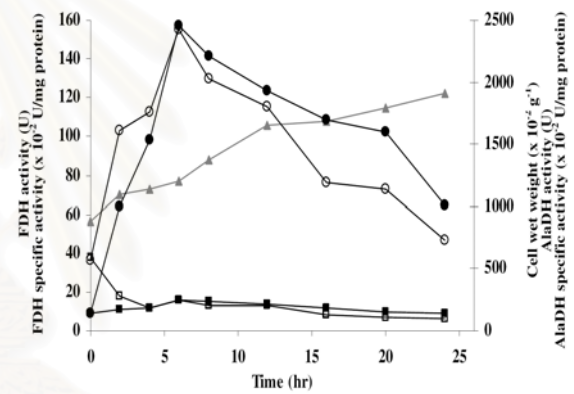
0.1 mM IPTG



0.2 mM IPTG



0.4 mM IPTG



0.8 mM IPTG

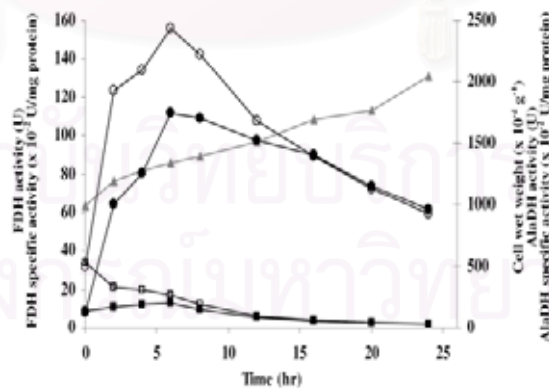


Figure 3.3 AlADH and FDH productions of *E. coli* KR harboring pETFA transformant No. 2 at various final concentrations of IPTG

- ▲ Cell wet weight ● AlADH activity ○ AlADH specific activity
 ■ FDH activity □ FDH specific activity

Table 3.2 AlaDH and FDH activities from crude extract of recombinant clones

Clone number	Cell wet weight (g)	Total activity (U) ^a		Total protein (mg)	Specific activity (U/mg protein)	
		AlaDH	FDH		AlaDH	FDH
pETAlaDH/ BL21 (DE3) ^b	0.80	1800.0	-	55.0	32.7	-
pETF ₂ FDH/ BL21 (DE3) ^b	0.90	-	140.0	44.0	-	3.2
pETF ₂ FA/ BL21 (DE3) ^b	0.85	1747.1	32.5	117.2	14.9	0.3
pETF ₂ FA/KR	1.14	2055.5	154.5	187.5	11.0	0.8

^a Total activity from 200 ml culture.

^b At optimum condition (Hatrongjitt, 2004).

3.5 Qualitative analysis of alanine production by *E. coli* KR using TLC technique

The *E. coli* KR containing plasmid pETFA was used to produce alanine by incubation of the recombinant cells with ammonium formate and pyruvate as described in section 2.11.1-2.11.2. Alanine can be detected on a reversed-phase TLC plate, which can separate optical isomers of the amino acid. This method is simple and rapid without using expensive impregnated plates or a chiral mobile phase. Figure 3.4 shows the chromatograms of FDAA alanine developed with acetonitrile: 50 mM triethylamine-phosphate buffer, pH 5.5 (35:65). A better separation was obtained after repeating the chromatography by putting the developed and dried plate back into the glass chamber for further development. The enantiomers were well-separated after the fifth development. The yellow spots of L-enantiomers move faster than those of the D-enantiomer because the FDAA D-enantiomers have greater affinity for the C₁₈ silica gel than the FDAA L-enantiomers. The *E. coli* BL21 (DE3) harboring pETFA (reference strain) showed equal amount of L- and D-form while *E. coli* KR harboring pETFA produced L-alanine as the main product.

3.6 Optimization of alanine production

E. coli KR harboring pETAlaDH and pETFA were cultured at their optimum condition for the enzyme induction as described in section 2.11.1. *E. coli* BL21 (DE3) harboring pETAlaDH and pETFA were used as reference strains. For alanine production, the five ml of cell suspension of each clone containing 0.2 g wet weight of washed cell, 0.5 M ammonium formate (pH 7.5) and various concentrations of pyruvate (0.2, 0.4 and 0.6 M) were made. The reactions were performed at 37 °C, 250 rpm with reciprocal shaking at various times (0, 2, 4, 6, 8, 10, 12, 16, 20 and 24 hr). Aliquots of the reaction mixture were collected for analysis of the amounts of D- and L-alanine production by HPLC as described in section 2.11.4. The peak of D- and L-isomers of alanine product from all samples were clearly separated as shown in Appendix D. The alanine production of each clones was shown in Figure 3.5.

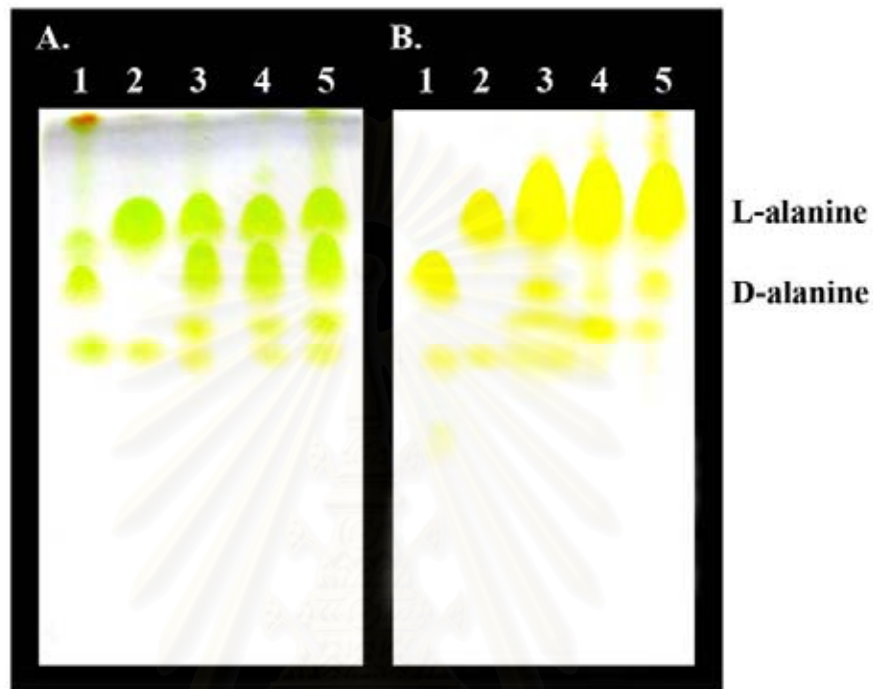


Figure 3.4 Separation of optical isomers of FDAA alanine on reversed phase TLC plate Each sample of FDAA alanine was spotted and developed in acetonitrile: 50 mM triethylamine-phosphate buffer, pH 5.5 (35:65) for 20 min. The enantiomers were well-separated after the fifth development. Lane 1: D-alanine, Lane 2: L-alanine, Lane 3-5 alanine product.

A) *E. coli* BL 21 (DE3) harboring pETFA

B) *E. coli* KR harboring pETFA

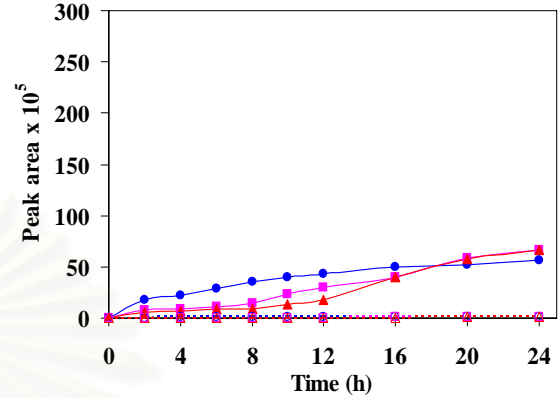
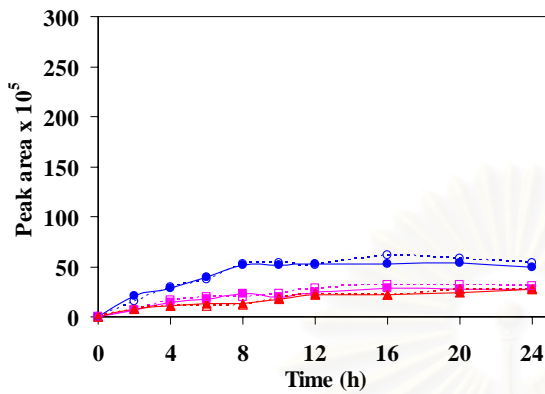
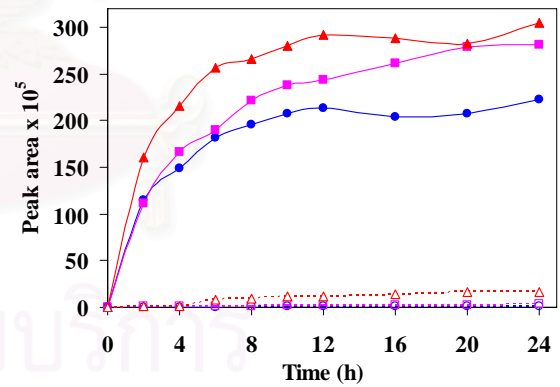
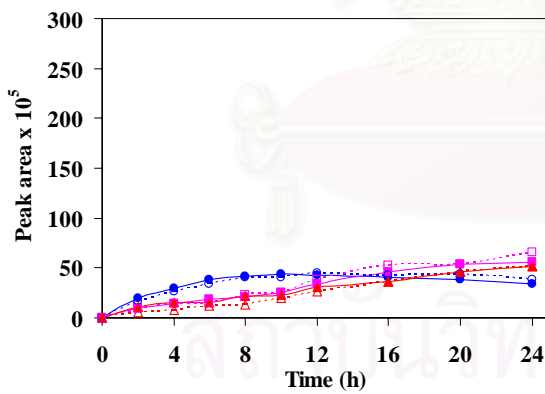
E. coli BL21 (DE3) harboring pETAlaDH*E. coli* KR harboring pETAlaDH*E. coli* BL21 (DE3) harboring pETFFA*E. coli* KR harboring pETFFA

Figure 3.5 Alanine production of various recombinant clones. Concentration of ammonium formate was fixed at 0.5 M.

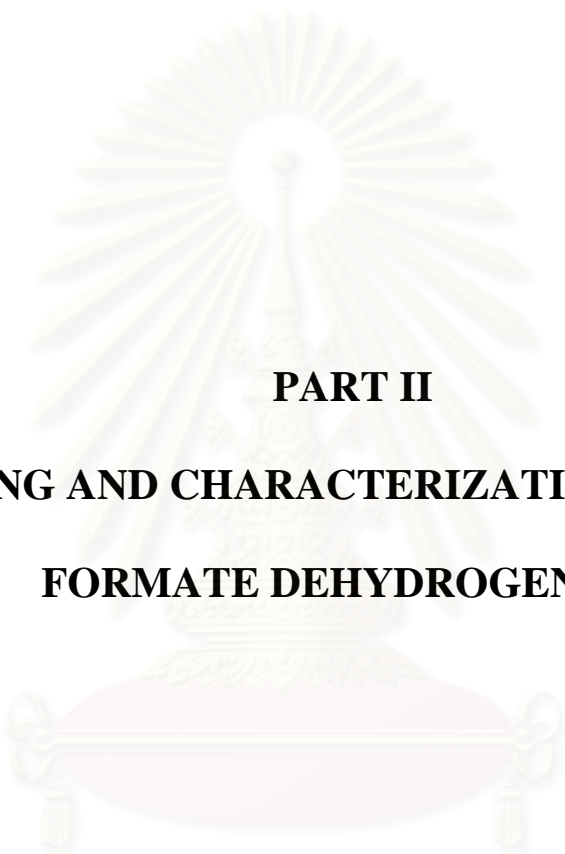
- (L-ala) 0.2 M pyruvate ■ (L-ala) 0.4 M pyruvate ▲ (L-ala) 0.6 M pyruvate
- (D-ala) 0.2 M pyruvate □ (D-ala) 0.4 M pyruvate △ (D-ala) 0.6 M pyruvate

In the reaction of *E. coli* BL21 (DE3) harboring pETAlaDH and pETFFA, amount of both isomers were nearly equal at all concentration of pyruvate. In contrast, D-alanine was produced less than 5% of total alanine product in the reaction using *E. coli* KR harboring pETAlaDH and pETFFA. The result was concordant with the TLC analysis. This indicated that alanine racemases influenced on a proportion of the L-alanine production. Nevertheless, a small amount of D-alanine still appeared in the reactions of *E. coli* KR although this strain was deficiency for both alanine racemase genes. This suggested that another mechanism for production of D-alanine might be occurred.

Total alanine production from *E. coli* KR containing pETFFA was 3 fold higher than that from *E. coli* BL21 (DE3) harboring pETFFA while L-alanine production was about 6 fold higher. This appearance should correlate with the amount of FDH produced by *E. coli* cells. As discussed in section 3.4, *E. coli* KR harboring pETFFA produced FDH 5 times higher than *E. coli* BL21 (DE3) containing pETFFA.

For the effect of pyruvate concentration on L-alanine production in *E. coli* KR harboring pETFFA, amount of L-alanine increased according to the increasing of pyruvate concentration similar to that found in *E. coli* TG1 harboring AlaDH and FDH genes in vector pUC119 (Galkin, *et al.*, 1997).

In this part, the recombinant *E. coli* clone which can produce optically pure of L-alanine (>95% enantiomeric excess) was successfully constructed from racemase deficiency (*alr*⁻, *dadX*⁻) mutant of *E. coli* K12. The coupling reaction of alanine dehydrogenase and formate dehydrogenase was introduced into the clone using pET system. Unexpectedly, the clone could produce formate dehydrogenase 5 fold higher than *E. coli* BL21 (DE3) harboring the same recombinant plasmid of AlaDH and FDH genes. This increasing amount of FDH led to 6 fold production of L-alanine. Since FDH showed strongly effect on L-alanine production, screening of the novel FDH was focused in the next part.



PART II

SCREENING AND CHARACTERIZATION OF A NOVEL

FORMATE DEHYDROGENASE

สถาบันวิทยบริการ
จุฬาลงกรณ์มหาวิทยาลัย

CHAPTER I

INTRODUCTION

In part I, pETFA harboring alanine dehydrogenase from *Aeromonas hydrophila* and the gene coding for NAD⁺ regenerating enzyme, formate dehydrogenase, from *Mycobacterium vaccae* N10 under T7 promoter was cloned into *E. coli* KR. The optical purity (~95%) of L-alanine was produced by the clone. By the way, the recombinant clone of pETFA showed imbalance level of AlaDH and FDH with specific activity of 11.0 and 0.8 U/mg protein, respectively. To produce high yield of L-alanine, FDHs that express high activity and high resistance to some factors, such as substrates, products, oxidation, and thermal inactivation, are required.

Therefore, in this part, screening of a novel formate dehydrogenase was performed. The enzyme gene was cloned and expressed in *E. coli* and the recombinant enzyme was characterized.



สถาบันวิทยบริการ
จุฬาลงกรณ์มหาวิทยาลัย

CHAPTER II

METHODS

2.1 Equipments

Electrophoresis unit: Mini protein, Bio-Rad, U.S.A.

Fraction collector: Frac-920, Amersham Biosciences, Sweden

Peristaltic pump: pump p-1, Pharmacia Biotech, Sweden

Other equipments used in this part were described in part I

2.2 Chemicals

Acrylamide: Merck, Germany

Ammonium persulphate: Sigma, U.S.A.

Ammonium sulphate: Carlo Erba Reagenti, Italy

5-Bromo-4-chloro-3-indolyl- β -D-galactosidase (X-gal): Sigma, U.S.A.

Butyl-Toyopearl 650M TSK gel: Tosoh, Japan

Coomassie brilliant blue G-250: Sigma, U.S.A.

Coomassie brilliant blue R-250: Sigma, U.S.A.

DEAE-Toyopearl 650M TSK gel: Tosoh, Japan

Dialysis tubing: Sigma, USA

Kanamycin: Sigma, U.S.A.

N, N'-methylene-bis-acrylamide: Sigma, U.S.A.

β -Nicotinamide adenine dinucleotide phosphate (NADP⁺): Sigma, U.S.A.

β -Nicotinamide adenine dinucleotide reduced form (NADH): Sigma, USA

Nitroblue tetrazolium: Koch-Light Laboratories Ltd., Japan

Phenylmethylsulfonyl fluoride (PMSF): Sigma, U.S.A.

Sodium formate: Fluka, Switzerland

Standard protein marker: Fermentas Inc., USA

N, N, N', N'-tetramethyl-1, 2-diaminoethane (TEMED): Carlo Erba Reagent, Italy

Other chemicals used in this part were described in part I

2.3 Enzymes and restriction enzymes

Lysozyme: Sigma, USA

Proteinase K: Sigma, USA

Restriction enzymes: New England BioLabs, Inc., U.S.A.; Zibenzyme, Sweden, and Fermentas, Lithuania.

RNaseA: Sigma, U.S.A.

Pfu DNA polymerase: Promega, U.S.A.

T₄ DNA ligase: New England BioLabs, Inc., U.S.A.

Taq DNA polymerase: Promega, U.S.A. NEB, U.S.A.

2.4 Bacterial strains

Escherichia coli DH12S, genotype: *mcrA* Δ (*mrr*, *hsdRMS*, *mcrBC*) ϕ 80d *lacZ* Δ M15 Δ *lacX74* *recA1* *deoR* Δ (*ara*,*leu*)7697 *araD139* *galU* *galK* *rpsL* F'[*proAB*⁺ *lacI*^qZ Δ M15] was used as a host for cloning.

Escherichia coli BL21 (DE3), genotype: F⁻ *ompT* *hsdS_B* (*r_B* *m_B*) *gal dem* (DE3) was used as a host for expression.

2.5 Plasmids

pET-17b, a vector for cloning and expression (Appendix A).

2.6 Determination of FDH activities

2.6.1 Crude extract preparation

Bacterial cells were grown at appropriated conditions. The cells were harvested by centrifugation at 8,000 xg for 15 min, then washed twice with cold 0.85% NaCl and centrifuged at 8,000 xg for 15 min. After that, the cell pellets were washed once with cold extraction buffer (0.1 M potassium phosphate buffer, pH 7.4 containing 0.1 mM PMSF and 1.0 mM EDTA) and centrifuged again. The cell pellets were stored at -80 °C until the next step. For enzyme extraction, the cell pellets were resuspended in 5 ml of cold extraction buffer and then broken by discontinuously sonication on ice with 5 sec pulse and 2 sec stop interval for 15 min by sonicator. Unbroken cell and cell debris were removed by centrifugation at 12,000 xg for 30 min. The supernatants were stored at 4 °C for enzyme and protein assays.

2.6.2 FDH activity assay

The activity of FDH was spectrophotometrically assayed. The 1 ml reaction mixture comprised of 200 μ l of 1 M potassium phosphate buffer (pH 7.0), 200 μ l of 0.5 M sodium formate and 5-200 μ l of the crude enzyme solution. In a blank tube, sodium formate was replaced by water. Incubation was carried out at 30 °C in a cuvette of 1-cm light path. The reaction was started by adding 100 μ l of 10 mM NAD⁺ or NADP⁺ and the initial velocity of the increase in absorbance of NADH or NADPH at 340 nm was monitored.

One unit of the enzyme is defined as the amount of enzyme that catalyzes the formation of 1 μ mol of NADPH and NADH in 1 min. Specific activity is expressed as units per milligram of protein.

2.6.3 Protein determination

Protein concentration was determined by the method of Lowry, *et al.*, (1951) using bovine serum albumin (BSA) as the protein standard as described in section 2.9.4 of part I.

2.7 Screening of a novel FDH

2.7.1 Screening of FDH from soil bacteria

Screening for formate dehydrogenase producing bacteria was done as follows. A spoonful of soil was suspended in 10 ml of water, and then 100 μ l of the supernatant was used to inoculate into 10 ml of basal medium (2 g of K₂HPO₄, 2 g of (NH₄)₂SO₄, 1 g of NaCl, 0.2 g of MgSO₄.7H₂O, 0.5 g of yeast extract, 0.02 μ g of biotin, 4 μ g of calcium pantothenate, 20 μ g of inositol, 4 μ g of nicotinic acid, 4 μ g of thiamine hydrochloride, 2 μ g of pyridoxine hydrochloride, 2 μ g of *p*-aminobenzoic acid, 2 μ g of riboflavin, and 0.1 μ g of folic acid in 1 liter of tap water (pH 7.0)) supplemented with 0.8% (wt/vol) methanol, 1% sodium formate, and 1% sodium carbonate. After aerobic cultivation at 30 °C, 250 rpm for 24 hr, the cell cultures were spread on enrichment medium agar plate and incubated at 37 °C overnight. Each selected colony was inoculated into LB medium (1% peptone, 0.5% yeast extract and 1% NaCl, pH 7.2), cultured under the same conditions as above. Afterward, the cells were assayed for

formate dehydrogenase activity as described in section 2.6. Then, the microorganisms showing high specific activity of formate dehydrogenase were sent to The Clinical Bacteriology Group, Department of Medical Sciences for species identification.

2.7.2 Screening of a novel FDH from bacterial culture collection

In addition to soil bacteria, the *Burkholderia cepacia* complex (BCC) bacteria which kindly provided by DMST-CC (Department of Medical Sciences, Thailand-Culture Collection) were selected for the screening of a novel FDH by PCR amplification. These bacteria can be divided into 3 groups as followings:

2.7.2.1 The reference bacteria

Ten strains of *Burkholderia cepacia* complex (BCC) of ten species were reference strain: *B. cepacia* LMG0122 (human isolated), *B. multivorans* LMG18825 (human isolated), *B. cenocepacia* LMG16656 (human isolated), *B. dolosa* LMG18943 (human isolated), *B. stabilis* LMG18870 (human isolated), *B. vietnamiensis* LMG10823 (environment isolated), *B. ambifaria* LMG51671 (environment isolated), *B. anthina* LMG20980, *B. pyrrocinia* LMG14191 (environment isolated) and *B. ubonensis* DMST6406 (environment isolated).

2.7.2.2 The local strains (isolated from human)

Twenty two of BCC isolated from human were *B. cepacia* (4 strains), *B. multivorans* (4 strains), *B. cenocepacia* (8 strains), *B. vietnamiensis* (3 strains), *B. stabilis* (2 strains) and *B. dolosa* (1 strain).

2.7.2.3 The local strains (isolated from environment)

Nine strains of BCC isolated from environment were *B. cepacia* (1 strain), *B. multivorans* (1 strain), *B. ambifaria* (1 strain), *B. pyrrocinia* (1 strain) and *B. ubonensis* (5 strains).

2.8 Oligonucleotide primer design

Two sets of primers for PCR amplification of a partial fragment of the formate dehydrogenase (FDH) gene homologs were designed (N1, C1, N2 and C2, Table 2.1) using the CODEHOP program (<http://blocks.fhcrc.org/codehop.html>) based on the conserved regions of amino acid sequences of the NAD⁺-dependent FDH annotated genes from *Paracoccus* sp. 12-A (BAB64941), *Ancylobacter aquaticus* KNK607M (BAC65346), *Moraxella* sp. (CAA73696), *Mycobacterium vaccae* N10 (BAB69476), *Pseudomonas* sp. 101 (P33160), *Burkholderia* sp. 383 (YP366697), *Burkholderia ambifaria* MC40-6 (ZP01552925), *Burkholderia cenocepacia* MC03 (YP001773637), *Burkholderia multivorans* ATCC17616 (YP001585382) and *Thiobacillus* sp. KNK65MA (BAC92737) as shown in Figure 2.1.

The primer sequences for inverse PCR amplification to derive the entire FDH gene and flanking sequences, and also those to amplify the complete coding sequence of the FDH homologs were designed by using FastPCR (<http://www.primerdigital.com/index.php?page=35>) as shown in Table 2.1.

2.9 PCR amplification

2.9.1 PCR amplification of partial FDH gene

The *Burkholderia cepacia* complex (BCC) was cultured in LB medium and then chromosomal DNA was extracted as described in section 2.6.1 of part I. The PCR for screening of FDH gene homolog was performed using the 4 primer pairs (N1-C1, N2-C2, N1-C2 and N2-C1, Table 2.1), in a total volume 25 μ l consisting of 20 mM Tris-HCl (pH 8.4), 50 mM KCl, 1.5 mM MgCl₂, 0.5 μ M of each primer, 0.2 mM dNTPs, 1 U of High Fidelity *Taq* DNA polymerase (Fermentas, Lithuania) and 0.7 μ g of chromosomal DNA template. The PCR thermal profile consisted of an initial denaturation at 95 °C for 3 min, 30 cycles of 95 °C for 1 min, 56 °C for 30 sec and 72 °C for 1 min, followed by a final extension at 72 °C for 7 min. The pUC119 containing FDH gene of *Mycobacterium vaccae* N10 (Galkin, *et al.*, 1995) was used as a positive control. For those samples whose PCR were negative, their template quality were checked by using universal primers for 16s rRNA gene (Mahenthalingam, *et al.*, 2000).

Table 2.1 Primers used in this study

Name	Sequence (5' to 3')	T_m (°C)	Purpose
FDHFN	GGAATTCC <u>CATATGG</u> CAAAGGTCCTGTG ^a	60	Error prone PCR
FDHRB	CGGGATCCCTCAGACCGCCTTCTTGAACCTG ^b	60	Error prone PCR
N1 ^c	GCGGATGTGGTTATTTCCCARCCNTTYTGGC	58	Partial fragment amplification
N2 ^c	ACCGCCGGNATHGGNTCVGAYCA	58	Partial fragment amplification
C1 ^d	GGYTGNNGRAACCANACRTC	56	Partial fragment amplification
C2 ^d	TGCCCCGCCGATAACKNGYYTGNGC	56	Partial fragment amplification
IFDHF1	CTGTTCGACGCGGCGATGATCGCG	58	Inverse PCR, Sequencing
IFDHF2	ACGGCGGCGACGTGTGGTTTCC	58	Inverse PCR, Sequencing
IFDHR1	TCGGCGGTCAGGTACGCGGGCC	58	Inverse PCR, Sequencing
FDH-F	GGAATTCC <u>CATATGG</u> CSACCGTCCTSTGCGTGC ^a	60	Complete FDH
FDH-R	CGGGATCCCTCATCAYGTCAGCCGGTACGACTGC ^b	60	Complete FDH
mutFDH	CCG GTG CCG GTC CGT GTA GTG CAG	60	Mutation

^{a, b} underline for *NdeI* and *BamHI*, respectively.

M13 forward^c (-40; GTTTTCCCAGTCACGAC) and reverse^d (-27; GGAAACAGCTATGACCATG) sequences were added to their 5'-end for direct sequencing.

CLUSTAL W (1.83) multiple sequence alignment

```

Mycobacterium      MAKVLCVLYDDPVDGYPKTYARDLDPKIDHYPGGQILPTPKAIDFTPGQLLGSVSGELGL 60
Pseudomonas       MAKVLCVLYDDPVDGYPKTYARDLDPKIDHYPGGQTLPTPKAIDFTPGQLLGSVSGELGL 60
Thiobacillus      MAKVLCVLYDDPVDGYPKTYARDLDPKIDHYPGGQTLPTPKAIDFTPGQLLGSVSGELGL 60
Ancylobacter      MAKVLCVLYDDPIDGYPTTYARDNLPKIDHYPGGQTLPTPKAIDFTPGTMLGSVSGELGL 60
Moraxella         MAKVVCVLYDDPINGYPTSYARDLPRIDKYPDGQTLPTPKAIDFTPGALLGSVSGELGL 60
Paracoccus        MAKVVCVLYDDPVDGYPKTYARDLDPKIDHYPGGQTLPTPKAIDFTVPGSLLGSVSGELGL 60
                  ***:*****:***:****.* ** *:*.** *****.* * :*****
                  N1
Mycobacterium      REYLESNGHTLVVTSKDKGPDVFERELVDADVVISQPFWPAYLTPERIAKAKNLKLALT 120
Pseudomonas       RKYLESNGHTLVVTSKDKGPDVFERELVDADVVISQPFWPAYLTPERIAKAKNLKLALT 120
Thiobacillus      RKYLESNGHTLVVTSKDKGPDVFEKELVDADIVISQPFWPAYLTPERFAKAKNLKLALT 120
Ancylobacter      RKYLESNGHTLVVTSKDKGPDVFEKELVDADIVISQPFWPAYLTPERFAKAKNLKLALT 120
Moraxella         RKYLESQGHVLTSSKDKGPDSELEKHLHDAEVIISQPFWPAYLTAERIAKAPKLKLALT 120
Paracoccus        RNYLEAQGHVLTSSKDKGPDSELEKHLHDAEVVISQPFWPAYLTAERIAKAPKLKLALT 120
                  *:***:.* * :****.* ***** :*:.* **:::*****.* **:* * :*****
                  N2
Mycobacterium      AGIGSDHVDLQSAIDRNVTVAEVTYCNSISVAEHVMMILSLVRNYLPSHEWARKGGWNI 180
Pseudomonas       AGIGSDHVDLQSAIDRNVTVAEVTYCNSISVAEHVMMILSLVRNYLPSHEWARKGGWNI 180
Thiobacillus      AGIGSDHVDLQSAIDRGITVAEVTYCNSISVAEHVMMILGLVRNYIPSHDWARGGWNI 180
Ancylobacter      AGIGSDHVDLQSAIDRGVTVAEVTYCNSISVAEHVMMILGLVRNYLPAHDWARKGGWNI 180
Moraxella         AGIGSDHVDLQAAIDRNITVAEVTYCNSNSVAEHVMMVLGLVRNYIPSHDWARGGWNI 180
Paracoccus        AGIGSDHVDLQAAIDRGITVAEVTFNCNSISVSEHVMMTALNLVRNYTPSHDWA VGGWNI 180
                  *****:***.:*****:*** **:* ***** *.***** *:*** :*****
Mycobacterium      ADCVSHAYDLEAMHVGTVAAGRIGLAVLRRRLAPFDVHLHYTDRHRLPESVEKELNLTWHA 240
Pseudomonas       ADCVSHAYDLEAMHVGTVAAGRIGLAVLRRRLAPFDVHLHYTDRHRLPESVEKELNLTWHA 240
Thiobacillus      ADCVEHSYDLEGMTVGSVAAGRIGLAVLRRRLAPFDVKLHYTDRHRLPEAVEKELGLVWHD 240
Ancylobacter      ADCVKHSYDLEAMSVGTVAAGRIGLAVLRRRLAPFDVKLHYTDRHRLPESVEKELNLTWHA 240
Moraxella         ADCVARSYDVEGMHVGTVAAGRIGLRLVRLAPFDMHLHYTDRHRLPEAVEKELNLTWHA 240
Paracoccus        ADCVTRS YDIEGMHVGTVAAGRIGLAVLRRRFKPFGMHLHYTDRHRLPREVELELDLTWHE 240
                  **** :*:*.** *:***** ** : **:::*****.* ** *.* **
Mycobacterium      TREDMYPVCDVVTLNCP LHPETE HMINDET LKLFKRGAY IVNTARGKLC DRDAVARALES 300
Pseudomonas       TREDMYPVCDVVTLNCP LHPETE HMINDET LKLFKRGAY IVNTARGKLC DRDAVARALES 300
Thiobacillus      TREDMYPHCDVVTLNVP LHPETE HMINDET LKLFKRGAY IVNTARGKLADRD AIVRAIES 300
Ancylobacter      SPTDMYPHCDVVTLNCP LHPETE HMINDET LKLFKRGAY IVNTARGKLC DRDAIARALEN 300
Moraxella         TREDMYGACDVVTLNCP LHPETE HMINDET LKLFKRGAY LVNTARGKLC DRDAIVRALES 300
Paracoccus        SPKDMFPACDVVTLNCP LHPETE HMINDET LKLFKRGAY LVNTARGKLC DRDAVARALES 300
                  : ** : ***** :*:*****:*****:*****:*****:*****:***:*.
                  C1          C2
Mycobacterium      GRLAGYAGDVWFPPAPKDPHWRTPYNGMTPHISGTTLTAQARYAAGTREILECFFEGR 360
Pseudomonas       GRLAGYAGDVWFPPAPKDPHWRTPYNGMTPHISGTTLTAQARYAAGTREILECFFEGR 360
Thiobacillus      GQLAGYAGDVWFPPAPKDPHWRTPMKEGMPHISGTTLSAQARYAAGTREILECFFEGR 360
Ancylobacter      GTLAGYAGDVWFPPAPADHPWRTPMANGMTPHMSGTSLTAQTRYAAGTREILECFFEGR 360
Moraxella         GRLAGYAGDVWFPPAPNDHPWRTPHNGMTPHISGTTLSAQTRYAAGTREILECYFEGR 360
Paracoccus        GQLAGYGGDVWFPPAPQDHPWRTPHNAMTPHISGTTLSAQARYAAGTREILECHFEGR 360
                  * ****.* ***** ** * :*:***:*.**:::*****.* *****
Mycobacterium      PIRDEYLIVQGGALAGTGAHSYSKGNATGGSEEAAKFKKAV- 401
Pseudomonas       PIRDEYLIVQGGALAGTGAHSYSKGNATGGSEEAAKFKKAV- 401
Thiobacillus      PIRDEYLIVQGGALAGTGAHSYSKGNATGGSEEAAKFKKAG- 401
Ancylobacter      PIRDEYLIVQGGNLAGVGAHSYSKGNATGGSEEAGKFKKAG- 401
Moraxella         PIRDEYLIVQGGGLAGVGAHSYSKGNATGGSEEAAKYEKLDA 402
Paracoccus        PIRDEYLIVQGGSLAGVGAHSYSKGNATGGSEEAAKFKKA-- 400
                  ***** ** * *****:*****:*****:*****:*****:*****:*****

```

Figure 2.1 Deduced amino acid sequence alignment of FDHs. Source of FDHs are *Mycobacterium vaccae* N10, *Pseudomonas* sp. 101, *Ancylobacter aquaticus*, *Thiobacillus* sp. KNK65MA, *Moraxella* sp. and *Paracoccus* sp. 12-A. Arrows indicate position of primers. Conserved residues, determined by the ClustalW algorithm, are shown as identical (*), conserved substitution (:), and semi-conserved substitution (.)

2.9.2 Determination of the partial FDH sequence

The conserve primers were used for amplification of FDH gene. The PCR products of the expected FDH gene from every strain were directly sequenced using either the M13 F or R primer by commercially First BASE Laboratories Sdn Bhd, Malaysia. In addition, some PCR products of expected partial FDH gene were ligated into pTZ57R/T. The ligated products were purified and introduced into *E. coli* DH12S by electroporation. The plasmid containing expected partial FDH fragment was extracted and sequenced. Then the obtained nucleotide sequences were used for design inverse PCR primers.

2.9.3 Inverse PCR amplification of the FDH gene

To determine the FDH flanking region from the 5 BCC strains, the chromosomal DNA of them were digested by the restriction enzymes (*Xho*I, *Pvu*II, *Hind*III, *Bam*HI, *Bgl*III and *Sma*I) for overnight at 37 °C. The digested products were purified using the QIAquick gel extraction kit as described in section 2.6.4 of part I and re-ligated with T4 DNA ligase at 16 °C for overnight. Then, the ligated products were purified with the QIAquick gel extraction kit and used as templates.

The inverse PCR (Figure 2.2) was done using the primers shown in Table 2.1. The inverse PCR reaction composed of 1X High Fidelity PCR buffer, 1.5 mM MgCl₂, 0.2 mM dNTP, 0.5 µM each forward and reverse primer, 1 U High Fidelity PCR enzyme mix (Fermentas, Lithuania) and 5 µl of ligated product. The PCR cycle was prenaturation at 95 °C for 3 min, 35 cycles of 95 °C for 40 sec, 56 °C for 45 sec, and 68 °C for 8 min then followed by 72 °C for 10 min. The inverse PCR product was separated by electrophoresis on 1% agarose gel. Each band of inverse PCR product was cut and purified by the QIAquick gel extraction kit as described above.

2.9.4 DNA sequencing and analysis

The PCR products from inverse PCR were directly sequenced using each inverse PCR primer. The nucleotide sequences were analysed by BLASTn (<http://blast.ncbi.nlm.nih.gov/Blast.cgi>) and checked for potential open reading frames (ORF) using ORF finder (<http://www.ncbi.nlm.nih.gov/gorf/gorf.html>).

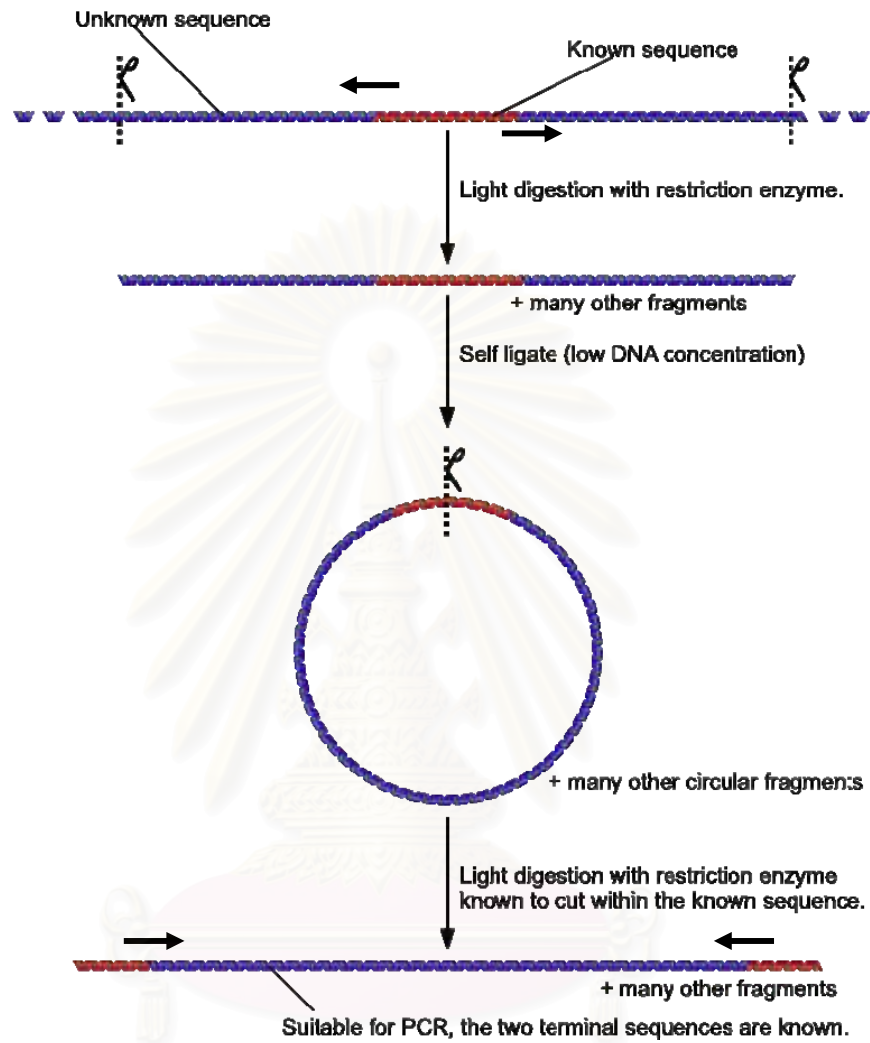


Figure 2.2 Diagram of inverse PCR

สถาบันวิทยบริการ
จุฬาลงกรณ์มหาวิทยาลัย

2.9.5 PCR amplification of the complete FDH gene

The entire FDH coding region from the different species were amplified by PCR in a total volume 25 μ l consisting of 40 mM 5X PhusionTM HF Buffer, 0.5 μ M of each FDH-F and FDH-R primers (Table 2.1), 0.2 mM dNTPs, 0.5 U of Phusion High-Fidelity DNA polymerase (NEB, USA) and 0.7 μ g of chromosomal DNA template. The PCR thermal profile consisted of an initial denaturation at 98 °C for 30 sec, 30 cycles of 98 °C for 10 sec, 60 °C for 20 sec and 72 °C for 30 sec, followed by a final extension at 72 °C for 7 min. Then, the PCR products were cloned into vector pET-17b in the further experiment.

2.10 Phylogenetic analysis

The amino acid sequences of NADP⁺-FDHs of BCC in this study, as well as NAD⁺-FDHs reference sequences obtained from the GenBank database were aligned, and neighbor-joining tree was constructed in MEGA4 (Tamura, *et al.*, 2007) using the PAM matrices model (Dayhoff, *et al.*, 1968).

2.11 Accession numbers

The complete nucleotide sequence of the FDH genes were deposited in the GenBank databases under accession numbers EU825920-EU825924 inclusively, which corresponds to *B. cepacia* 15507, *B. multivorans* 12938, *B. cenocepacia* 11197, *B. stabilis* 15516 and *B. pyrrocinia* 15515, respectively.

2.12 Cloning of the FDH genes in different BCC isolates into pET-17b

The PCR products of each complete FDH gene was digested with *Nde*I–*Bam*HI and then inserted into *Nde*I–*Bam*HI sites of pET-17b to construct BceFDH, BmuFDH, BcnFDH, BstFDH and BpyFDH for *B. cepacia* 15507, *B. multivorans* 12938, *B. cenocepacia* 11197, *B. stabilis* 15516 and *B. pyrrocinia* 15515, respectively as shown in Figure 2.3. The ligation products were transformed into *E. coli* DH12S by electroporation. The transformed cells were grown on LB agar plate containing 100 μ g/ml ampicillin at 37 °C for 16 hr. Cells containing the recombinant plasmids, which had FDH gene, were screened by colony PCR and checked by agarose gel

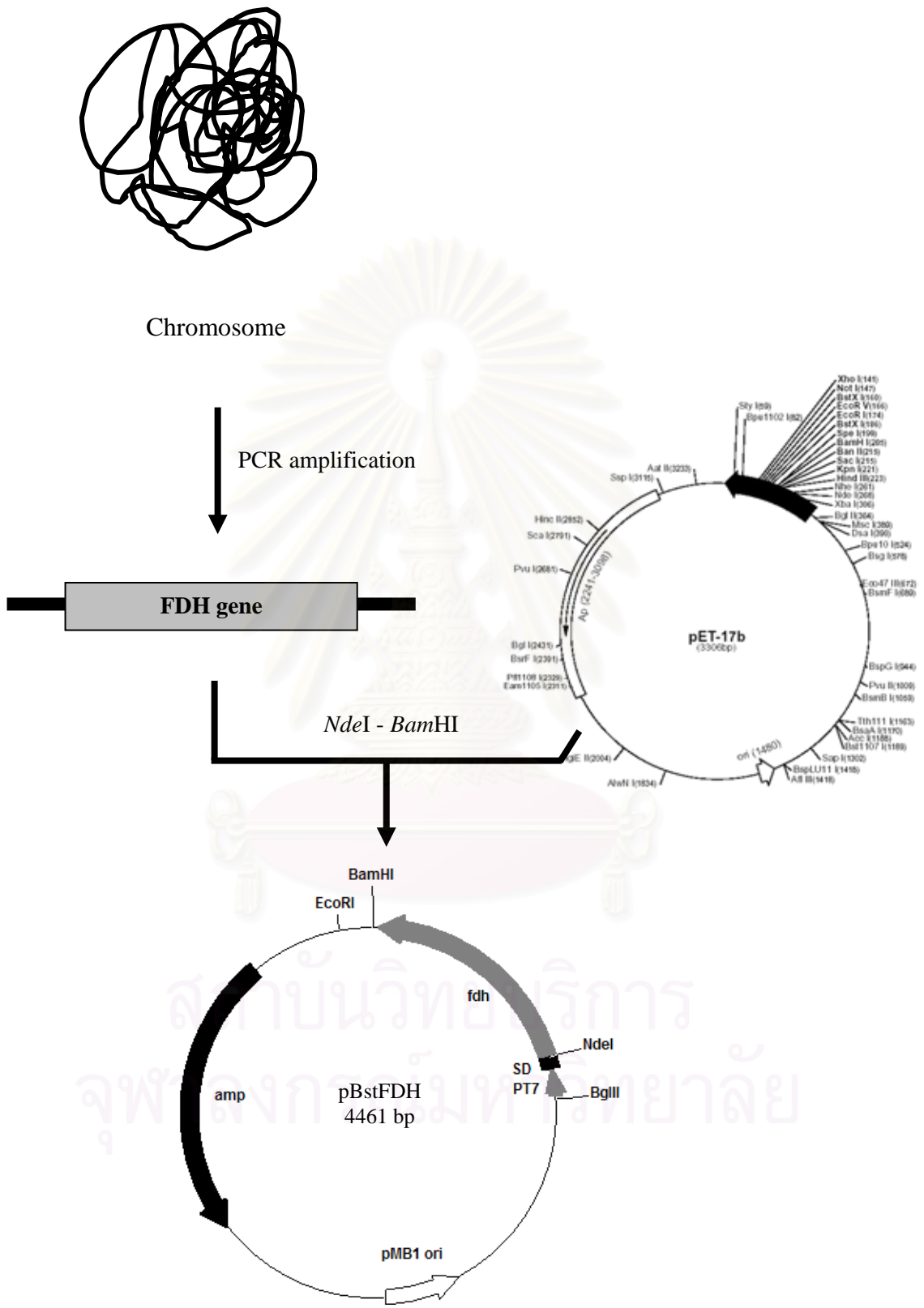


Figure 2.3 Construction of the representative BstFDH.

electrophoresis. After transformation into *E. coli* BL21 (DE3), the inserted FDH genes were confirmed by DNA sequencing. The transformed cells were grown on LB agar plates containing 100 µg/ml ampicillin at 37 °C for 16 hr. Then, crude extracts were prepared and assayed for the enzyme activity of FDH and protein determination.

2.13 Optimization of the recombinant FDH production by varying IPTG concentration and induction time

The *E. coli* BL21 (DE3) containing recombinant plasmid was grown in 5 ml of LB-medium supplemented with 100 µg/ml ampicillin at 37 °C overnight. After that, 1% of each cell culture was inoculated into 100 ml LB-medium containing 100 µg/ml ampicillin and shaken at 37 °C, 250 rpm. When the turbidity of the cultures at 600 nm had reached 0.6, IPTG at final concentration of 0, 0.01, 0.1, 0.2, 0.3, 0.4 mM was added to induce enzyme production. Aliquots 1 ml of cell cultures was harvested by centrifugation at various times for 0, 2, 4, 8, 16, 20 and 24 hr. Then, the cell pellets were resuspended in 100 µl of 5x sample buffer except 50 µl for 0 hr sample. The 7 µl of cell samples of crude extracts was run on 12.5% gel SDS-PAGE.

2.14 Polyacrylamide gel electrophoresis

2.14.1 SDS-polyacrylamide gel electrophoresis

The SDS-PAGE system was performed according to the method of Bollag, *et al.*, 1996. The slab gel system consisted of 0.1% SDS (W/V) in 10% separating gel and 5% stacking gel. Tris-glycine (25 mM Tris, 192 mM glycine and 0.1% SDS), pH 8.3 was used as electrode buffer. The gel preparation was described in Appendix E. The sample was mixed with 5x sample buffer (60 mM Tris-HCl pH 6.8, 25% glycerol, 2% SDS, 0.1% bromophenol blue and 14.4 mM β-mercaptoethanol) by ratio 5: 1 and boiled for 10 min before loading to the gel. The electrophoresis was run from cathode towards anode at constant current (20 mA) at room temperature. The molecular weight marker proteins were β-galactosidase (116,000 Da), bovine serum albumin (66,200 Da), ovalbumin (45,000 Da), lactate dehydrogenase (35,000 Da), restriction endonuclease Bsp98I (25,000 Da), β-lactoglobulin (18,400 Da) and lysozyme (14,400 Da). After electrophoresis, the gel was performed for protein staining.

2.14.2 Non-denaturing gel electrophoresis

Discontinuous PAGE was performed on the slab gel of a 7.7% separating gel and a 5% stacking gel. Tris-glycine buffer, pH 8.3 (25 mM Tris and 192 mM glycine) was used as electrode buffer. Preparation of solution and polyacrylamide gels was described in Appendix F. The enzyme was mixed with 5x sample buffer (312.5 mM Tris-HCl, pH 6.8, 50% glycerol and 0.05% bromophenol blue) by ratio 5: 1 and loaded onto the gel. The electrophoresis was run from cathode towards anode at constant current (20 mA). For activity staining, the experiment was done at 4°C. After electrophoresis, the gel was developed by protein and activity staining.

2.14.3 Protein staining

The gel was moved to a box containing coomassie staining solution (1% coomassie Blue R-250, 45% methanol, and 10% glacial acetic acid). The gel was agitated for 30 min on the shaker. The stain solution was poured out and the coomassie destaining solution (10% methanol and 10% glacial acetic acid) was added. The gel was gently destained for several times until gel background was clear.

2.14.4 Activity staining

After resolution of protein through 7.7% (w/v) native PAGE as described in section 2.15.2, the enzyme activity was assayed in 10 ml of 0.1 M ammonium formate, 5 mg/ml nitroblue tetrazolium, 0.5 mg/ml phenazine methosulfate and 0.5 M potassium phosphate buffer (pH 7.0) with 50 mM of either NAD⁺ or NADP⁺. The gel was gently shaken at room temperature for 5 min. After the brown band had appeared, the staining reaction was stopped by pouring off the staining solution and was then quickly rinsed several times with deionized water until gel background was clear.

2.15 Site-directed mutagenesis of FDH

To study of the FDH, site-directed mutagenesis was performed at the essential amino acid residues for coenzyme binding using megaprimer-based mutagenesis (Rajiv, *et al.*, 2004). The strategies require two rounds of PCR amplification using two flanking primers and one internal mutagenic primer in single tube PCR (Figure 2.4). The primer

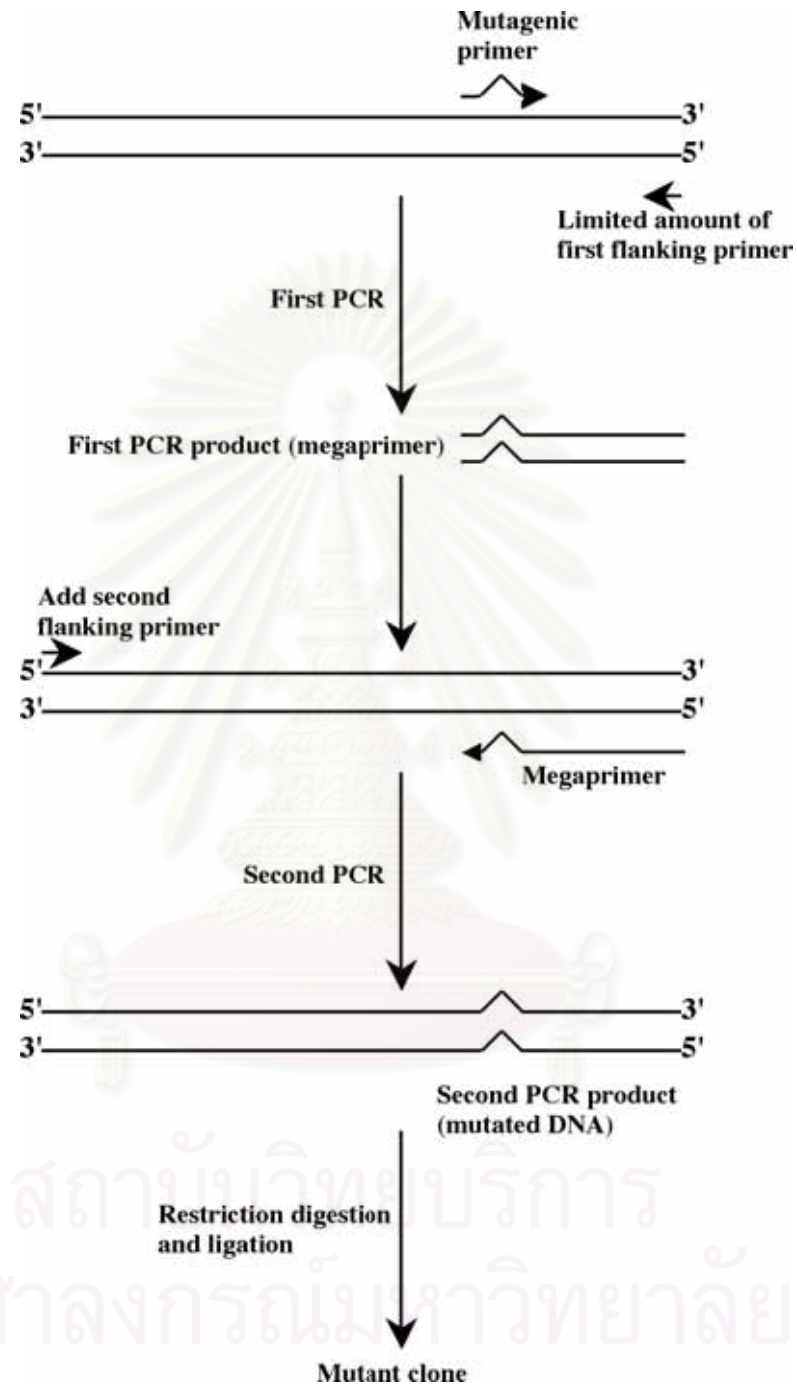


Figure 2.4 Megaprimer PCR mutagenesis strategy

used in this part is shown in Table 2.1. The PCR reaction in a total volume 50 μ l consisted of 40 mM 5X Phusion[™] HF Buffer, 0.2 mM dNTP, 1 pmole of mutagenic reverse primer, 0.05 pmole of forward flanking primer, 0.5 U of Phusion High-Fidelity DNA polymerase (NEB, USA) and 100 ng of DNA template. The PCR thermal profile consisted of an initial denaturation at 98 °C for 0.30 min followed by 5 cycles of 98 °C for 0.10 min, 56 °C for 0.20 min and 72 °C for 0.30 min, followed by a final extension at 72 °C for 35 min. Then for second round of PCR, the 1 pmole reverse flanking primer was added into the same tube and continuously run PCR followed by 25 cycles of 98 °C for 0.10 min, 60 °C for 0.20 min and 72 °C for 0.30 min, after followed by a final extension at 72 °C for 10 min. The PCR product was purified and cloned into pJET2.1 vector and transform to *E. coli* DH12S. The plasmid isolated from selected colonies was sequenced. Then the mutant fragment was digested with *Nde*I and *Bam*HI and cloned into pET-17b. Consequently, the mutant recombinant plasmid was transformed into *E. coli* BL21 (DE3) host cell. After that, the FDH activity and protein concentration were determined. Moreover, optimization of the FDH production and its cofactor preference were performed as described above.

2.16 Purification of formate dehydrogenase

2.16.1 Preparation of crude extract

The transformant pBstFDH 15516 was grown in 3 liter of LB medium, pH 7.2, containing 100 μ g/ml ampicillin, shaken at 37 °C, 250 rpm. When the turbidity of the cultures at 600 nm had reached 0.6, the cultivation was continued at 37 °C for 8 hr before cell harvesting without induction. The cell cultivation, crude extract preparation, assay for FDH activity and protein determination were performed as described above.

2.16.2 Enzyme purification procedures

The crude extract from section 2.16.1 was purified by the following steps. All operations were done at 4 °C. The working buffer used in all steps was 10 mM potassium phosphate buffer, pH 7.4 containing 0.1 mM PMSF and 1 mM EDTA.

2.16.2.1 DEAE-Toyopearl column chromatography

The activated DEAE-Toyopearl was prepared by washing with 0.5 N NaOH for 2-3 times, and rewashed by deionized water until the pH reached 8.0. The activated DEAE-Toyopearl was then resuspended in the working buffer, packed into 2.3 x 18.5 cm column and equilibrated with the same buffer for 5-10 column volume at flow rate 1 ml/min.

The crude enzyme solution from section 2.16.1 was applied to the DEAE-Toyopearl column. The unbound proteins were eluted from the column with the buffer until the absorbance at 280 nm was nearly zero. After that, the buffer was changed by making linear salt gradient of 0 to 0.5 M KCl in the working buffer in order to elute the bound proteins from the column. The 3 ml fractions were collected using a fraction collector. The protein profile was determined by measuring the absorbance at 280 nm. FDH activity was assayed using the method as described in the section 2.6.2. The fractions containing FDH activity was pooled and dialyzed against the buffer. The FDH activity and protein concentration of pooled fraction were measured as described above.

2.16.2.2 Butyl-Toyopearl column chromatography

Butyl-Toyopearl was washed with deionized water for 2-3 times, and then resuspended in the working buffer containing 25% saturated ammonium sulfate and packed into 2.3 x 18.5 cm column followed by equilibrating with the same buffer for 5-10 column volume at flow rate 1 ml/min.

The pooled active fraction from section 2.16.2.1 was slowly adjusted to 25% saturation with fine ammonium sulfate and stirred gently at least 30 min. Then, the protein solution was applied to the column at flow rate 1 ml/min. The unbound proteins were eluted from the column with the buffer containing 25% saturated ammonium sulfate until the absorbance at 280 nm was nearly zero. Stepwise elution of the bound protein was performed at 20%, 15%, 10%, 5% and 0% saturated ammonium sulfate in the same working buffer at the flow rate of 1 ml/min. Two milliliter fractions were collected by using fraction collector and assayed for both protein concentration and FDH activity. Protein profile was determined by measuring an absorbance at 280 nm. FDH activity was assayed by using the method as described above. The fractions

containing FDH activity were pooled and dialyzed against the working buffer. After desalting, the enzyme was concentrated with aquasorb. The FDH activity and protein concentration were determined.

2.17 Characterization of formate dehydrogenase

2.17.1 Coenzyme specificity of formate dehydrogenase

The purified FDH was used to study coenzyme specificity at final concentration of 10 mM NADP⁺ and NAD⁺. The result was expressed as a percentage of the relative activity.

2.17.2 Effect of pH on formate dehydrogenase activity

The effect of pH on the FDH activity was examined under the standard assay conditions at various pHs. The 200 mM buffer used were acetate buffer for pH 4.0 to 6.0, potassium phosphate buffer for pH 6.0 to 8.5, Tris-HCl buffer for pH 7.0 to 9.0 and glycine-KCl-KOH buffer for pH 8.5 to 12.5. The pH of each reaction mixture was measured with a pH meter at room temperature after the reaction. Then, the percentage of relative activity against the final pH of each reaction was plotted.

2.17.3 Effect of temperature on formate dehydrogenase activity

The effect of temperature on the FDH activity was determined under the standard assay condition at various temperatures from 30 °C to 80 °C. The percentage of relative activity was plotted against the temperature used for assay of the FDH activity.

2.17.4 Effect of pH on formate dehydrogenase stability

The purified FDH was used to study for pH stability. After the enzyme had been incubated at 30 °C for 20 min in each of the 10 mM buffer at various pHs, an aliquot of the enzyme solution was withdrawn for measured the remaining activity of enzyme under the standard assay condition. The 10 mM acetate buffer for pH 4.0 to 6.0, potassium phosphate buffer for pH 6.0 to 8.5, Tris-HCl buffer for pH 7.0 to 9.0 and glycine-KCl-KOH buffer for pH 8.5 to 12.5 were used. The percentage of FDH relative activity was plotted against the incubated pH.

2.17.5 Effect of temperature on formate dehydrogenase stability

After the purified FDH was incubated at various temperatures from 30 °C to 80 °C for 10 min to determine the effect of temperature on the stability of the FDH, the activity of FDH was assayed under the standard condition. Afterward, to study of the temperature and time that the enzyme still remained activity, the enzyme was incubated at the high temperature for 45 °C to 60 °C and collected at various time for enzyme activity assay under the standard condition. The percentage of relative activity was plotted against the temperature and time used.

2.18 Kinetic studies of formate dehydrogenase

A series of steady-state kinetic analysis were carried out in order to investigate the kinetic parameters as described below.

The initial velocity studies for the oxidation reaction were carried out under the standard reaction condition, except that various amounts of formate and NADP⁺ or NAD⁺ were used. When using formate and NADP⁺ as substrates, the concentrations of formate were 40, 60, 100 and 200 mM while those of NADP⁺ were 0.25, 0.5, 0.75, 1.0 and 1.5 mM. For formate and NAD⁺, the concentrations of NAD⁺ were 0.3, 0.5, 0.7, 0.8 and 1.0 mM where as those of formate were 20, 40, 60, 80 and 100 mM. The Lineweaver-Burke plots (double-reciprocal plots) of the initial velocities against formate concentrations at a series of fixed concentrations of NADP⁺ or NAD⁺ and the secondary plots of y intercepts against the reciprocal concentrations of NADP⁺ or NAD⁺ were made. K_m of formate and NADP⁺ or NAD⁺ was determined from these two plots, respectively.

CHAPTER III

RESULTS

3.1 Screening of formate dehydrogenase (FDH) in bacteria

Formate dehydrogenase producing bacteria were screened from 6 soil samples as described in section 2.7. After identification, they were *Burkholderia cepacia* (2 strains), *Burkholderia cenocepacia* (2 strains), *Burkholderia multivorans* (1 strain), *Acinetobacter lwoffii* (1 strain), *Alcaligenes faecalis* (1 strain), *Pseudomonas putida* (1 strain) and *Pseudomonas syringae* (1 strain). Comparison of FDH activity amongst these bacteria (0.4-10 mU/mg protein) revealed that *Burkholderia* and *Pseudomonas* possessed the high FDH activity. PCR amplification of partial FDH gene with primer IPCRF1-IPCRR1 and IPCRF2-IPCRR1 (section 2.9) followed by nucleotide sequencing of the PCR products showed that the expected partial FDH sequence of *P. putida* and *P. migulae* were 100% identity to that of *Pseudomonas* sp. 101 which was already reported (Tishkov, *et al.*, 1993) while the sequence from *Burkholderia* spp. revealed moderate difference to those from other FDH organisms in Genbank database. *Burkholderia cepacia* complex (BCC) is a group of gram-negative bacteria distributed in natural environments that are comprised of at least 10 genomovars or species (Mahenthiralingam, *et al.*, 2000 and Vandamme, *et al.*, 2002). Moreover, bacteria in this group have a diversity in genetic. Therefore, the *Burkholderia* spp. was chosen as target for novel FDH.

3.2 Distribution of FDH gene in *Burkholderia cepacia* complex (BCC)

Forty six strains of *Burkholderia cepacia* complex (BCC) used in this study comprised of 5 isolated bacteria from section 3.1 which were *Burkholderia cepacia* (2 strains), *Burkholderia cenocepacia* (2 strains), *Burkholderia multivorans* (1 strain) and 41 strains from culture collection which were *B. cepacia* (8 strains), *B. multivorans* (7 strains), *B. cenocepacia* (11 strains), *B. stabilis* (3 strains), *B. vietnamiensis* (4 strains), *B. dolosa* (2), *B. ambifaria* (2 strains), *B. anthina* (1 strains), *B. pyrrocinia* (2 strains) and *B. ubonensis* (6 strains) as shown in Table 3.1.

For the distribution of FDH gene in BCC, primers were designed at the conserved sequence of the well known NAD⁺-dependent FDHs. The result in Figure 3.1 showed the

Table 3.1 The presence of the FDH gene in BCC

Former genomovar designation	Bacteria	Source of isolation (no. of strains = 46)	Presence of FDH gene
I	<i>B. cepacia</i>	Environment (3)	+(2), -(1)
		Human (5)	+(4), -(1)
II	<i>B. multivorans</i>	Environment (2)	+(1), -(1)
		Human (5)	+(2), -(3)
III	<i>B. cenocepacia</i>	Environment (2)	+(1), -(1)
		Human (9)	+(8), -(1)
IV	<i>B. stabilis</i>	Human (3)	+(3)
V	<i>B. vietnamiensis</i>	Environment (1)	-(1)
		Human (3)	-(3)
VI	<i>B. dolosa</i>	Human (2)	-(2)
VII	<i>B. ambifaria</i>	Environment (2)	-(2)
VIII	<i>B. anthina</i>	Human (1)	-(1)
IX	<i>B. pyrrocinia</i>	Environment (2)	+(1), -(1)
X	<i>B. ubonensis</i>	Environment (6)	-(6)

Presence (+) or absence (-) of FDH amplicons following PCR with the 4 N-C primer sets for the indicated number of isolates in parenthesis.

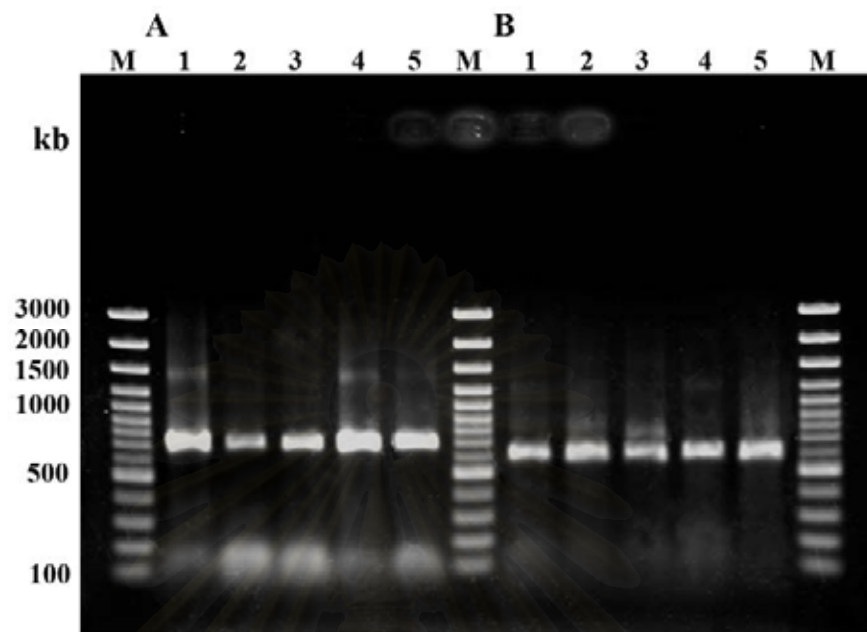


Figure 3.1 PCR amplification of the partial FDH gene

A. N1-C1 primer

Lane M = 100 bp DNA ladder

Lane 1 = *B. cenocepacia* 11197

Lane 2 = *B. multivorans* 12938

Lane 3 = *B. cepacia* 15507

Lane 4 = *B. pyrrocinia* 15515

Lane 5 = *B. stabilis* 15516

B. N2-C1 primer

Lane M = 100 bp DNA ladder

Lane 1 = *B. cenocepacia* 11197

Lane 2 = *B. multivorans* 12938

Lane 3 = *B. cepacia* 15507

Lane 4 = *B. pyrrocinia* 15515

Lane 5 = *B. stabilis* 15516

a representative of BCC that obtained a 700 bp PCR product when using primer N1-C1 and a 600 bp when using primer N2-C1. Sequencing of these partial fragments and subsequent BLASTn searches of the GenBank database confirmed the likely identity of the overlapping amplicon fragment as from FDH genes, rather than misamplifications or degenerate pseudogene amplifications, and thus the actual presence of the FDH gene in all cases. As summarized in Table 3.1, 22 out of the 46 tested BCC strains derived from 10 species were found to be positive for the FDH gene by PCR amplification with the 4 N-C primer sets. These were comprised of 5 species of BCC, that is; *B. cepacia* (6 positive strains from 8 tested strains), *B. multivorans* (3 positive strains from 7 tested strains), *B. cenocepacia* (9 positive strains from 11 tested strains), *B. stabilis* (3 positive strains from 3 tested strains) and *B. pyrrocinia* (1 positive strain from 2 tested strains). On the other hand, all tested strains of the species *B. vietnamiensis* (4 strains), *B. dolosa* (2 strains), *B. ambifaria* (2 strains), *B. anthina* (1 strain) and *B. ubonensis* (6 strains) were PCR negative for the FDH gene.

3.3 Determination of flanking region surrounding the FDH gene

Since the result in section 3.2 suggested that only 5 of the 10 species of BCC, those from *B. cepacia*, *B. multivorans*, *B. cenocepacia*, *B. stabilis* and *B. pyrrocinia*, contained partial gene fragment of FDH gene(s). Determination of the 5' and 3' ends of each FDH gene was performed for one representative strain from each of the five species by inverse PCR.

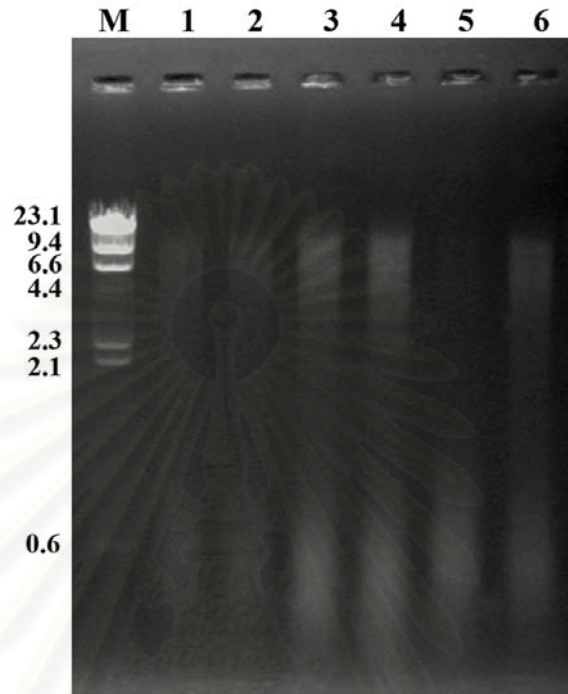


Figure 3.2 Chromosomal DNA digestion of a representative of BCC (*B. stabilis* 15516) Lane M = λ -HindIII DNA marker, lane 1 = HindIII, lane 2 = XhoI, lane 3 = PvuII, lane 4 = SmaI, lane 5 = BglII, and lane 6 = BamHI.

สถาบันวิทยบริการ
จุฬาลงกรณ์มหาวิทยาลัย

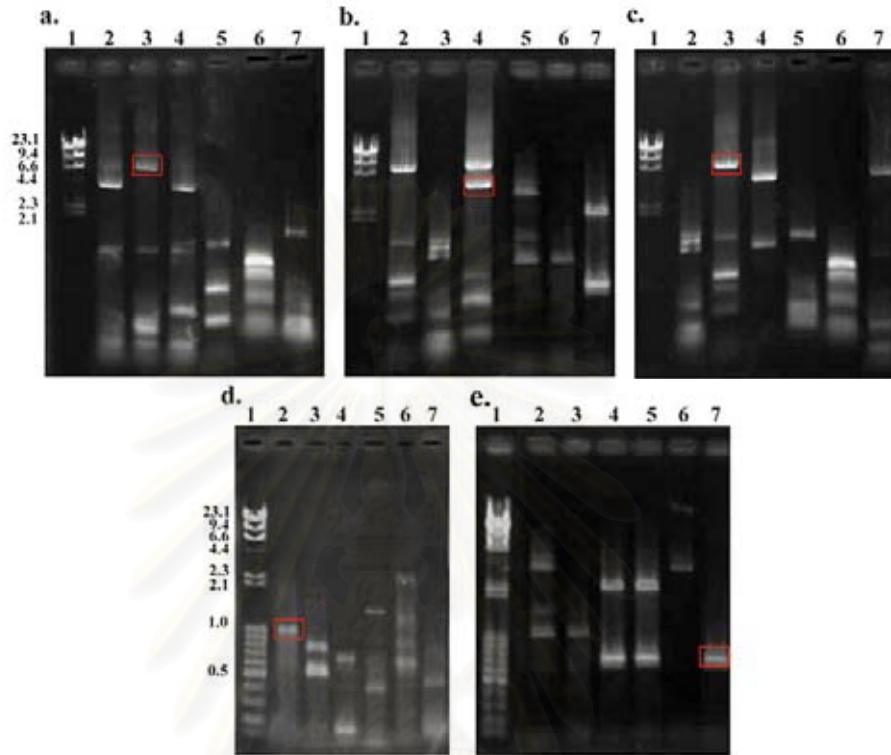


Figure 3.3 The inverse PCR products of 5 BCC species: *B. cepacia* 15507 (a), *B. multivorans* 12938 (b), *B. cenocepacia* 11197 (c), *B. stabilis* 15516 (d), and *B. pyrrocinia* 15515 (e). Lane 1 = λ -*Hind*III DNA marker and 100 bp DNA ladder; lane 2-6 = Inverse PCR product when chromosomal DNA were digested by *Hind*III, *Xho*I, *Pvu*II, *Sma*I, *Bgl*III and *Bam*HI, respectively. Red boxes indicate the specific inverse PCR products.

flanking sequence (~1 kb and ~700 bp, respectively) were obtained from the chromosomal DNA digested with *Hind*III and *Bam*HI (Figure 3.3d and 3.3e). The complete nucleotide sequence and deduce amino acid sequence of the entire FDH of the 5 BCC were shown in Figure 3.4 and 3.5, respectively.

3.4 Cloning of FDH genes

The whole FDH gene of these five representative strains were amplified with the subsequently designed primers FDH-F and FDH-R, and then directionally cloned into pET-17b at *Nde*I and *Bam*HI site. The recombinant plasmids so obtain were designated as pBceFDH, pBmuFDH, pBcnFDH, pBstFDH and pBpyFDH for *B. cepacia* 15507, *B. multivorans* 12938, *B. cenocepacia* 11197, *B. stabilis* 15516 and *B. pyrrocinia* 15515, respectively. After transformation into *E. coli* BL21 (DE3), the inserted FDH genes were confirmed by agarose gel electrophoresis (Figure 3.6) and DNA sequencing. The complete nucleotide sequences were 1,161 bp in length encoding a predicted 386 amino acids as shown in Figure 3.5.

3.5 Analysis of the nucleotide sequences

BLASTn analysis showed 88-93% similarity in the coding sequence of the FDH gene amongst 5 BCC. The sequence of FDH gene from *B. cenocepacia* 11197, a representative of 5 species, showed high similarity in BLASTn analysis with 98% to *B. cenocepacia* AU1054 (CP000378), 98% to *B. cenocepacia* HI2424 (CP000460), 97% to *B. cenocepacia* MCO-3 (CP000960), 93% to *Burkholderia* sp. 383 (CP000150), 88% to *B. multivorans* ACTT17616 (CP000870) and 73% to *B. ambifaria* MC40-6 (CP001026) (Table 3.2). In contrast, no similarity was found with the reported complete genome sequence of *B. cenocepacia* J2315 (NC_011000-011002), *B. ambifaria* AMMD (CP000440-000442), *B. vietnamiensis* G4 (NC_009254-009256) and *B. dolosa* AUO158 (CH482382).

The BLASTn analysis of the 5' and 3' flanking sequences of the FDH genes, from *B. cepacia* 15507, *B. multivorans* 12938 and *B. cenocepacia* 11197, showed a similar gene organization. Partial sequences of FAD-dependent pyridine nucleotide-disulphide oxidoreductase and GntR family transcriptional regulator were located 5' and

	FDH-F →	
B_cenocepacia	ATGGCTACCGTCCTGTGCGTGTCTACCCCGATCCCGTCGACGGCTATCCGCCGCGCTAC	60
B_cepacia	ATGGCCACCGTCCTGTGCGTGTCTACCCCGATCCCGTCGACGGCTATCCGCCGCGCTAC	60
B_pyrrrocinia	ATGGCGACCGTCCTGTGCGTGTCTACCCCGATCCCGTCGACGGCTATCCGCCGCGCTAC	60
B_stabilis	ATGGCGACCGTCCTGTGCGTGTCTACCCCGATCCCGTCGACGGCTATCCGCCGCGCTAC	60
B_multivorans	ATGGCCACCGTCCTGTGCGTGTCTACCCCGACCCCGTCGACGGCTATCCGCCGCGCTAC	60

B_cenocepacia	GTGCGCGACACGATTCCGGTCATCAGCCTACGCGGACGGTCAAACCGCGCCGACGCGG	120
B_cepacia	GTGCGCGACGCGATTCCGGTCATCAGCCTACGCGGACGGGCAAACCGCGCCGACGCGG	120
B_pyrrrocinia	GTGCGCGACGCGATTCCGGTCATCAGCAATACGCCGACGGACAAACCGCGCCGACGCGG	120
B_stabilis	GTGCGCGACACGATTCCGGTCATCAGCCTACGCGGACGGACAAACCGCGCCGACGCGG	120
B_multivorans	GTGCGCGACACGATTCCCGTCATCAGCCTACGCGGACGGCCAGCTCGCGCCGACGCGG	120

B_cenocepacia	GCCGGCCCGCCTGGCTTCCGGCCCGGGCGAACTCGTCGGCTCGGTGTCCGGCCGCTCGGC	180
B_cepacia	GCCGGCCCGCCCGGCTTCCGGCCCGGGCGAACTCGTCGGCTCGGTGTCCGGCCGCTCGGC	180
B_pyrrrocinia	GCCGGCCCGCCTCGGCTTCCGGCCCGGGCGAACTCGTCGGCTCGGTGTCCGGCCGCTCGGC	180
B_stabilis	GCCGGCCCGCCCGGTTTCCGGCCCGGGCGAACTCGTCGGCTCGGTGTCCGGCCGCTCGGC	180
B_multivorans	TCCGGCCCGCCCGGTTTCCGGCCCGGGCGAACTCGTCGGCTCGGTATCCGGCCGCTCGGC	180
	**** *	
B_cenocepacia	TTGCGCGGCTATATGGAGGCGCACGGCCATACGCTGATCGTACAGGACGACAAGGACGGC	240
B_cepacia	TTGCGCGGCTATCTGGAGGCGCACGGCCACACGCTGATCGTACAGGACGACAAGGACGGC	240
B_pyrrrocinia	TTGCGCGGCTATCTGGAGGCGCACGGTACACGCTGATCGTGACGAGCGACAAGGACGGC	240
B_stabilis	CTGCGCGGCTACCTGGAAGCGCACGGTACACGCTGATCGTGACGAGTGACAAGGACGGC	240
B_multivorans	TTGCGCGACTATCTGGCGGCGCACGGTACATACGCTGATCGTGACGAGCGACAAGGACGGC	240

B_cenocepacia	CCCGATTCCGAATTCGAGCGCCGGCTGCCCGAAGCGGACGTTGGTATTCGCGAGCCGTTT	300
B_cepacia	CCCGATTCCGAATTCGAGCGCCGGCTGCCCGAAGCGGACGTTGGTATTCGCGAGCCGTTT	300
B_pyrrrocinia	CCCGACTCCGAGTTCGAGCGCCGGCTGCCCGACGCGGACGTTGGTATTCGCGAGCCGTTT	300
B_stabilis	CCCGATTCCGAATTCGAACGCCGGCTGCCCGACGCGGACGTTGGTATTCGCGAGCCGTTT	300
B_multivorans	CCCGACTCCGAATTCGAGCGCCGGCTGCCCGAAGCGGACGTTGGTATTCGCGAGCCGTTT	300

B_cenocepacia	TGGCCCGGTACCTGAGCGCGGAACGCATCGCCCGCGCGCGAAGCTCAAGCTCGCGCTG	360
B_cepacia	TGGCCCGGTACCTGAGCGCGGAACGCATTGCCCGCGCGCGCGAAGCTGAAGCTCGCGCTG	360
B_pyrrrocinia	TGGCCCGGTACCTGAGCGCGGAACGGATCGCCCGCGCGCGCGAAGCTGAAGCTCGCGCTG	360
B_stabilis	TGGCCCGGTACCTGACCGCGGAACGGATCGCCCGCGCGCGCGAAGCTCAGGCTCGCGCTG	360
B_multivorans	TGGCCCGGTATCTGACCGCGGAGGGGATCGCGCGCGCGCGCGAAGCTCGCGCTG	360

B_cenocepacia	ACGGCCGGCATCGGCTCCGATCAGCTCGATCTGGACGCCCGCGCACGCGCGCATACAG	420
B_cepacia	ACGGCTGGCATCGGCTCCGATCAGCTCGATCTCGACGCCCGCGCGCGCGCATGTCACC	420
B_pyrrrocinia	ACGGCCGGCATCGGCTCCGATCAGCTCGATCTCGACGCCCGCGCGCGCGCATACAG	420
B_stabilis	ACGGCCGGCATCGGCTCCGATCATGTCATCTCGACGCCCGCGCGCGCGCATACAG	420
B_multivorans	ACTGCGGGCATCGGCTCCGATCAGCTCGATCTCGCGCGCGCGCGCGCGCGCGCATACAG	420

B_cenocepacia	GTTGCCGAAGTACCCGGCTCGAACAGCATCAGCGTGGCCGAGCAGTGGTGGTATGACGAGC	480
B_cepacia	GTCGCCGAAGTACCCGGCTCGAACAGCATCAGCGTGGCCGAGCAGTGGTGGTATGACGAGC	480
B_pyrrrocinia	GTCGCCGAAGTACCCGGCTCGAACAGCATCAGCGTGGCCGAGCAGTGGTGGTATGACGAGC	480
B_stabilis	GTCGCCGAAGTACCCGGCTCGAACAGCATCAGCGTGGCCGAGCAGTGGTGGTATGACGAGC	480
B_multivorans	GTCGCCGAAGTACCCGGATCGAACAGCGTACGCGTGGCCGAGCAGTGGTGGTATGACGAGC	480

B_cenocepacia	CTCGCGCTGGTGGCGCAACTACCTGCCGTCGCATGCGGTGCGCGCAGAGGGCGGCTGGAAC	540
B_cepacia	CTCGCGCTGGTGGCGCAACTACCTGCCGTCGCATGCGGTGCGCGCAGCAAGGGCGGCTGGAAC	540
B_pyrrrocinia	CTCGCGCTGGTGGCGCAACTACCTGCCGTCGCATGCGGTGCGCGCAGCAAGGGCGGCTGGAAC	540
B_stabilis	CTCGCGCTGGTGGCGCAACTACCTGCCGTCGCATGCGGTGCGCGCAGCAAGGGCGGCTGGAAC	540
B_multivorans	CTTGGCTCGTGGCGCAACTATCTGCCGTCGCACGCGATGCGCGCAGCAAGGGCGGCTGGAAC	540

B_cenocepacia	ATCGCCGACTGCGTGTGCGCGAGCTACGACGTCGAAGGAATGCATTTCCGCACGGTCCGC	600
B_cepacia	ATCGCGGATTGCGTGTGCGCGAGCTACGACGTCGAGGGCATGCATTTCCGCACGGTCCGC	600
B_pyrrrocinia	ATCGCCGATTGCGTGTGCGCGAGCTACGACGTCGAAGGCATGCATTTCCGCACGGTCCGC	600
B_stabilis	ATCGCCGATTGCGTGTGCGCGAGCTACGACGTCGAAGGGATGCATTTCCGCACGGTCCGC	600
B_multivorans	ATCGCCGACTGCGTATCGCGAGCTACGACATCGAGGGCATGCATTTCCGCACGGTCCGC	600

(continued)

Figure 3.4 Alignment of the coding nucleotide sequence of FDH gene from five BCC

The arrows indicate position of primer for full FDH amplification.

B_cenocepacia	GCGGGGCGCATCGGCCTCGCGGTGCTGCGCCGGCTGCAACCGTTTCGGCCTGCATCTGCAC	660
B_cepacia	GCGGGGCGCATCGGGCTCGCCGTGCTGCGGGCGGCTGAAGCCGTTTCGGCCTGCAGCTGCAC	660
B_pyrocinia	GCGGGGCGCATCGGCCTCGCGGTGCTGCGCCGGCTGAAGCCGTTTCGGCCTGCATCTGCAC	660
B_stabilis	GCGGGGCGCATCGGTCTCGCGGTGTTGCGCCGGCTGAAGTCGTTTCGGCCTGCACCTGCAC	660
B_multivorans	GCCGGCCGCATCGGGCTCGCGGTGCTGCGGGCGGCTGAAGCCGTTTCGGGCTGGCGCTGCAC	660
	*** ** ***** ** ** ** **	
B_cenocepacia	TACACGCAGCGCCACCGGCTGGATGCATCGATCGAGCAGGCGCTCGCGCTCACGTATCAC	720
B_cepacia	TACACGCAGCGCCACCGGCTCGAGCGGTCGGTCGAGCAGGAACTCGCGCTCACGTATCAC	720
B_pyrocinia	TACACGCAGCGCCACCGGCTCGAGCGCCCGATCGAGAAGGAACTCGCGCTCACGTATCAC	720
B_stabilis	TACACGCAGCGCCACCGGCTCGAGCGCCGATCGAGCAGGAACTCGGGCTCACGTATCAC	720
B_multivorans	TATACGCAGCGGCATCGGCTCGATCCGGCGATCGAACCGAACTCGCGCTGACCTATCAC	720
	*** ** ***** ** ** **	
B_cenocepacia	GCCGACGTGGCGTCGCTCGCGAGCGCGGTCGATATCGTCAACCTGCAGATTCGGCTGTAC	780
B_cepacia	GCCGATGCCGCGTCGCTCGCGAGCGCGTCGACATCGTCAACCTGCAGATCCCGCTTAC	780
B_pyrocinia	GCCGATGCCGCGTCGCTCGCAGGTGCCGTCGATATCGTGAACCTGCAGATTCGGCTGTAC	780
B_stabilis	GCCGATCCCGCGTCGCTCGCCGCGCGGTCGACATCGTCAACCTGCAGATCCCGCTGTAC	780
B_multivorans	GCGGACGTCCGCGTCGCTCGCGAGCGCGGTCGACATCGTGAATCGTGAATCGCGCTGTAT	780
	*** ** ***** ** ** **	
B_cenocepacia	CCGTCGACCCGAGCACCTGTTTCGACGCGGCGATGATCGCGCGAATGAAGCGCGGCGCGTAT	840
B_cepacia	CCGTCGACCGGAGCACCTGTTTCGACGCGGCGATGATCGCGCGCATGAAGCGCGGCGCGTAC	840
B_pyrocinia	CCGTCGACCCGAGCACCTGTTTCGACGCGGCGATGATCGCGCGGATGAAGCGCGGCGCATA	840
B_stabilis	CCGTCGACCCGAGCACCTGTTTCGACGCGGCGATGATCGCGCGGATGAAGCGCGGCGCGTAC	840
B_multivorans	CCGTCGACCCGAGCATCTGTTTCGATGCCGCAATGATCGCGCGCATGAAGCGCGGCGCGTAT	840
	***** ** ** **	
B_cenocepacia	CTGATCAACACCCGCGCGCGAAGCTGGTCGACCGCGACGCGGTCGTAATGCGCTCACG	900
B_cepacia	CTGATCAACACCCGCGCGCGAAGCTGGTCGACCGCGACGCGGTCGTAATGCCGTCACG	900
B_pyrocinia	CTGGTCAACACCCGCGCGTGCGAAGCTGGTCGACCGCGACGCGGTCGTCGTCGCCGTGACG	900
B_stabilis	CTGATCAACACCCGCGCGCGAAGCTGGTCGATCGCGATGCCGTCGTCGCGCGGTCACG	900
B_multivorans	CTGATCAACACCCGCGCGCGAAGCTGGTCGATCGCGATGCCGTCGTCGCGACGCGGTCGCG	900
	*** ***** ** ** **	
B_cenocepacia	TCCGGCCATCTCGCCGGCTATGGCGGCGACGTGTGGTTTCCGAGCCGGCGCGCCGGAT	960
B_cepacia	TCCGGGCATCTCGCGGGCTACGGCGGCGACGTGTGGTTTCCCGAGCCGGCGCGCCGGAT	960
B_pyrocinia	TCCGGGCATCTCGCGGGCTACGGCGGCGACGTGTGGTTTCCCGAGCCGGCGCGCCGGAT	960
B_stabilis	TCCGGCCATCTCGCCGGCTACGGCGGCGACGTGTGGTTTCCCGAGCCGGCGCGCCGGAT	960
B_multivorans	TCCGGCCATCTCGCCGGCTACGGCGGCGACGTGTGGTTTCCCGAGCCGGCGACCCGGCCGAT	960
	*** ** ***** ** ** **	
B_cenocepacia	CACCCGTGGCGCAGATGCCGTTCAACGGGATGACGCCGCACATCTCCGGCAGCTCGTTG	1020
B_cepacia	CACCCGTGGCGCGCGATGCCGTTCAACGGGATGACCCCGCACATCTCCGGCAGCTCGCTG	1020
B_pyrocinia	CATCCGTGGCGCAGATGCCGTTCAACGGGATGACGCCGCACATCTCCGGCAGCTCGCTG	1020
B_stabilis	CACCCGTGGCGCGCGATGCCGTTCAACGGGATGACGCCGCACATCTCCGGCAGCTCGCTG	1020
B_multivorans	CATCCGTGGCGCGCGATGCCGTTCAACGGGATGACGCCGCATATCTCCGGCAGCTCGCTG	1020
	*** ***** ** ** **	
B_cenocepacia	TCCGCGCAGGCGCGCTATGCGGCCGGCACGCTGGAGATCCTGCAATGCTGGTTTCGACGGC	1080
B_cepacia	TCCGCGCAGGCGCGCTATGCGGCCGGCACGCTGGAGATCCTGCAATGCTGGTTTCGACGGC	1080
B_pyrocinia	TCCGCTCAGGCGCGTTATGCGGCCGGCACGCTGGAAATCCTGCAATGCTGGTTTCGACGGC	1080
B_stabilis	TCCGCGCAGGCGCGCTATGCGGCCGGCACGCTGGAGATCCTGCAATGCTGGTTTCGACGGC	1080
B_multivorans	TCCGCGCAGGCGCGCTACGCGGCCGGTACGCTCGAAATCTGCAATGCTGGTTTCGACGGC	1080
	*** ** ***** ** ** **	
B_cenocepacia	AGGCCGATCCGCAACGAATACCTGATCGTCGACGGCGGACGCTCGCGGGCACCGGCGCG	1140
B_cepacia	AAGCCGATCCGCAACGAATACCTGATCGTCGACGGCGGACGCTCGCGGGACCGGCGCG	1140
B_pyrocinia	AAGCCGATCCGGAACGAATACCTGATCGTCGACGGCGGACGCTCGCGGGACCGGCTGCG	1140
B_stabilis	CGGCCGATCCGCAATGAATACCTGATCGTCGACGGCGGACGCTCGCGGGACCGGCGCG	1140
B_multivorans	CGGCCGATTCCGAGGCCATACCTGATCGTCGACGGCGGACGCTCGCGGGACCGGCGGAG	1140
	***** ** **	
B_cenocepacia	CAGTCGTACCGGCTGACATGA	1161
B_cepacia	CAGTCGTACCGGCTGACATGA	1161
B_pyrocinia	CAGTCGTACCGGCTGACATGA	1161
B_stabilis	CAGTCGTACCGGCTGACATGA	1161
B_multivorans	CAGTCGTACCGGCTGACATGA	1161
	***** ** **	

←

FDH-R

Figure 3.4 Alignment of the coding nucleotide sequence of FDH gene of five BCC

The arrows indicate position of primer for full FDH amplification.

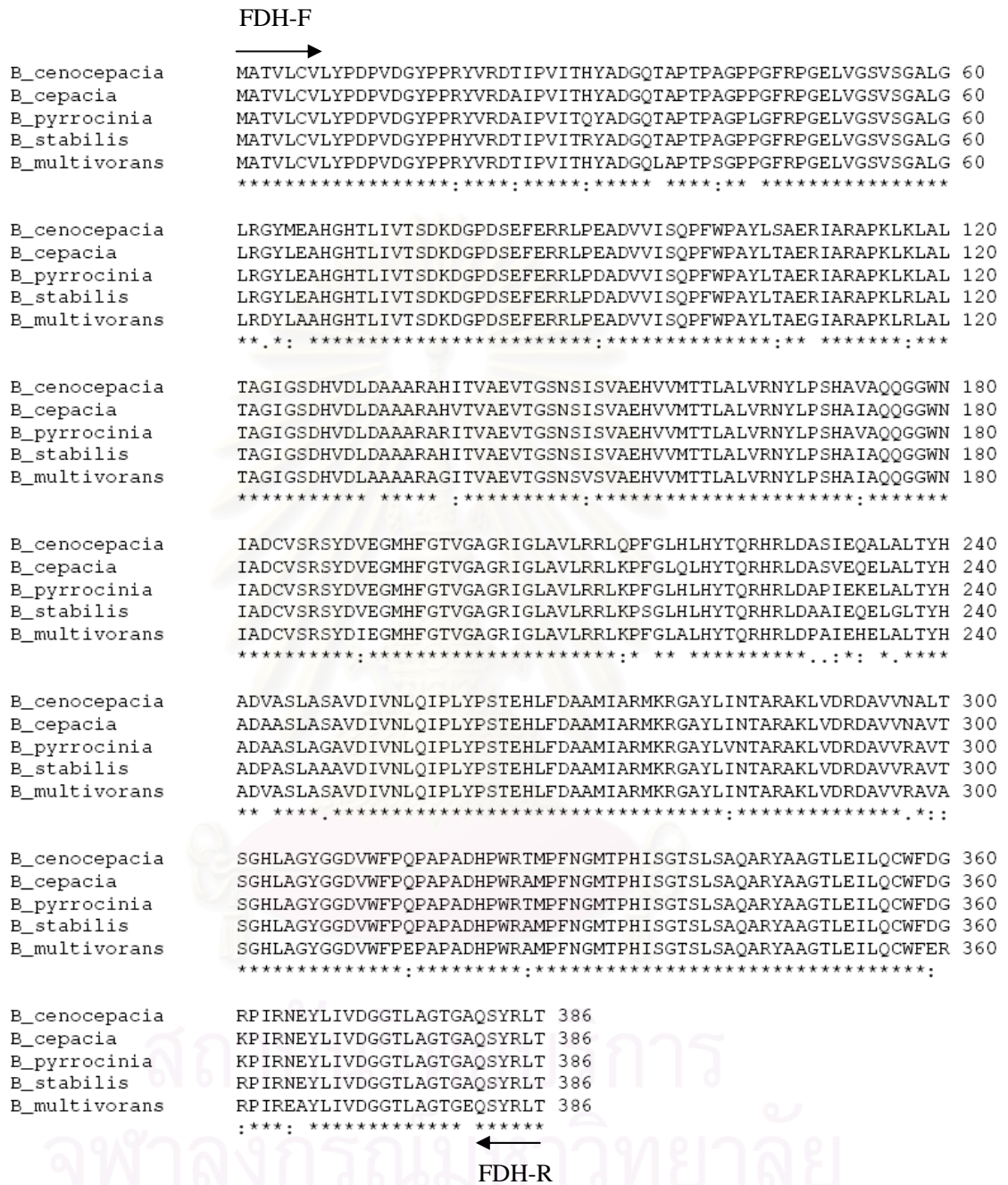


Figure 3.5 Amino acid sequence alignment of 5 FDHs from BCC The arrows indicate position of primer for full FDH.

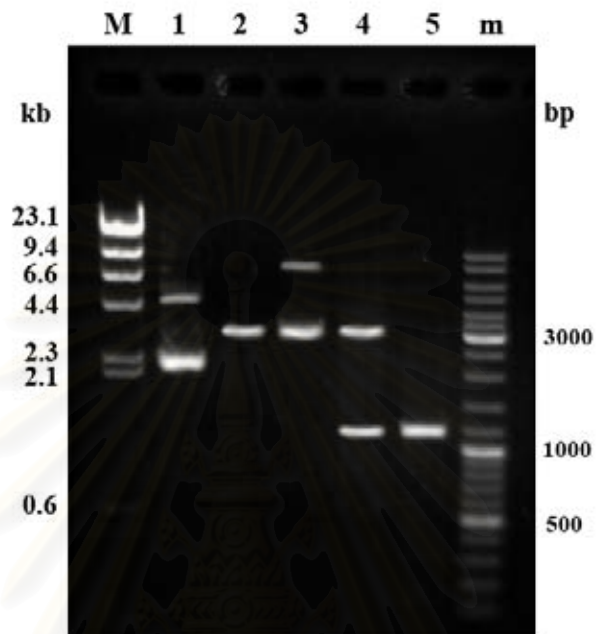


Figure 3.6 Restriction pattern of pBstFDH

Lane M = λ /*Hind*III standard DNA marker

Lane 1 = undigested pET-17b

Lane 2 = *Nde*I-*Bam*HI digested pET-17b

Lane 3 = undigested pBstFDH

Lane 4 = *Nde*I- *Bam*HI digested pBstFDH

Lane 5 = amplified product of FDH gene

Lane m = 100 bp DNA ladder

Table 3.2 The percentage of nucleotide sequence identities of FDH genes

Bacteria	BceFDH 15507	BmuFDH 12938	BcnFDH 11197	BstFDH 15516	BpyFDH 15515
BceFDH 15507	100	88	93	92	93
BmuFDH 12938	88	100	88	88	88
BcnFDH 11197	93	88	100	92	93
BstFDH 15516	92	88	92	100	93
BpyFDH 15515	93	88	93	93	100
<i>B. cenocepacia</i> HI2424	93	88	98	92	93
<i>B. cenocepacia</i> AU1054	93	88	98	92	93
<i>B. cenocepacia</i> MC03	93	88	97	92	92
<i>B.</i> 383	93	88	93	91	93
<i>B. multivorans</i> ATCC17616	88	99	88	88	88
<i>B. ambifaria</i> MC40-6	73	73	73	74	73
<i>Ancylobacter aquaticus</i>	69	67	71	69	70
<i>Hyphomicrobium</i>	67	66	66	67	67
<i>Moraxella</i>	68	67	69	68	69
<i>Mycobacterium vacce</i> N10	73	71	73	73	73
<i>Paracoccus</i> sp. 12A	71	70	72	72	72
<i>Thiobacillus</i>	72	69	72	71	72

สถาบันวิทยบริการ
จุฬาลงกรณ์มหาวิทยาลัย

3' of the FDH gene, respectively (Figure 3.7). However, the 5' and 3' flanking sequences from *B. stabilis* 15516 and *B. pyrrocinia* 15515 were incomplete and too short to be analyzed. Searching of the genomic organization and location of the FDH gene in the available genome sequences of *Burkholderia* sp. 383, *B. cenocepacia* AU1054, *B. cenocepacia* HI2424, *B. cenocepacia* MCO-3 and *B. multivorans* ATCC17616 revealed a similar pattern as our description above, supporting homologs by synteny as well as sequence similarity.

However, for the three species which obtained the complete 5' and 3' non-coding sequences, and thus could distinguish the flanking genes, in addition to the two species with only partial non-coding sequences, a putative promoter sequence did not find in the adjacent 5' non-coding region of the BCC-FDH gene using the BPROM program (<http://linux1.softberry.com/berry.phtml?topic=bprom&group=programs&subgroup=gfi> ndb).

3.6 Comparison of the deduced amino acid sequences from the five FDH genes

The deduced amino acid sequences of the FDH genes from *B. cepacia* 15507, *B. multivorans* 12938, *B. cenocepacia* 11197, *B. pyrrocinia* 15515 and *B. stabilis* 15516 were aligned against those from other known (annotated) bacterial NAD⁺-FDH sequences in the Genbank database using CLUSTALW2 (<http://www.ebi.ac.uk/Tools/clustalw2/index.html>) as shown in Figure 3.8. The sequence identity of the deduced amino acid sequences were ~91-96% identical amongst the five BCC species, and 65-70%, 40-43%, 44-45% by comparison to other bacterial NAD⁺-FDHs, fungi and plant, respectively (Table 3.3). Putative catalytically important amino acid residues of FDH (Figure 3.8 with highlight) were conserved in these FDH sequences of all five BCC strains, except that Q315 was replaced by E315 in *B. multivorans*. The dendrogram based upon the amino acid sequences of some reported FDH genes shows that amino acid sequences of FDH from the five BCC strains were distinct from the other bacterial NAD⁺-FDHs (Figure 3.9).



 **FAD-dependent pyridine nucleotide-disulphide oxidoreductase**

 **Transcriptional regulator, GntR family**

Figure 3.7 The flanking genes at upstream and downstream of the FDH genes

สถาบันวิทยบริการ
จุฬาลงกรณ์มหาวิทยาลัย

Table 3.3 The percentage of deduced amino acid sequence identities of FDHs

Bacteria	BceFDH 15507	BmuFDH 12938	BcnFDH 11197	BstFDH 15516	BpyFDH 15515
BceFDH 15507	100	93	96	96	96
BmuFDH 12938	93	100	92	93	91
BcnFDH 11197	96	92	100	95	95
BstFDH 15516	96	93	95	100	95
BpyFDH 15515	96	91	95	95	100
<i>B. cenocepacia</i> HI2424	96	92	99	95	95
<i>B. cenocepacia</i> AU1054	96	92	99	95	95
<i>B. cenocepacia</i> MC03	97	92	98	95	95
<i>B. 383</i>	97	91	96	95	95
<i>B. multivorans</i> ATCC17616	93	100	92	93	91
<i>B. ambifaria</i> MC40-6	75	73	74	75	76
<i>Ancylobacter aquaticus</i>	67	65	66	66	67
<i>Hyphomicrobium</i>	67	65	66	67	68
<i>Moraxella</i>	68	67	68	69	70
<i>Mycobacterium vacce</i> N10	69	67	69	69	70
<i>Paracoccus</i> sp. 12A	70	67	68	69	70
<i>Pseudomonas</i> sp.	69	67	69	69	70
<i>Thiobacillus</i>	67	66	67	68	68
<i>Candida boidinii</i>	41	40	41	41	42
<i>Aspergillus nidulans</i>	43	42	42	43	43
<i>Solanum tuberosum</i>	45	44	44	45	45

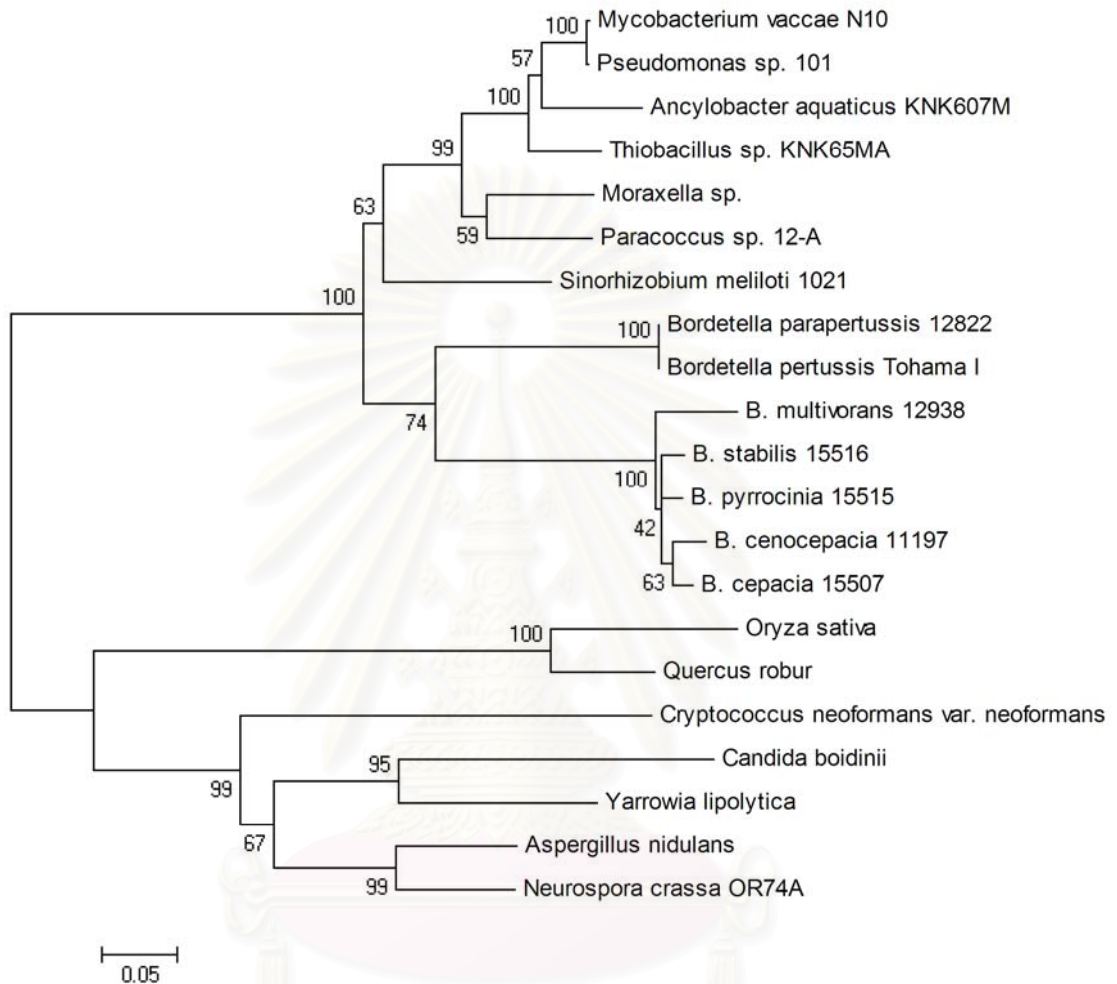


Figure 3.9 Neighbor-joining based dendrogram of FDH gene. Neighbor-joining tree was constructed in MEGA4 using the PAM matrices model. Bootstrap values and genetic distance scale are shown.

3.7 Optimization of FDH production by varying IPTG concentration and induction time

For IPTG concentration and induction time course study, the transformant clone of pBceFDH 15507, pBmuFDH 12938, pBcnFDH 11197, pBstFDH 15516 and pBpyFDH 15515 were grown and induced by IPTG at various final concentrations of 0, 0.01, 0.1, 0.2, 0.3 and 0.4 mM before cell was harvested at various times: 0, 2, 4, 8, 16, 20 and 24 hr. The protein patterns of cell *E. coli* BL21 (DE3) harboring pBstFDH 15516, the representative clone, indicated that when the cells were grown without induction by IPTG, the recombinant proteins were principally expressed. Contrastingly, no expression could be detected when the induction were performed at 0.01-0.4 mM final concentration of IPTG (after the culture OD₆₀₀ reach 0.6, and induced 1-24 hr) (Figure 3.10). The same result was observed when the other 4 recombinant clones were used.

3.8 Determination of recombinant FDH activity from BCC

The expression of recombinant FDH from five BCC strains was performed in *E. coli* BL21 (DE3) containing pBceFDH 15507, pBmuFDH 12938, pBcnFDH 11197, pBstFDH 15516 and pBpyFDH without induction by IPTG. Surprisingly, NADP⁺ can act as the coenzyme. The result indicated that BstFDH 15516, BpyFDH 15515 and BcnFDH 11197 showed activity toward NADP⁺ over NAD⁺. The specific activities of the crude recombinant enzymes were 0.4-1.8 U/mg of protein in the presence of NADP⁺ (Table 3.4). The BceFDH 15507 and BmuFDH 12938 showed very low level of FDH activity for NADP⁺. Moreover, the activity toward NAD⁺ could not be detected. Thus, BcnFDH 11197, BpyFDH 15515 and BstFDH 15516 which possessed the high recombinant FDH activity were selected for further study.

3.9 Coenzyme dependence of recombinant FDH

To support the potential of coenzyme preference on NADP⁺ over NAD⁺, recombinant FDH activity was examined by activity staining of native PAGE gel using NAD⁺ or NADP⁺. FDH from *Mycobacterium vaccae* N10, acted on NAD⁺ but not NADP⁺, was used as a control. Each *Burkholderia* recombinant enzyme showed a single activity band when they were stained in the complete reaction mixture containing NAD⁺

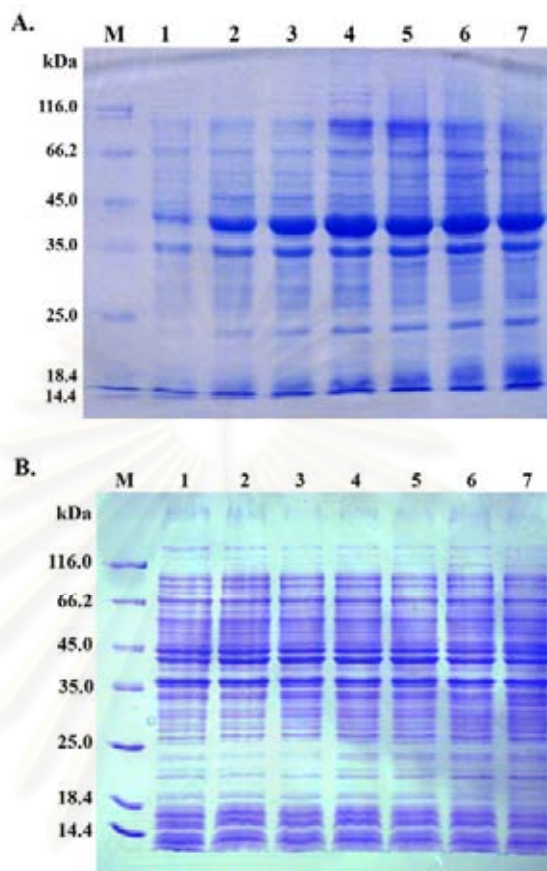


Figure 3.10 Protein pattern of *E. coli* BL21 (DE3) harboring pBstFDH clone at various induction times detected by SDS-PAGE

A: 0 mM IPTG

Lane M = protein marker

Lane 1-7 = cell of transformant at various induction times:
0, 2, 4, 8, 16, 20 and 24 hr, respectively.

B: 0.01 mM IPTG

Lane M = protein marker

Lane 1-7 = cell of transformant at various induction times:
0, 2, 4, 8, 16, 20 and 24 hr, respectively.

Table 3.4 FDH activity from crude extract of recombinant clones

clones	Cell wet weight (g)	Total activity (U) ^a		Total protein (mg)	Specific activity (U/mg protein)	
		NADP ⁺	NAD ⁺		NADP ⁺	NAD ⁺
pET-17b	0.97	-	-	45.6	-	-
pBceFDH 15507 ^b	1.00	1.4	-	52.2	0.03	-
pBmuFDH 12938 ^b	1.05	2.7	-	47.1	0.1	-
pBcnFDH 11197 ^b	1.03	52.9	2.1	47.8	1.1	0.04
pBpyFDH 15515	1.00	20.4	2.6	51.9	0.4	0.05
pBstFDH 15516	1.19	82.4	5.8	44.9	1.8	0.13
Mutant pBstFDH 15516	0.87	3.0	21.1	46.8	0.1	0.45

^aTotal activity from 200 ml culture.

^bScreen from soil isolated.

or NADP^+ , which coincided in position with the major band obtained from coomassie blue staining. NADP^+ gave a stronger band when compared to that of NAD^+ whilst the opposite data was obtained when NAD^+ -FDH from *Mycobacterium vaccae* N10 was used (Figure 3.11). No activity band was seen in the reaction mixture without coenzyme (NAD^+ or NADP^+ , structure in Appendix G), substrate (ammonium formate) or recombinant enzyme (data not shown). The data is thus consistent with the notion that the NADP^+ utilization is by recombinant FDH and not to other contaminating *E. coli* enzyme, and that, therefore, these BCC enzymes are NADP^+ -dependent FDH. Moreover, the recombinant enzymes were unlikely to require metal ions as cofactor since 200 mM of EDTA did not significantly affect the enzyme activities.

3.10 Site-directed mutagenesis of FDH

As described above, the FDH from recombinant clones of BCC showed the pattern of coenzyme preference to NADP^+ over than NAD^+ , moreover, Gln223, an amino acid residue at coenzyme binding site of NADP^+ -FDH is substituted by Asp in NAD^+ -FDH (Figure 3.8). Therefore, the model structures of BstFDH- NAD^+ complex and BstFDH- NADP^+ complex were constructed via the Automated Protein Modeling Server SWISS-MODEL (<http://www.expasy.org>). The structure of protein in databank coded 2NAD (*Pseudomonas* sp. 101 FDH) was used as a template for BstFDH- NAD^+ complex. Since, the 3D structure of NADP^+ -dependent FDH was not available in PDB database, the conformation of NADP^+ bound to glyoxylate reductase from *Pyrococcus horikoshii* OT3 (protein databank code 2dbq, a homologue enzyme of CboFDH) was used as a template for prediction of BstFDH- NADP^+ complex. The predicted interactions between NADP^+ and Gln as well as those of NAD^+ and Asp were shown in Figure 3.12. The negative charge of phosphate group of NADP^+ was blocked by the negative charge of Asp. This might allow NAD^+ -FDH to accept NAD^+ greater than NADP^+ . Contradictorily, uncharged Gln seemed to accept both NAD^+ and NADP^+ . To prove the important role of Gln223 in NADP^+ -FDH, the recombinant plasmid pBstFDH 15516 was selected to perform site-directed mutagenesis using megaprimer-based mutagenesis strategies. Gln223 residue at the conserved coenzyme binding sequence Gly(Ala)XGlyXXGlyX₁₇Gln of NADP^+ -FDH was substituted with Asp by changing CAG to GAC. Subsequently, coenzyme specificity of the mutant was determined.

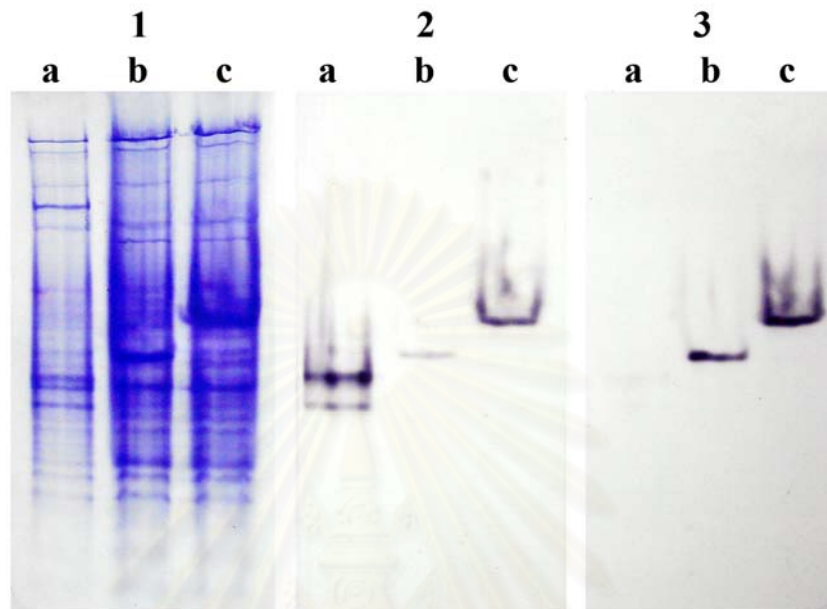
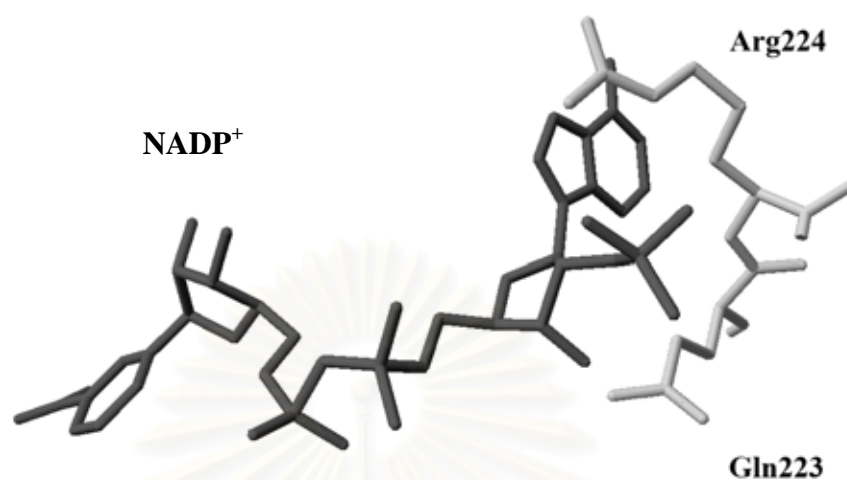


Figure 3.11 Coenzyme specificity of the crude recombinant FDH enzyme from *Mycobacterium vaccae* N10, BcnFDH 11197 and BstFDH 15516

The recombinant FDH enzyme was resolved through a native-PAGE and stained for FDH activity. 1 = coomassie blue stain, 2 = enzyme activity stain with NAD⁺ and 3 = enzyme activity stain with NADP⁺. The character above each lane (a, b, c) stands for *Mycobacterium vaccae* N10, BcnFDH 11197 and BstFDH 15516, respectively.

A



B

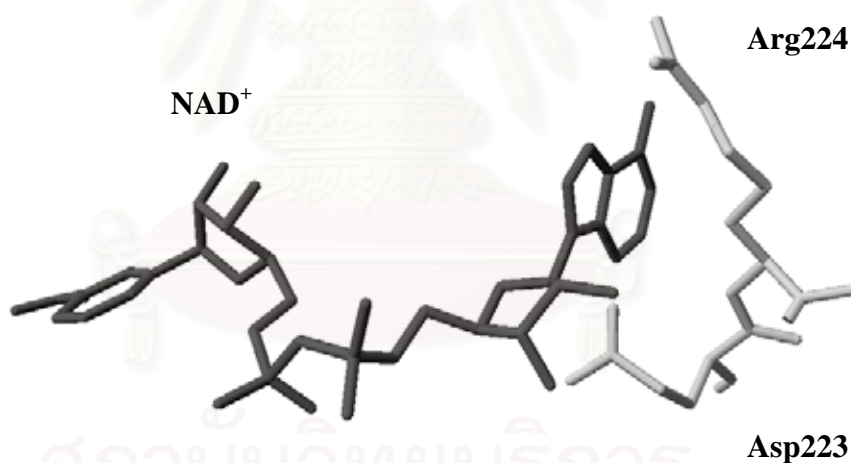


Figure 3.12 Structure of the *B. stabilis* 15516 wild-type and mutant enzymes (A) Model of wild-type enzyme with NADP⁺ bound to the nucleotide binding site. (B) Model of Gln223Asp mutant enzyme with NAD⁺ bound to the nucleotide binding site. Residue 223 is shown in light grey. The model structure was constructed by the Automated Protein Modeling Server SWISS-MODEL (<http://www.expasy.org>) using 2NAD (PseFDH) and 2dbq (*Pyrococcus horikoshii* OT3) as templates for coenzyme NAD⁺ and NADP⁺, respectively.

3.10.1 Cloning of mutant FDH

The 1.2 kb PCR fragments of the FDH gene from *B. stabilis* 15516 obtained by megaprimer-based mutagenesis strategies as described in section 2.14 (Figure 3.13) was cloned into pET-17b at *NdeI*-*Bam*HI site to generate mutant pBstFDH and transformed to *E. coli* BL21 (DE3) and then determined by *NdeI*-*Bam*HI (Figure 3.14). After that, the recombinant FDH plasmid was sequenced. The result exhibited the substitution of CAG to GAC. The mutant clone was determined for the FDH activity and coenzyme specificity.

3.10.2 Optimization of mutant FDH activity by varying IPTG concentration and induction time

For IPTG concentration and induction time course study, the mutant was grown and induced by IPTG at various final concentration of 0, 0.1, and 0.2 mM before cell was harvested at various times: 0, 2, 4, 8, 16, 20 and 24 hr. The result indicated that Gln223Asp mutant showed the similar result to the wild-type. When cells were grown without induction by IPTG, the recombinant proteins were principally expressed as soluble proteins. In contrast, no expression could be detected in both soluble protein and inclusion bodies when 0.1-0.2 mM final concentrations of IPTG were added (Figure 3.15).

3.10.3 Determination of mutant FDH activity

FDH activity and specific activity of Gln223Asp mutant of pBstFDH 15516 for NADP⁺ were 3.0 U and 0.1 U/mg protein and those for NAD⁺ were 21.1 U and 0.4 U/mg protein, respectively as shown in Table 3.4.

3.10.4 Cofactor dependence of the mutant FDH

To study the coenzyme specificity, the mutant FDH was separated by native PAGE. The activity stain of the Gln223Asp mutant showed only a single activity band when stained in the complete reaction mixture containing NAD⁺ but not NADP⁺ as shown in Figure 3.16. This activity band coincided in position with the major band obtained from coomassie blue staining. Unlike the mutant, recombinant wild-type

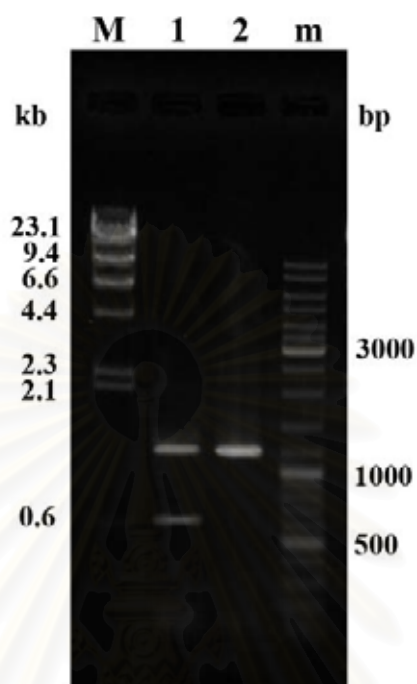


Figure 3.13 PCR amplification of FDH gene using megaprimer-based mutagenesis strategies

Lane M = λ /*Hind*III standard DNA marker

Lane 1 = PCR product of megaprimer-based mutagenesis

Lane 2 = reamplified product

Lane m = 100 bp DNA ladder

สภามหาวิทยาลัย
จุฬาลงกรณ์มหาวิทยาลัย

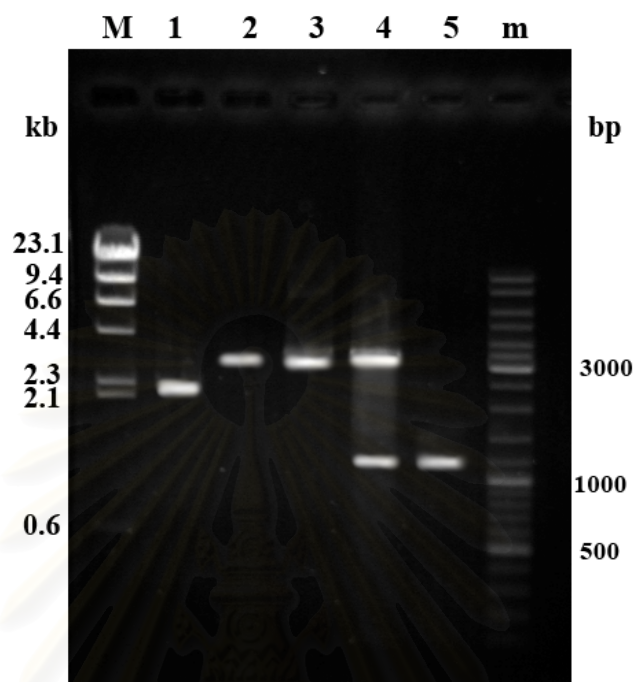


Figure 3.14 Restriction pattern of mutant pBstFDH

Lane M = λ /HindIII standard DNA marker

Lane 1 = undigested pET-17b

Lane 2 = *NdeI*-*Bam*HI digested pET-17b

Lane 3 = undigested mutant pBstFDH

Lane 4 = *NdeI*-*Bam*HI digested mutant pBstFDH

Lane 5 = amplified product of FDH gene

Lane m = 100 bp DNA ladder

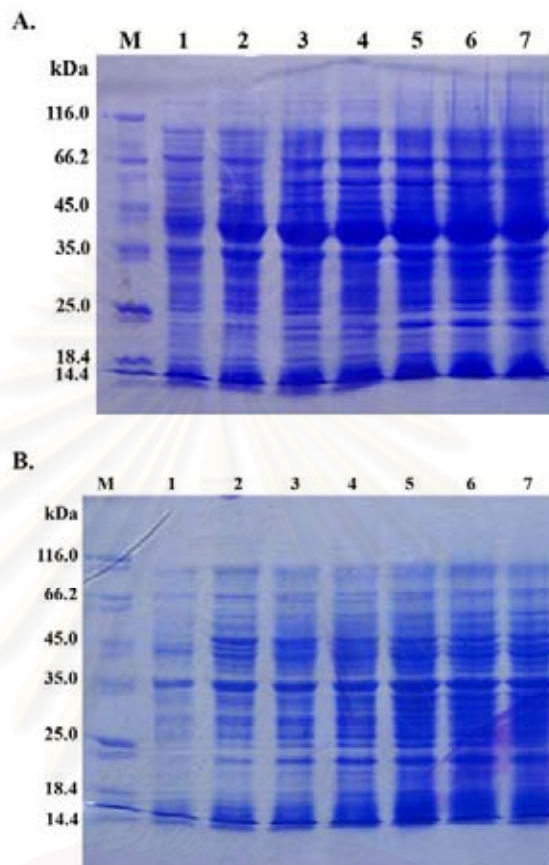


Figure 3.15 Protein pattern of cell harboring mutant pBstFDH at various induction times detected by SDS-PAGE

A: 0 mM IPTG

Lane M = protein marker

Lane 1-7 = mutant cells at various induction times:
0, 2, 4, 8, 16, 20 and 24 hr, respectively.

B: 0.2 mM IPTG

Lane M = protein marker

Lane 1-7 = mutant cells at various induction times:
0, 2, 4, 8, 16, 20 and 24 hr, respectively.

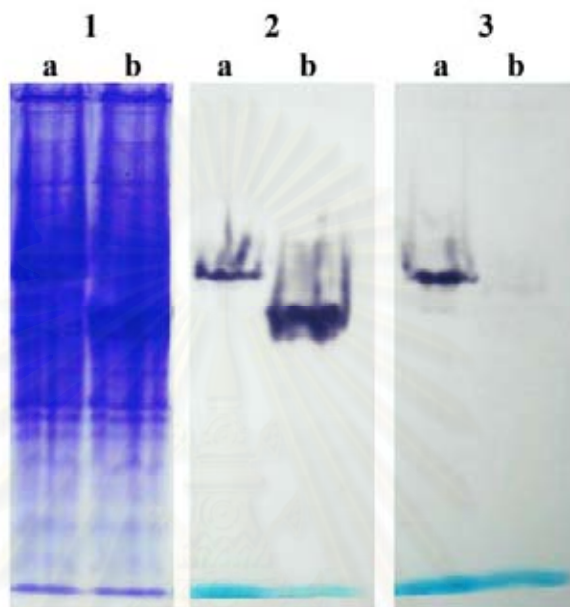


Figure 3.16 Coenzyme preference of the crude FDH from pBstFDH 15516 and the mutant clone The FDHs were separated through a native-PAGE and stained for FDH activity. 1 = coomassie blue stain, 2 = activity stain with NAD^+ and 3 = activity stain with NADP^+ . The character above each lane (a, b) stands for *B. stabilis* 15516 and the mutant clone, respectively.

จุฬาลงกรณ์มหาวิทยาลัย

enzyme showed the single activity band with both NAD^+ and NADP^+ . The result indicated that the substitution at Gln223 by Asp altered the coenzyme preference of BstFDH from NADP^+ to NAD^+ .

3.11 Purification of formate dehydrogenase

3.11.1 Preparation of crude extract

Thirteen grams of *E. coli* BL21 (DE3) cell harboring pBstFDH 15516 obtained by cultivation of the cells in 3 L of LB medium supplemented with 100 g/ml ampicillin without induction of IPTG as described in section 3.7 were used as source of FDH. Crude extract contained 1,152 units of FDH with 855 mg proteins. Thus, the specific activity of the enzyme in the crude preparation was 1.4 units/mg protein.

3.11.2 DEAE-Toyopearl column chromatography

The crude enzyme was applied onto DEAE-Toyopearl column as described in section 2.16.2.1. The chromatographic profile was shown in Figure 3.17. FDH was eluted as unbound protein as indicated in the profile. The fractions with FDH activity were pooled, dialyzed against the buffer, concentrated by aquasorb to reduce enzyme volume. After this purification step, the remaining protein was 220 mg with 1,056 total activity and the specificity activity was 4.8 units/mg protein. Thus, the enzyme was purified 3.56 fold with 91.7% recovery.

3.11.3 Butyl-Toyopearl column chromatography

The pooled active fraction from DEAE-Toyopearl column was applied to the Butyl-Toyopearl column as described in section 2.16.2.2. The chromatographic profile was shown in Figure 3.18. The unbound proteins were eluted from column with phosphate buffer containing 25% saturated ammonium sulfate. The bound proteins were eluted by negative salt stepwise method with the phosphate buffer containing 25, 20, 15 and 0% saturated ammonium sulfate, respectively. The FDH was eluted with the phosphate buffer containing 10% salt saturation. The pooled fraction containing FDH activity was dialyzed against the buffer and concentrated by aquasorb. This operation obtained the enzyme with 98 mg remaining protein and 523 units of FDH activity. The specific activity of the enzyme was 5.3 units/mg protein. From this final step, the FDH

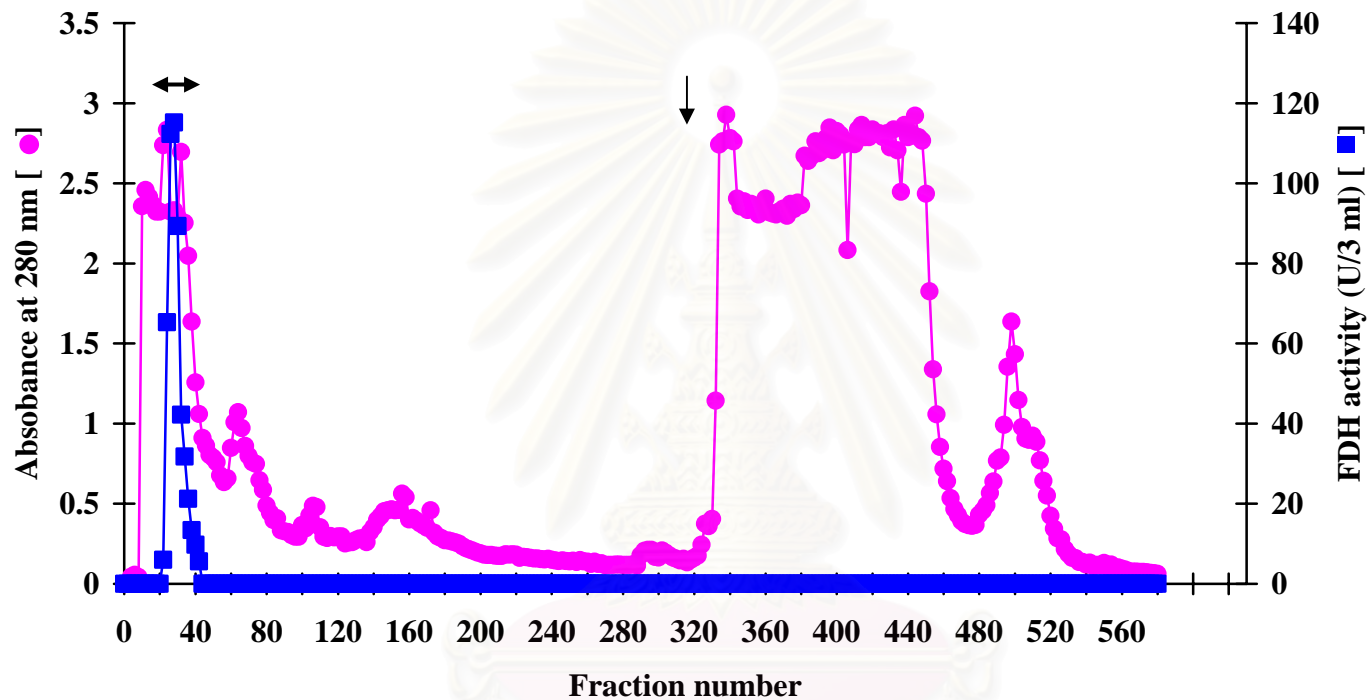


Figure 3.17 Purification of formate dehydrogenase from pBstFDH 15516 clone by DEAE - Toyopearl column

The enzyme solution was applied to DEAE -Toyopearl column and washed with 10 mM potassium phosphate buffer, pH 7.4 containing 1 mM EDTA until A_{280} decreased to base line. The bound proteins were eluted by 0-0.5 M KCl in the same buffer at the flow rate of 1ml/min. The fractions of 3 ml were collected. The arrow indicates where gradient started (\downarrow). The protein peak from fraction number 23 to 39 was pooled (\longleftrightarrow).

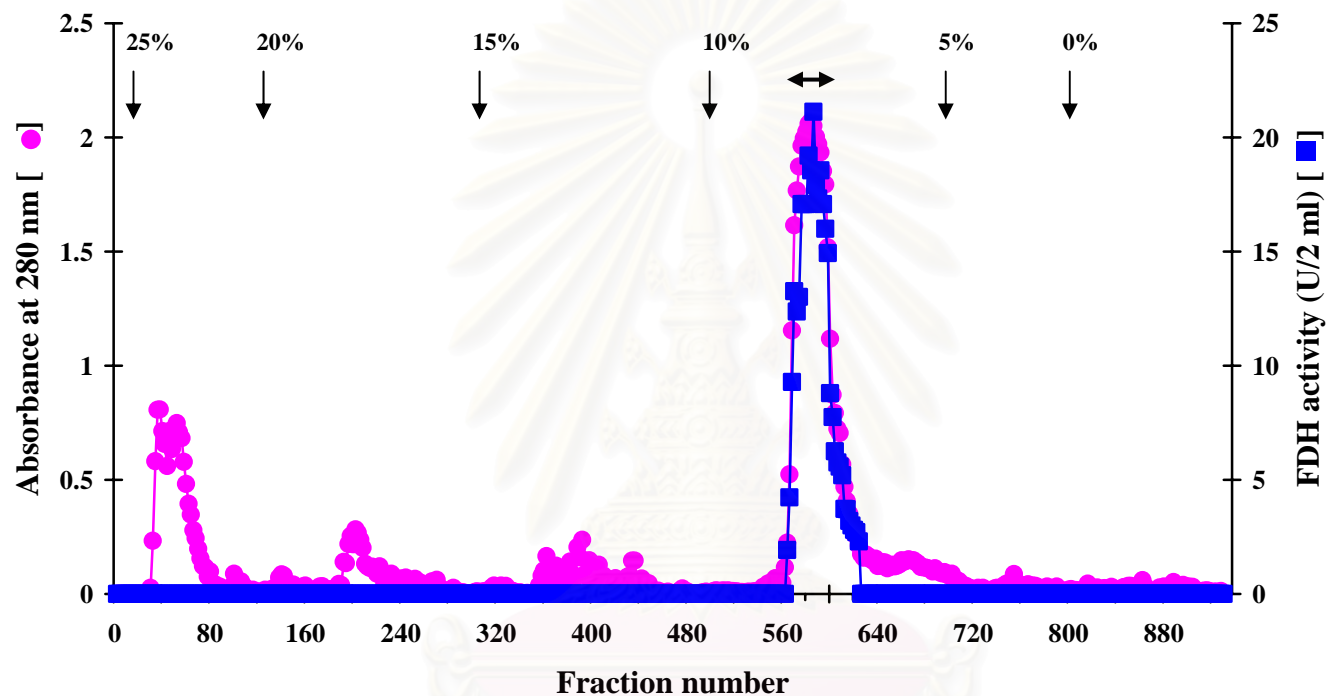


Figure 3.18 Purification of formate dehydrogenase from recombinant pBstFDH 15516 clone by Butyl-Toyopearl column.

The enzyme solution was applied to Butyl-Toyopearl column and washed with 25% saturated ammonium sulfate in 10 mM potassium phosphate buffer, pH 7.4 containing 1 mM EDTA until A_{280} decreased to base line. Stepwise elution of bound protein was performed at 20%, 15%, 10%, 5% and 0% saturated ammonium sulfate in the same buffer at the flow rate of 1 ml/ min. The fractions of 2 ml were collected. The arrow indicates where each stepwise started. The protein peak from fraction number 568 to 604 was pooled (\longleftrightarrow).

was purified 3.96 fold with about 45.4% recovery compared with the crude extract as shown in Table 3.5. The purified enzyme from this step was kept at 4°C for further experiments.

3.11.4 Determination of enzyme purity and protein pattern

The enzyme from each step of the purification was examined to purity and protein pattern by SDS-PAGE. In addition, the purified enzyme from the last step of purification was run on non-denaturing PAGE followed by protein and activity staining as shown in Figure 3.19. The purified enzyme in lane 4A on SDS-PAGE showed a single band which corresponded with a single protein band in lane 1B and its activity staining in lane 2B on native-PAGE. The result indicated that FDH from Butyl-Toyopearl column was purified to homogeneity. The molecular weight of FDH subunit was calculated to be 42 kDa by its mobility in SDS-PAGE compared with those of standard proteins.

3.12 Characterization of formate dehydrogenase

3.12.1 Coenzyme specificity of formate dehydrogenase

Coenzyme specificity of FDH was investigated as described in section 2.17.1. FDH required NADP⁺ as a natural coenzyme over NAD⁺ which showed 37.73% relative activity to that of NADP⁺.

3.12.2 Effect of pH on formate dehydrogenase activity

The effect of pH on the enzyme activity was determined at various pHs of buffers ranged from 6.0 to 12.5 as mentioned in section 2.17.2. The result was shown in Figure 3.20. The enzyme performed maximal activity at pH 6.0-7.5.

3.12.3 Effect of temperature on formate dehydrogenase activity

The effect of temperature on the enzyme activity was examined as described in section 2.17.3. The temperature was varied from 30 °C to 80 °C. The result was shown in Figure 3.21. The enzyme exhibited the highest activity at 60 °C.

Table 3.5 Purification of formate dehydrogenase from *E. coli* BL21 (DE3) cell harboring FDH gene from *Burkholderia stabilis* 15516^a

Purification steps	Total activity (unit)	Total protein (mg)	Specific activity (unit/mg protein)	% Recovery	Purification fold
Crude enzyme	1152	855	1.4	100	1
DEAE-Toyopearl	1056	220	4.8	91.7	3.56
Butyl-Toyopearl	523	98	5.3	45.4	3.96

^a Crude extract was prepared from 3 L (13 g cell wet weight) of cell culture.

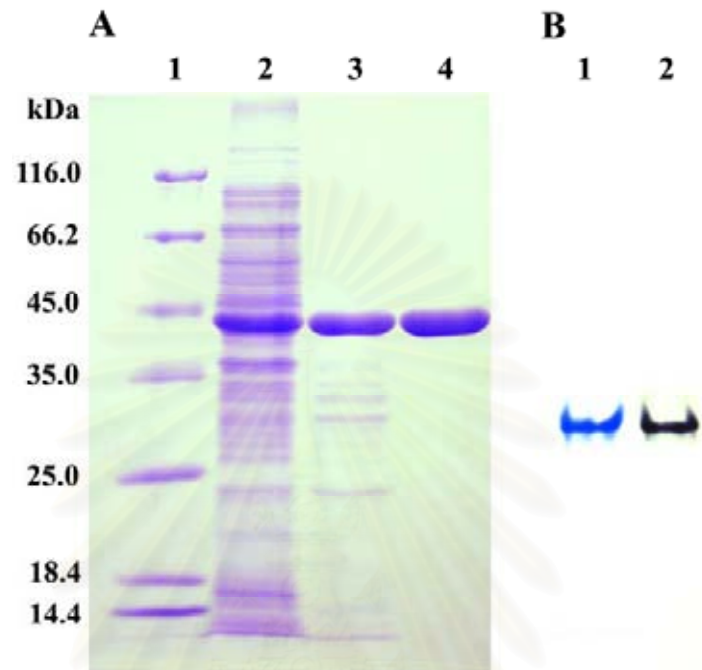


Figure 3.19 Protein pattern from each step of purification investigated by SDS-PAGE and the purified FDH at last step examined by native-PAGE.

A: 12.5% SDS-PAGE

Lane 1 = protein marker

Lane 2 = crude extract

Lane 3 = DEAE-Toyopearl column

Lane 4 = Butyl-Toyopearl column

B: 7.7% native-PAGE

Lane 1 = Butyl-Toyopearl column (protein staining)

Lane 2 = Butyl-Toyopearl column (activity staining)

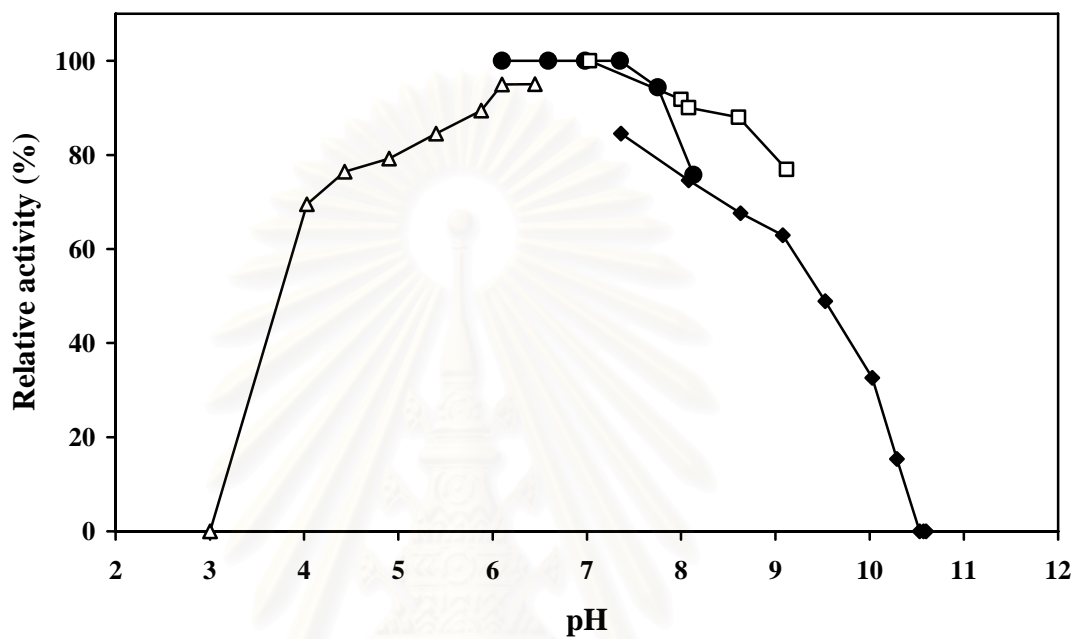


Figure 3.20 Effect of pH on formate dehydrogenase activity. The FDH activities were measured at different pHs with 200 mM potassium acetate buffer (Δ), phosphate buffer (\bullet), Tris-HCl buffer (\square) and glycine-KCl-KOH buffer (\blacklozenge).

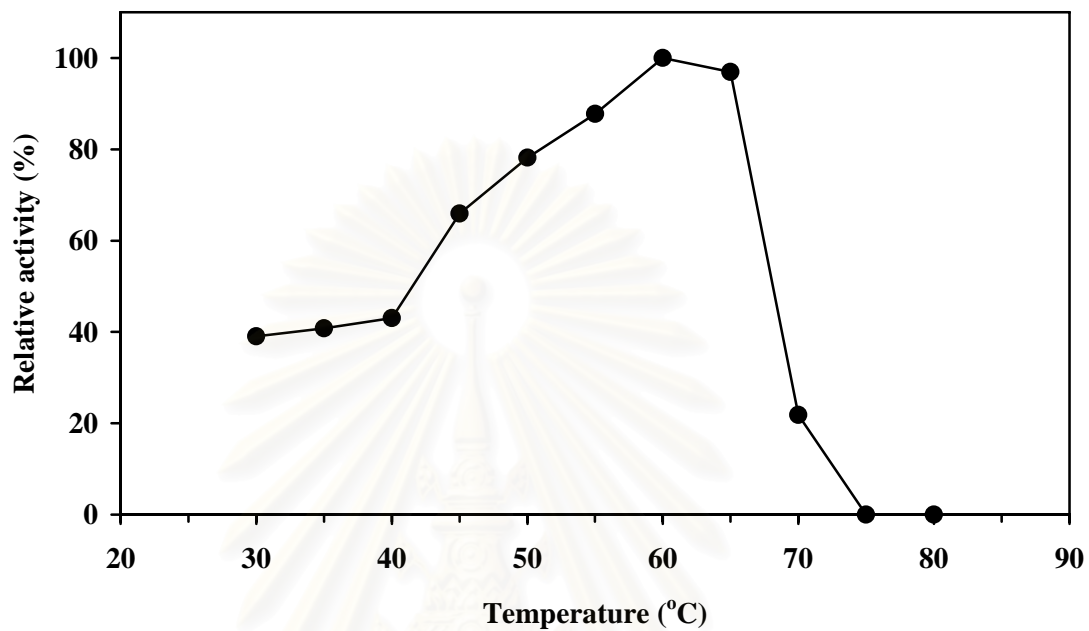


Figure 3.21 Effect of temperature on formate dehydrogenase activity.

The FDH activities (●) were measured at various temperatures varying from 30 °C to 80 °C.

สถาบันวิทยบริการ
จุฬาลงกรณ์มหาวิทยาลัย

3.12.4 Effect of pH on formate dehydrogenase stability

The pH stability of FDH was studied as described in section 2.17.4. The enzyme was preincubated at 30 °C for 20 min in various 10 mM buffers at various pHs ranging from 4.0 to 12.5. The result was shown in Figure 3.22. The remaining activities were over 60% at pH ranged from 4.0 to 12.5. Moreover, the enzyme showed the full activity at pH 6.0-8.0.

3.12.5 Effect of temperature on formate dehydrogenase stability

The temperature stability of FDH was studied as described in section 2.17.5. The enzyme was preincubated at various temperatures ranged from 30 °C to 70 °C for 10 min. The enzyme activity of non-preincubated enzyme was defined as 100% relative activity. As shown in Figure 3.23A, the enzyme retained its full activity at temperature up to 45 °C and lost about half of its activity at over 65 °C. At 70 °C, FDH absolutely lost its activity. Moreover, the enzyme was advanced in its long time tolerance on temperature at 45 °C, 50 °C, 55 °C, and 60 °C by incubation for 0 to 62 hr and measured its activity. The remained activities were performed as the percentage of the initial activity as shown in Figure 3.23B. The enzyme was fully stable at 45 °C for 16 hr and retained 50% of its activity after treatment for 36 hr. The enzyme activity was relatively decreased with increasing of incubation time. At 50 and 55 °C, the enzyme showed the full activity for 10 hr, whilst at 36 hr 50% activity was remained. In addition, the FDH could retain 50% activity at least 5 hr at 60 °C and the activity was completely lost after incubation for 40 hr.

3.13 Kinetic studies of formate dehydrogenase

3.13.1 Initial velocity studies for oxidative reaction of formate with NADP⁺ and NAD⁺

A series of steady-state kinetic analysis was carried out to investigate the kinetic parameters of FDH. The concentration of formate was varied in the presence of several fixed concentration of NADP⁺ or NAD⁺. Double-reciprocal plots of initial velocity against reciprocals of formate concentrations gave a family of straight lines, which intersected in the upper left quadrant as shown in Figure 3.24A and 3.24C. These

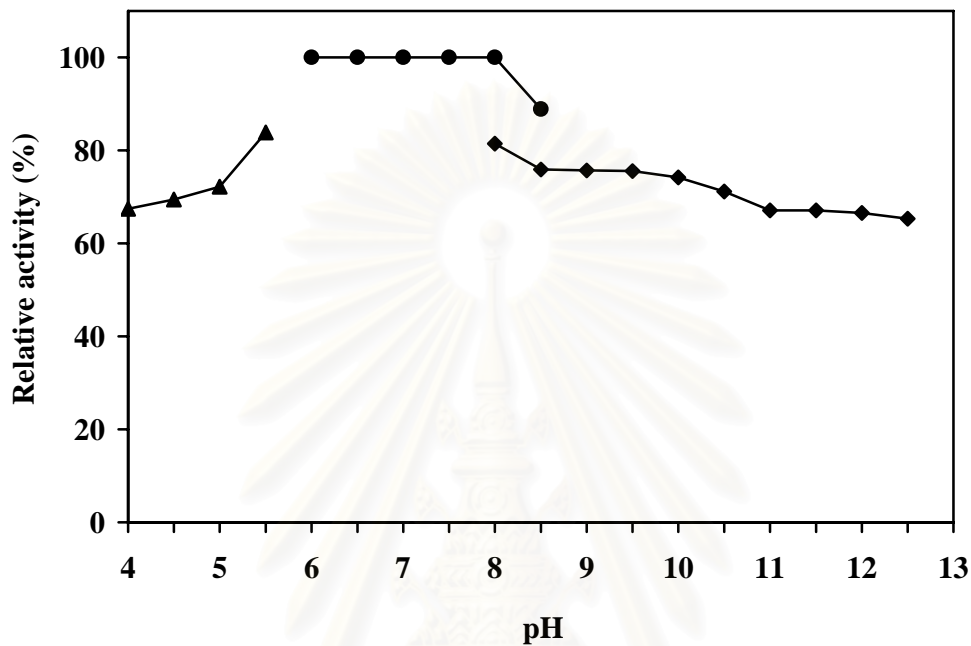
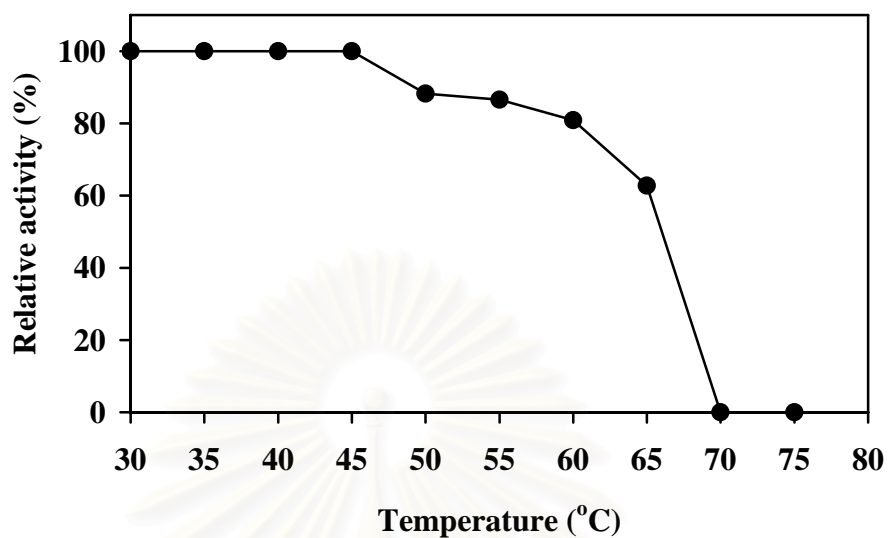


Figure 3.22 Effect of pH on formate dehydrogenase stability.

The enzymes in buffers at various pHs ranged from 4.0 to 12.5 were incubated at 30 °C for 20 min and then the relative activities were assayed. The 10 mM buffers used were acetate buffer (pH 4.0- 6.0; ▲), potassium phosphate buffer (pH 6.0-8.5; ●) and glycine-KCl-KOH buffer (pH 8.5-12.5; ◆).

A



B

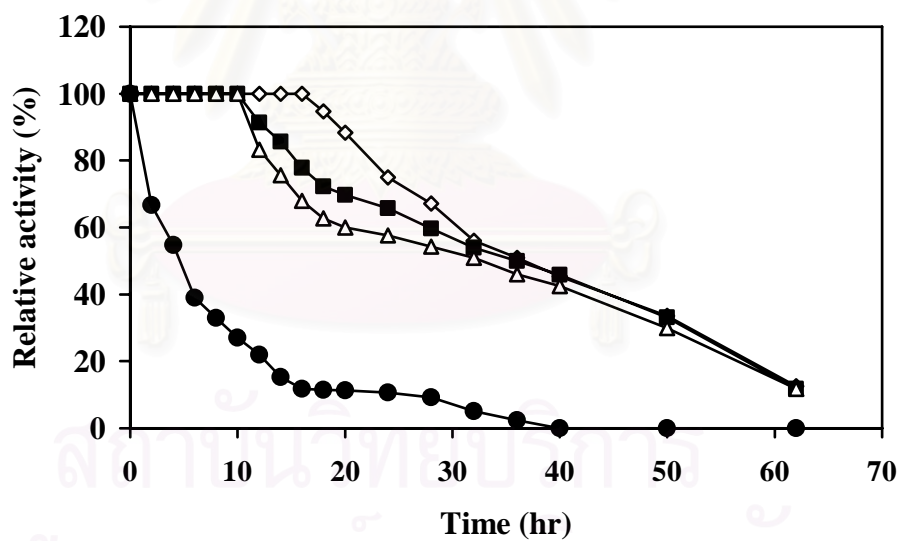
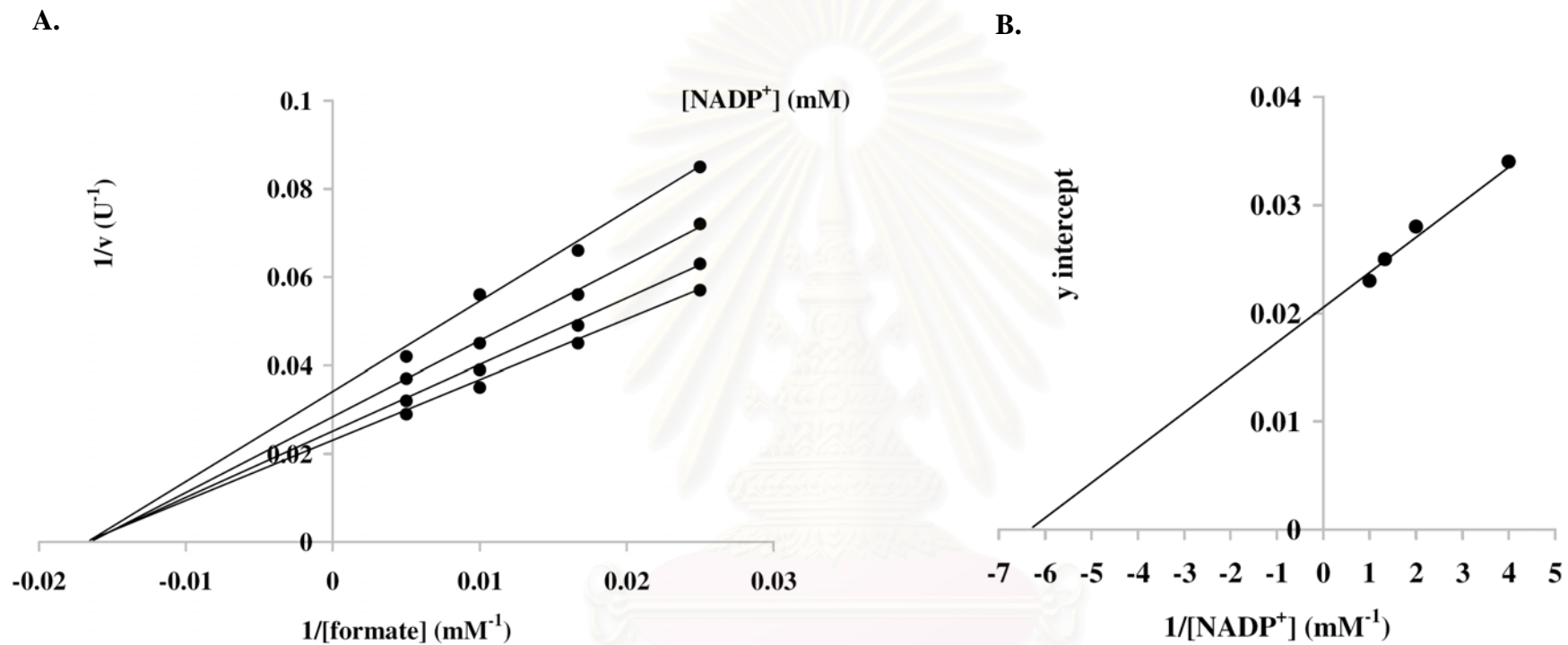


Figure 3.23 Effect of temperature on formate dehydrogenase stability.

A. The effect of temperature on enzyme stability was performed at 30 to 75 °C for 10 min before the activity was determined under standard condition at 30 °C.

B. The enzyme stability was tested at 45, 50, 55 and 60 °C and the activity was assayed under standard condition at 30 °C.

◇ 45 °C ■ 50 °C △ 55 °C ● 60 °C



(continued)

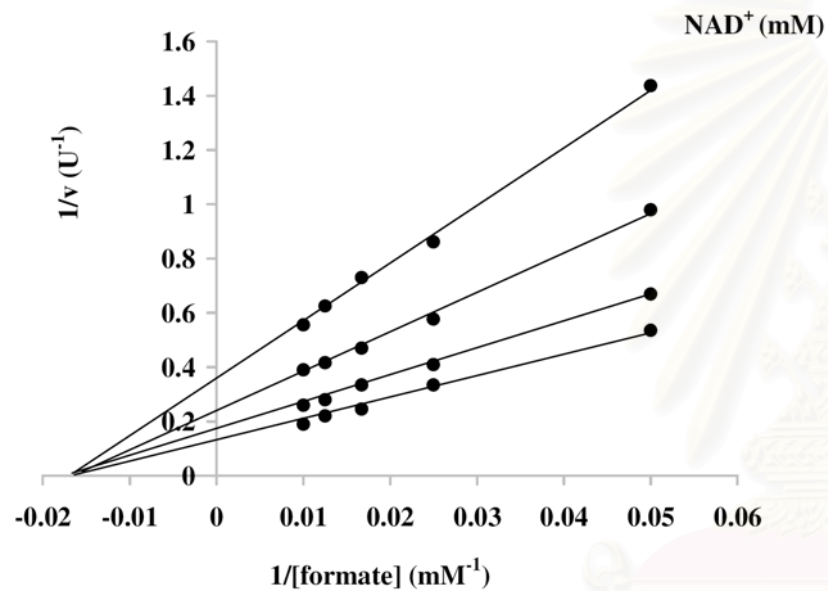
Figure 3.24 Initial velocity patterns

A. Double-reciprocal plots of initial velocities versus formate concentrations at a series of fixed concentrations of $NADP^+$.

Concentrations of $NADP^+$ were 0.25, 0.5, 0.75, 1.0 and 1.5 mM, respectively.

B. Secondary plots of y intercepts versus reciprocal $NADP^+$ concentrations.

C.



D.

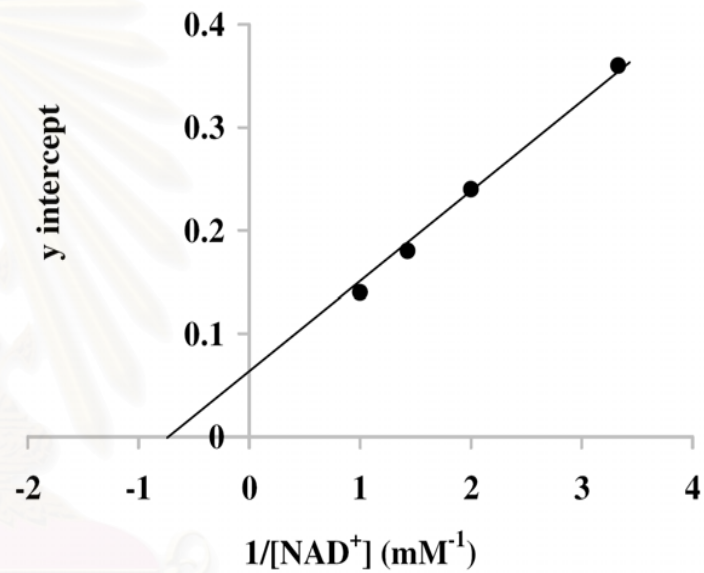


Figure 3.24 Initial velocity patterns.

C. Double-reciprocal plots of initial velocities versus formate concentrations at a series of fixed concentrations of NAD^+ .

Concentrations of NAD^+ were 0.3, 0.5, 0.7, 0.8 and 1.0 mM, respectively.

D. Secondary plots of y intercepts versus reciprocal NAD^+ concentrations.

results showed that the reaction proceeds via the formation of a ternary complex of the enzyme with NADP⁺ or NAD⁺ and formate (Cleland, 1971). The apparent K_m value for formate was calculated to be 62.5 mM. From the secondary plots of intercept at the ordinate versus reciprocal concentrations of NADP⁺ or NAD⁺, the apparent K_m value for NADP⁺ or NAD⁺ was calculated to be 0.16 mM or 1.43 mM as shown in Figure 3.24B and 3.24D, respectively.

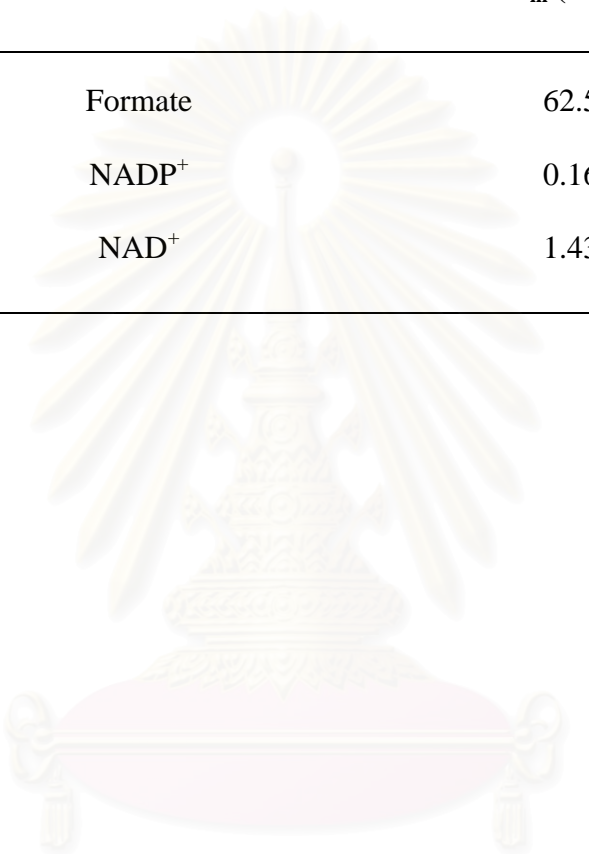
The apparent K_m values of the substrates of FDH were summarized in Table 3.6.



สถาบันวิทยบริการ
จุฬาลงกรณ์มหาวิทยาลัย

Table 3.6 The apparent K_m values of substrates of formate dehydrogenase from *E. coli* BL21 (DE3) harboring pBstFDH 15516

Substrate	K_m (mM)
Formate	62.5
NADP ⁺	0.16
NAD ⁺	1.43



สถาบันวิทยบริการ
จุฬาลงกรณ์มหาวิทยาลัย

CHAPTER IV

DISCUSSION

Formate dehydrogenases (FDH) are a large set of enzymes which catalyse the oxidation of formate to carbon dioxide coupled to the reduction of NAD(P)^+ to NAD(P)H . The FDH enzyme family is comprised of several distinct groups of enzymes that vary in molecular mass, complex quaternary structure, the presence and type of various prosthetic groups, substrate specificity and their liability towards oxygen (Popov and Lamzin, 1994). FDH has been selected as a NAD^+ regenerator to developing the system for amino acid production because 1) Formate, as a substrate for the FDH, is one of the cheapest hydrogen sources and does not inhibit most other dehydrogenases. 2) The CO_2 product can be easily removed from the reaction mixture. 3) The reaction has a favorable equilibrium strongly shifted towards CO_2 and NADH formation. 4) The enzyme has a broad pH optimum range of activity for 6-9.

In this part of my research, a novel FDH was screened in order to improve the yield of L-alanine production from the coupling reaction of recombinant alanine dehydrogenase and formate dehydrogenase.

Up to the present, the various FDH-producing organisms without prosthetic groups have been reported such as bacteria: *Pseudomonas* sp.101 (Tishkov, *et al.*, 1993), *Moraxella* sp. C-2 (EMBL Accession O08375), *Mycobacterium vaccae* N10 (Galkin, *et al.*, 1995), *Hyphomicrobium* strain JT-17 (FERM P-16973), *Paracoccus* sp. 12-A (Shinoda, *et al.*, 2002), *Ancylobacter aquaticus* (Nanba, *et al.*, 2003a) and *Thiobacillus* sp. KNK65MA (Nanba, *et al.*, 2003b), yeasts: *Hansenula polymorpha* (Hollenberg and Janowiez, 1989), *Candida methylica* (Allen and Holbrook, 1995), *Candida boidinii* (Sakai, *et al.*, 1997) and *Pichia pastoris* (Goldberg, *et al.*, 2002), and fungi: *Aspergillus nidulans* (Saleeba, *et al.*, 1992) and *Neurospora crassa* (Chow and RajBhandarg, 1993). However, these reported FDHs accept NAD^+ as the natural coenzyme. Moreover, of the occurring NAD^+ -dependent FDHs currently known, only the FDHs from bacteria show a high activity and stability (Tiskov and Popov, 2004), making them of greater interest in potential biotechnological applications.

In this study, we found a novel FDH from *Burkholderia cepacia* complex (BCC) that prefers NADP⁺ as the electron acceptor with a much higher specific activity than that for NAD⁺. This kind of FDH has not been reported before.

Burkholderia cepacia complex (BCC), a group of gram-negative bacteria distributed in natural environments, comprised of at least 10 genomovars or species (LiPuma, 2007). BCC is a group which contains potentially opportunistic human pathogens, as well as plant pathogens, because of the capability of some members causing opportunistic infections in vulnerable individuals and, perhaps, especially people with cystic fibrosis. In contrast with their clinical epidemiology, members and isolates of the BCC can interact with plants beneficially around their roots and foliage forms in the natural habitat. During these interactions, BCC facilitate highly beneficial processes such as the breakdown of pollutants or enhancement of crop growth (Mahenthiralingam, *et al.*, 2008). On the other hand, BCC products and enzymes were used widely in the clinical impacts, industry, agriculture, biotechnology, bioremediation, biocontrols and environments (Chiarini, *et al.*, 2006; 2008; Heungens and Parke, 2001).

In this study, at least some, but not all, isolates from five out of 10 species of BCC, namely *B. cepacia*, *B. multivorans*, *B. cenocepacia*, *B. stabilis* and *B. pyrrocinia*, were found to contain a FDH gene. Nevertheless, the presence of the FDH gene, as detected by PCR amplification with four primer sets, was not detected in all the tested strains of *B. vietnamiensis*, *B. dolosa*, *B. ambifaria*, *B. anthina* and *B. ubonensis*. Whether this reflects a true absence in the genome, or sequence variation at the primer binding sites, but the variation in apparent FDH presence within isolates of the same species, as well as between species, suggests the loss and gain of the FDH gene. However, the FDH gene does not form in all strains of each BCC species (Table 3.1). Moreover, the FDH gene has been found in most of clinical isolates, this suggests that the gene may play a key role in cell function and survival in host condition as shown that it was also found in genome sequencing of various pathogenic organisms (Tishkov and Popov, 2006).

The completed FDH genes of *B. cepacia* 11197, *B. multivorans* 12938, *B. cenocepacia* 15507, *B. pyrrocinia* 15515 and *B. stabilis* 15516 are equal in length of nucleotide sequences for 1161 bp encoding 386 amino acid residues. Consistent with the trend that FDH genes show high primary sequence identity (80-85%) within the same

genus and relatively high levels (50-55%) between enzymes from different groups (Popov and Lamzin, 1994), the 5 BCC FDHs show a high amino acid sequence identity (91-96%) amongst themselves and also a relatively high sequence identity (65-70%) to those of currently reported bacterial NAD⁺-FDHs. They show the conserved amino acid residues and the important key amino acids for FDH catalysis (Figure 3.8). The dendrogram revealed the BCC-FDH has a unique lineage differ from other FDHs (Figure 3.9).

The catalytic mechanism of NAD⁺-dependent FDH is specified by the direct transfer of hydride ion from the substrate onto the C4-atom of the nicotinamide moiety of NAD⁺ without the acid-base catalysis stages that are present in the reactions catalyzed by other related dehydrogenases (Tishkov and Popov, 2004). All reported FDHs have an almost an identical set of catalytically essential amino acid residues in the active center (Popov and Lamzin, 1994). The Gln313-His332 (numbering in PseFDH) pair in the active center is conserved in all FDHs and also BCC-FDH (Gln315-His334) and is equivalent to the Glu-His pair in the active center the proton relay system, which is required for steps of acid-base catalysis of D-specific 2-hydroxy acid dehydrogenases (Tishkov and Popov, 2004). The presence of the Gln in FDHs is believed to be essential for the broad pH affinity profile towards substrate (Tishkov, *et al.*, 1996). However, in novel and direct contrast, in the BCC-FDH gene sequences reported here the catalytically important residue of the residue Gln315 is substituted with Glu315 in *B. multivorans* 12938. This substitution is also found in the reported genome sequence of *B. multivorans* ATCC17616 (YP001585382), and so is unlikely to either be a sequencing artifact or stochastic detection of a recent deleterious mutation. It thus remains of interest to evaluate if the catalytic mechanism of FDH from *B. multivorans* is different from previous FDHs and proceeds through acid-base catalysis.

The BCC-FDHs reported here have a relatively low subunit molecular mass of ~42 kDa as detected by SDS-PAGE, which corresponded with those calculated from theoretical MW of deduced amino acid sequences. The theoretical MW from their deduced amino acid sequences that were 41.419, 41.469, 41.518, 41.550 and 41.492 kDa corresponded with BceFDH 15507, BmuFDH 12938, BcnFDH 11197, BstFDH 15516 and BpyFDH 15515, respectively. The theoretical isoelectric point (pI) of the recombinant FDH from each strain was 6.19 (*B. cepacia* 15507 and *B. multivorans*

12938), 6.23 (*B. cenocepacia* 11197), 6.34 (*B. stabilis* 15516) and 6.53 (*B. pyrrocinia* 15515), respectively. The enzymes were unlikely to require divalent metal ions, such as molybdenum or iron, as well as prosthetic groups, as they were not inhibited by EDTA.

In the coenzyme preference, the previous reports have revealed that the majority of NAD⁺-dependent FDHs are highly specific towards NAD⁺ and do not utilize NADP⁺ as a coenzyme. However, at least one of them from bacteria PseFDH displays dual coenzyme specificity. Under optimal reaction conditions the activity of PseFDH towards NADP⁺ reaches nearly 30% of that with NAD⁺ (Tishkov and Popov, 2006). The FDH activity from *Ancylobacter aquaticus* with NADP⁺ is 2.4% of the activity with NAD⁺ (Nanba, *et al.*, 2003a) and that from *Thiobacillus* sp. KNK65MK shows 4% of the activity with NAD⁺ (Nanba, *et al.*, 2003b). While the reported FDH from yeast can not utilize NADP⁺ as a coenzyme (Serov, *et al.*, 2002).

In this study, BCC-FDH clearly preferred NADP⁺ as the natural cofactor with a markedly strong band of NADP⁺ when compared to that of NAD⁺ of activity stain in native PAGE (Figure 3.11). Moreover, the crude enzyme specific activity of BCC-FDH that was up to 25.2-folds higher with NADP⁺ than NAD⁺. The FDH specific activity from *B. cenocepacia* 11197, *B. pyrrocinia* 15515 and *B. stabilis* 15516 with NAD⁺ were 3.96, 12.44 and 7.10% of the activity with NADP⁺, respectively. The results indicate that the BCC-FDH enzymes from 5 species outlined in this report are a novel NADP⁺-dependent FDH. BCC-FDH can be distinguished to 2 types, (i) NADP⁺ accepted enzyme such as FDH from *B. cenocepacia* 11197, *B. cepacia* 15507 and *B. multivorans* 12938, however, FDH from *B. cepacia* 15507 and *B. multivorans* 12938 showed the very low level of enzyme activity toward NADP⁺ and no activity toward NAD⁺. (ii) NADP⁺ and NAD⁺ accepted enzyme, which NADP⁺ is preferred over NAD⁺ such as FDH from *B. stabilis* 15516 and *B. pyrrocinia* 15515. It is interesting that the BCC-FDHs show a variety of coenzyme preference. Especially, the FDH from *B. stabilis* 15516 and *B. pyrrocinia* 15515 can accept both coenzymes. Moreover, the FDH from *B. cenocepacia* 11197 significantly accepts NADP⁺ as coenzyme. Characterization of this novel type of FDH is needed for application in biotechnology and various industries.

All NAD⁺-FDHs and other enzymes in their superfamily, D-specific 2-hydroxy acid dehydrogenases, contain the coenzyme conserved nucleotide binding sequence as Gly(Ala)XGlyXXGlyX₁₇Asp for NAD⁺ (Popov and Lamzin, 1994), where the

conserved Asp residue interacts with 2'- and 3'-OH groups of adenosine ribose and is a major determinant of the specificity for NAD^+ (Serov, *et al.*, 2002). Mutagenesis of FDH, including at this site, with a view to changing the coenzyme specificity from NAD^+ to NADP^+ has been reported in *Candida methylica* (Gul-Karaguler, *et al.*, 2001), *Saccharomyces cerevisiae*, *Pseudomonas* sp. 101 (Serov, *et al.*, 2002) and *Candida boidinii* (CboFDH) (Rozzell, *et al.*, 2004), with promising results. However, whilst these and, especially, the combined Asp195Gln/Tyr196His mutation of CboFDH (Andreadeli, *et al.*, 2008) show a higher $(K_{\text{cat}}/K_{\text{m}})^{\text{NADP}^+}/(K_{\text{cat}}/K_{\text{m}})^{\text{NAD}^+}$ when compared with those of wild-type enzymes, NAD^+ remains their preferred coenzyme. For the NADP^+ -dependent FDH from 5 BCC species, Gln223 (Asp195 in CboFDH) substituted the Asp of the coenzyme nucleotide binding conserved sequence of NAD^+ -FDHs as changed to GlyXGlyXXGlyX₁₇Gln. This indicates that Gln223 is likely to potentially have important roles in NADP^+ specificity.

To confirm that Gln223 is essential for NADP^+ specificity, we performed the site-directed mutagenesis on this position of FDH from *B. stabilis* 15516 that changed Gln223 to Asp. The result showed that the coenzyme preference of mutant enzyme Gln223Asp was completely reversed from NADP^+ to NAD^+ . This suggested that the Gln223 is essential for NADP^+ binding site. The predicted structures display the mark different between interaction of NADP^+ on Gln and NAD^+ on Asp. Due to the negative charge of phosphate group of NADP^+ is blocked by the negative charge of Asp, this might allow the NAD^+ enzyme accepts NAD^+ greater than NADP^+ . On the other hand, Gln has no charge that allows it to accept both the NADP^+ and NAD^+ . This might be implied that the coenzyme binding site of BCC-FDH has a special architecture which is suitable for dual coenzyme NADP^+ and NAD^+ , although they prefer NADP^+ over NAD^+ . However, three dimensional modeling studies are required to confirm this inference.

For characterization of the BCC-FDH enzyme, FDH from *B. stabilis* 15516 was chosen due to its highest FDH activity and favor of dual coenzymes NADP^+ and NAD^+ . The apparent K_{m} values for sodium formate, NADP^+ and NAD^+ are 62.5, 0.16 and 1.43 mM, respectively. Comparison with NAD^+ -dependent FDH from other organisms revealed the lower substrate affinity of BCC-FDH. The K_{m} for formate of NAD^+ -dependent FDH from plant, fungi and bacteria are in range of 0.0033-0.6, 1.67-40, and 0.077-15 mM, respectively whilst K_{m} value for NAD^+ are in the range of 0.0057-0.07,

0.032-5.5 and 0.048-0.18 for plant, fungi and bacteria, respectively. Among bacterial-NAD⁺-dependent FDH, only the enzyme from *Ancylobacter aquaticus* and *Thiobacillus* sp. exhibit the NADP⁺ activity with 2.4 and 4.2% of the activity for NAD⁺. Yeast- FDH can not use the NADP⁺ as a coenzyme (Serov, *et al*, 2002).

The pH for FDH activity of *B. stabilis* 15516 is widely range between pH at 4-10 and the optimal pH for expression of full FDH activity is 6-7.5. The data from the BRENDA enzyme database also indicates that the optimal pH of NAD⁺-dependent FDHs are in range of 5.2 to 8.0 (www.brenda-enzymes.org). BstFDH 15516, like other reported FDHs, can tolerate in a wide range of pH at 4-12. *Ancylobacter aquaticus* shows FDH activity of 60% and 65% at pH 5.0 and 10.5, respectively while *Thiobacillus* sp. has an activity of 80% and 65% at pH 5.0 and 10.0, respectively.

FDH from *B. stabilis* 15516 has the broad range of the activity at temperature between 30 °C and 70 °C. It expressed the full activity at optimal temperature of 60 °C. At 70 °C, FDH retained its activity about 20%. In addition, the bacterial NAD⁺-FDH from *Arthrobacter* sp., *Pseudomonas* sp., *Ancylobacter aquaticus*, *Paracoccus* sp. 12A and *Thiobacillus* sp., revealed the temperature optimum at 30, 40, 50, 55 and 58 °C, respectively (www.brenda-enzymes.org). BstFDH 15516 expressed its full temperature stability when incubation was performed for 10 min at 30-45 °C. The enzyme showed the temperature tolerance with remaining activity at 65 °C over 60% while the NAD⁺-FDH from *Ancylobacter aquaticus* showed the temperature stability for the activity of 45% at 60 °C and that from *Thiobacillus* sp. remained the activity of 30% at 65 °C (www.brenda-enzymes.org). For prolong incubation of BstFDH 15516 at high temperature, full activity was observed at 45 °C until 16 hr where as 50% activity was retained at 36 hr. Upon treatment at 50 and 55 °C, it showed the full activity for 10 hr while at 36 hr showed 50% remaining activity. Moreover, the BstFDH 15516 could remain a 50% activity at least 5 hr when it was incubated at 60 °C.

Even though BstFDH can not directly used in NADH regeneration system of alanine dehydrogenase for L-alanine production, its Gln223Asp mutant that used NAD⁺ as a major coenzyme can be applied. However, the further mutagenesis of the mutated enzyme is needed to improve or increase the FDH activity.

This is the first reported on a novel native FDH from *B. cepacia* complex which prefers NADP⁺ as a natural coenzyme over NAD⁺. Though K_m for formate seems high, it

shows an advantage in pH and high temperature stability. It would be applied on NADPH regeneration for production of many valuable products that widely useable in food and pharmaceutical industries.



สถาบันวิทยบริการ
จุฬาลงกรณ์มหาวิทยาลัย

CONCLUSIONS

Part I: Improvement of host cell for alanine production

1. T7 RNA polymerase gene was inserted into chromosome of *E. coli* MB2795, the alanine racemase deficiency strain. The recombinant strain was named *E. coli* KR.
2. *E. coli* KR harboring pETAlaDH or pETFAla could produce optical purity of L-alanine (> 95%).
3. Formate dehydrogenase can increase yield of L-alanine production in *E. coli* KR.
4. L-alanine production by *E. coli* KR harboring pETFAla was 6 fold higher than that produced by *E. coli* BL21 harboring pETFAla.

Part II: Screening of a novel formate dehydrogenase to improve alanine production

1. Distribution of FDH was determined among 46 strains from 10 species of the *Burkholderia cepacia* complex (BCC). Five out of 10 species, namely *B. cepacia*, *B. multivorans*, *B. cenocepacia*, *B. stabilis* and *B. pyrrocinia* were found to contain a FDH gene.
2. The complete FDH gene of 5 strains of BCC was equal in length of nucleotide sequence for 1,161 bp encoding 386 amino acid residues.
3. The 5 BCC FDHs showed a high amino acid sequence identity (91-96%) amongst themselves and also a relatively high sequence identity (65-70%) to those reported bacterial NAD⁺-FDHs.
4. FDH from pBstFDH clone was purified to homogeneity and characterized its properties. It was proven to be a novel NADP⁺-FDH.
5. Gln223Asp mutant of FDH from *B. stabilis* 15516 showed completely change in coenzyme preference from NADP⁺ to NAD⁺.

REFERENCES

- Aharonowitz, Y., and Friedrich, C. G. 1980. Alanine dehydrogenase of the beta-lactam antibiotic producer *Streptomyces clavuligerus*. *Arch. Microbiol.* 125: 137–142.
- Allais, J. J., Louktibi, A., and Baratti, J. 1983. Oxidation of methanol by the yeast *Pichia pastoris*. Purification and properties of the formate dehydrogenase. *Agric. Biol. Chem.* 47: 2547–2554.
- Allen, S. J., and Holbrook, J. J. 1995. Isolation, sequence and overexpression of the gene encoding NAD-dependent formate dehydrogenase from the methylotrophic yeast *Candida methylica*. *Gene.* 162: 99–104.
- Andreadeli, A., Platis, D., Tishkov, V. I., Popov, V. O., and Labrou, N. E. 2008. Structure-guided alteration of coenzyme specificity of formate dehydrogenase by saturation mutagenesis to enable efficient utilization of NADP⁺. *FEBS J.* 275: 3859–3869.
- Asano, Y., Sekigawa, T., Inukai, H., and Nakazawa, A. 1988. Purification and properties of formate dehydrogenase from *Moraxella* sp. strain C-1. *J. Bacteriol.* 170: 3189–3193.
- Avilova, T. V., Egorova, O. A., Loanesyan, L. S., and Egorov, A. M. 1985. Biosynthesis, isolation and properties of NAD-dependent formate dehydrogenase from the yeast *Candida methylica*. *Eur. J. Biochem.* 152: 657–662.
- Babel, W., and Mothes, G. 1980. The role of formate dehydrogenase in serine pathway bacteria. (in German). *Z. Allg. Mikrobiol.* 20:167–175.
- Bellion, E., and Tan, F. 1987. An NAD⁺-dependent alanine dehydrogenase from a methylotrophic bacterium. *Biochem. J.* 244: 565–570.
- Bommarius, A. S., Schwarm, M., Stingl, K., Kottenhahn, M., Huthmacher, K., and Drauz, K. 1995. Synthesis and use of enantiometrically pure *tert*-leucine. *Tetrahedron-Asymmetry.* 6: 2851–2888.
- Brunhuber, N. M. W., and Blanchard, J. S. 1994. The biochemistry and enzymology of amino acid dehydrogenases. *Crit. Rev. Biochem. Mol. Biol.* 29: 415–467.
- Caballero, F. J., Cardenas, J., and Castillo, F. 1989. Purification and properties of L-alanine dehydrogenase of the phototrophic bacterium *Rhodobacter capsulatus* E1F1. *J. Bacteriol.* 171: 3205–3210.

- Carrea, G., Bovara, R., Longhi, R., and Barani, R. 1984. Enzymatic reduction of dehydrocholic acid to 12-ketochenodeoxycholic acid with NADH regeneration. *Enzyme Microb. Technol.* 6: 307–311.
- Carugo, O., and Argos, P. 1997a. NADP-dependent enzymes. I: Conserved stereochemistry of cofactor binding. *Proteins.* 28: 10–28.
- Carugo, O., and Argos, P. 1997b. NADP-dependent enzymes. II: Evolution of the mono- and dinucleotide binding domains. *Proteins.* 28: 29–40.
- Chiarini, L., Bevivino, A., Dalmastr, I. C., Tabacchioni, S., and Visca, P. 2006. *Burkholderia cepacia* complex species: Health hazards and biotechnological potential. *Trends in Microbiol.* 14: 277–286.
- Chow, C. M., and Raj Bhandary, U. L. 1993. Developmental regulation of the gene for formate dehydrogenase in *Neurospora crassa*. *J. Bacteriol.* 175: 3703–3709.
- Chowdhury, E. K., Saitoh, T., Nagata, S., Ashiuchi, M., and Misono, H. 1998. Alanine dehydrogenase from *Enterobacter aerogenes*: Purification, characterization, and primary structure. *Biosci. Biotechnol. Biochem.* 62: 2357–2363.
- Colas des Francs-Small, C., Ambard-Bretteville, F., Small, I. D., and Remy, R. 1993. Identification of a major soluble protein in mitochondria from nonphotosynthetic tissues as NAD-dependent formate dehydrogenase. *Plant Physiol.* 102: 1171–1177.
- Damrau, F. 1962. Benign prostatic hypertrophy: Amino acid therapy for symptomatic relief. *J. Am. Geriatrics. Soc.* 10: 426–430.
- Davidson, D. C. 1951. Studies on plant formic dehydrogenase. *Biochem. J.* 49: 520–526.
- Davies, P., and Mosbach, K. 1974. The application of immobilized NAD⁺ in an enzyme electrode and in model enzyme reactor. *Biochim. Biophys. Acta.* 370: 329–338.
- Dower, G. E., Yakush, A., Nazzal, S. B., Jutzy, R. V., and Ruiz, C. E. 1988. Deriving the 12-lead electrocardiogram from four (EASI) electrodes. *J. Electrocard.*, 21: 182–187
- Drauz, K., and Waldmann, H. editors. 1995. Enzyme catalysis in organic synthesis. Weinheim, Germany: VCH. p 597.
- Egorov, A. M., Avilova, T. V. Dikov, M. M., Popov, V. O., Rodionov, Y. V., and Berezin, I. V. 1979. NAD-dependent formate dehydrogenase from methylotrophic bacterium, strain 1. *Eur. J. Biochem.* 99: 569–576.

- Eisenberg, M. A., and Star, C. 1968. Synthesis of 7-oxo-8-aminopelargonic acid, a biotin vitamin, in cell-free extracts of *Escherichia coli* biotin auxotrophs. *J. Bacteriol.* 96: 1291–1297.
- Ernst, M., Kaup, B., Muller, M., Bringer-Meyer, S., and Sahm, H. 2005. Enantioselective reduction of carbonyl compounds by whole-cell biotransformation, combining a formate dehydrogenase and a (*R*)-specific alcohol dehydrogenase. *Appl. Microbiol. Biotechnol.* 66: 629–634.
- Farinelli, M. P., Fry, D. W., and Richardson, K. E. 1983. Isolation, purification, and partial characterization of formate dehydrogenase from soybean seed. *Plant Physiol.* 73: 858–859.
- Federick, M. A., Roger, B., Robert, E. K., David, D. M., Seidman, J. G. John, A. S., and Kevin, S. 1995. *Short protocols in molecular biology*. 3rd ed. USA. John Wiley & Sons. pp. 2–12.
- Feinblatt, H. M., and Gant, J. C. 1958. Palliative treatment of benign prostatic hypertrophy value of glycine-alanine-glutamic acid combination. *J. Maine. Med. Assoc.* 46: 99–102.
- Ferry, J. G. 1990. Formate dehydrogenase. *FEMS Microbiol. Rev.* 7: 377–382.
- Fiolitakis, E., and Wandrey, C. 1983. *Enzyme Technol. Proc.* (Vol. III), Rotenburg Fermentation Symposium 1982, (Lafferty, R. M., ed.), Springer-Verlag. pp. 273–284.
- Galkin, A., Kulakova, L., Ashida, H., Sawa, Y., and Esaki, N. 1999. Cold-adapted alanine dehydrogenases from two antarctic bacterial strains: gene cloning, protein characterization, and comparison with mesophilic and thermophilic counterparts. *Appl. Envir. Microbiol.* 65: 4014–4020.
- Galkin, A., Kulakova, L., Tishkov, V., Esaki, N., and Soda, K. 1995. Cloning of formate dehydrogenase gene from a methanol-utilizing bacterium *Mycobacterium vaccae* N10. *Appli. Microbiol. Biotechnol.* 44: 479–483.
- Galkin, A., Kulakova, L., Yamamoto, H., Tanizawa, K., Tanaka, H., Esaki, N., and Soda, K. 1997a. Conversion of α -keto acids to D-amino acids by coupling of four enzyme reactions. *J. Ferment. Bioeng.* 83: 299–300.

- Galkin, A., Kulakova, L., Yoshimura, T., Soda, K., and Esaki, N. 1997b. Synthesis of optically active amino acids from α -keto acids with *Escherichia coli* cells expressing heterologous genes. *Appl. Envir. Microb.* 63: 4651–4656.
- Germano, G. J., and Anderson, K. E. 1968. Purification and properties of L-alanine dehydrogenase from *Desulfovibrio desulfuricans*. *J. Bacteriol.* 96: 55–60.
- Goncalves, L. P. B., Antunes, O. A. C., Pinto, G. F., and Oestreicher. 2000. Simultaneous enzymatic synthesis of (S)-3-fluoroalanine and (R)-3-fluoroalanine acid. *Tetrahedron- Asymmetry.* 11: 1465–1468.
- Graham, A., and Boxer, D. H. 1981. The organization of formate dehydrogenase in the cytoplasmic membrane of *Escherichia coli*. *Biochem. J.* 195: 627–637.
- Gu, K. F., and Chang, T. M. 1990. Conversion of ammonia or urea into essential amino acids, L-leucine, L-valine, and L-isoleucine using artificial cells containing an immobilized multienzyme system and dextran-NAD L-lactic dehydrogenase for coenzyme recycling. *Appl. Biochem. Biotechnol.* 26: 115–124.
- Gul-Karaguler, N., Sessions, R. B., Clarke, A. R., and Holbrook, J. 2001. A single mutation in the NAD-specific formate dehydrogenase from *Candida methylca* allows the enzyme to use NADP. *Biotechnol. Lett.* 23: 283–287.
- Hashimoto, A., Nishikawa, T., Oka, T., Takahashi, K., and Hayashi, T. 1992. Determination of free amino acid enantiomers in rat brain and serum by high-performance liquid chromatography after derivatization with N-tert-butylloxycarbonyl-L-cysteine and o-phthaldialdehyde. *J. Chromatography.* 582: 41–48.
- Hatch, M., Bourke, E., and Costello, J. 1977. New enzymic method for serum oxalate determination. *Clin. Chem.* 23: 76–78.
- Hatrongjitt, R. 2004. Alanine production by *Escherichia coli* transformed with alanine dehydrogenase and formate dehydrogenase genes. Master's Thesis, Department of Biochemistry, Faculty of Science, Chulalongkorn University.
- Heungens, K. K., and Parke, J. L. 2001. Post infection biological control of oomycete pathogens of pea by *Burkholderia cepacia* AMMDR1. *Phytopathology.* 91: 383–391.

- Holes, P., Kleerebezein, M., Kuipers, O. P., Ferain, T., Delcour, J., and DeVos, W. M. 2003. Process for the production of alanine by recombinant microorganisms. *United States Patent: 662720*. p 13.
- Hollenberg, C. P., and Janowicz, Z. 1989. DNA-molecules coding for FMDH control regions and structured gene for a protein having FMDH activity and their uses. *European patent EP 0299 108 A1, Bulletin 89/03*.
- Hou, C. T., Patel, R. N., Laskin, A. I., and Barnabe, N. 1982. NAD-linked formate dehydrogenase from methanol-grown *Pichia pastoris* NRRL-Y-7556. *Arch. Biochem. Biophys.* 216: 296-305.
- Hummel, W. 1999. Large-scale applications of NAD(P)-dependent oxidoreductases: Recent developments. *Trends Biotechnol.* 17: 487–492.
- Hummel, W., and Kula, M. R., 1989. Dehydrogenases for the synthesis of chiral compounds. *Eur. J. Biochem* 184: 1–13.
- Iida, M., Kitamura-Kimura, K., Maeda, H., and Mineki, S. 1992. Purification and characterization of a NAD⁺-dependent formate dehydrogenase produced by *Paracoccus* sp. *Biosci. Biotechnol. Biochem.* 56: 1966–1970.
- Irwin, J. A., Gudmundsson, H. M., Marteinson, V. T., Hreggvidsson, G. O., Lanzetti, A. J., Alfredsson, G. A., and Engel, P. C. 2001. Characterization of alanine and malate dehydrogenases from a marine psychrophile strain PA-43. *Extremophiles.* 5: 199–211.
- Itoh, N., Morikawa, R., Itoh, N., and Morikawa, R. 1983. Crystallization and properties of L-alanine dehydrogenase from *Streptomyces phaeochromogenes*. *Agric. Biol. Chem.* 47: 2511–2519.
- Izumi, Y., Kanzaki, H., Morita, S., Futazuka, H., and Yamada, H. 1989. Characterization of crystalline formate dehydrogenase from *Candida methanolica*. *Eur. J. Biochem.* 182: 333–341.
- Johnson, P. A., and Quayle, J. R. 1964. Microbial growth on C₁ compounds. 6. Oxidation of methanol, formaldehyde and formate by methanol-grown *Pseudomonas* AM1. *Biochem. J.* 93: 281–290.
- Jormakka, M., Byrne, B., and Iwata, S. 2003. Formate dehydrogenase-a versatile enzyme in changing environments. *Curr. Opin. Struct. Biol.* 13: 418–423.

- Kato, N., Kano, M., Tani, Y., and Ogata, K. 1974. Purification and characterization of formate dehydrogenase in a methanol-utilizing yeast, *Kloeckera* sp. No. 2201. *Agric. Biol. Chem.* 38: 111–116.
- Kato, N., Sahn, H., and Wagner, F. 1979. Steady-state kinetics of formaldehyde dehydrogenase and formate dehydrogenase from methanol-utilizing yeast, *Candida boidinii*. *Biochim. Biophys. Acta.* 566: 12–20.
- Kato, Y., Fukumoto, K., and Asano, Y. 1993. Enzymatic synthesis of L- β -chloroalanine using amino acid dehydrogenase. *Appl. Microbiol. Biotechnol.* 39: 301–304.
- Keradjopoulos, D., and Holldorf, A. W. 1979. Purification and properties of alanine dehydrogenase from *Halobacterium salinarium*. *Biochim. Biophys. Acta.* 570: 1–10
- Kim, E. K., and Fitt, P. S. 1977. Partial Purification and properties of *Halobacterium cutirubrum* L-alanine dehydrogenase. *Biochem. J.* 161: 313–320.
- Klibanov, A. M., Alberti, B. N., and Zale, S. E. 1982. Enzymatic synthesis of formic acid from H₂ and CO₂ and production of hydrogen from formic acid. *Biotechnol. Bioeng.* 24: 25–36.
- Kuroda, S., Tanizawa, K., Sakamoto, Y., Tanaka, H., and Soda, K. 1990. Alanine dehydrogenases from two *Bacillus* species with distinct thermostabilities: Molecular cloning, DNA and protein sequence determination, and structural comparison with other NAD(P)⁽⁺⁾-dependent dehydrogenases. *Biochemistry.* 29: 1009–1015.
- Kwan, C. H. R., Hon, Y.T. P., and Renneberg, R. 2004. Amperometric biosensor for rapid determination of alanine. *Analytica. Chimica. Acta.* 523: 81–88.
- Lin, S-S., Miyawaki, O., and Nakamura, K. 1997. Continuous production of L-Alanine with NADH regeneration by a nanofiltration membrane reactor. *Biosci. Biotech. Biochem.* 61: 2029–2033.
- LiPuma, J. J. 2007. Update on *Burkholderia* nomenclature and resistance. *Clin. Microbiol. News.* 29: 65–69.
- Lowry, O. H., Rosebrough, N. J., Farr, A. L., and Randall, R. J. 1951. Protein measurement with Folin phenol reagent. *J. Biol. Chem.* 193: 265–275.

- Mahenthiralingam, E., Bischof, J., Byrne, S. K., Radomski, C., Davies, J. E., AV-Gay, Y., and Vandamme, P. 2000. DNA-based diagnostic approaches for identification of *Burkholderia cepacia* complex, *Burkholderia vietnamiensis*, *Burkholderia multivorans*, *Burkholderia stabilis*, and *Burkholderia cepacia* genomovar I and III. *J. Clin. Microbiol.* 38: 3165–3173.
- Mathews, M. B., and Vennesland, B. 1950. Enzymic oxidation of formic acid. *J. Biol. Chem.* 186: 667–682.
- Matsunaga, T., and Kamiya, S. 1987. Use of magnetic particles isolated from magnetotactic bacteria for enzyme immobilization. *Appl. Microbiol. Biotechnol.* 26: 328–332.
- Mueller, P., and Werner, D. 1982. Alanine dehydrogenase from bacterioids and free living cells of *Rhizobium japonicum*. *Z. Naturforsch. C.* 37: 927-936.
- Muller, U., Willnow, P., Rusching, U., and Hopner, T. 1978. Formate dehydrogenase from *Pseudomonas oxalaticus*. *Eur. J. Biochem.* 83: 485–498.
- Nagata, Y., Iida, T., and Sakai, M. 2001. Enantiomeric resolution of amino acids by thin-layer chromatography. *J. Molecular Catalysis B: Enzymatic.* 12: 105–108.
- Nakamura, K., Aizawa, M., and Miyawaki, O. 1988. Electroenzymology coenzyme regeneration. Springer-Verlag, Berlin, Heidelberg. p 100.
- Nanba, H., Takaoka, Y., and Hasegawa, J. 2003a. Purification and characterization of formate dehydrogenase from *Ancylobacter aquaticus* strain KNK607M and cloning of the gene. *Biosci. Biotechnol. Biochem.* 67: 720–728.
- Nanba, H., Takaoka, Y., and Hasegawa, J. 2003b. Purification and characterization of formate dehydrogenase from *Ancylobacter aquaticus* strain KNK607M and cloning of the gene. *Biosci. Biotechnol. Biochem.* 67: 720–728.
- Nath, P. K., Izumi, Y., and Yamada, H. 1990. NADH production from NAD⁺ with a formate dehydrogenase system involving immobilized cells of a methylotrophic *Arthrobacter* strain. *Enzymes Microb. Technol.* 12: 28–32.
- Nitta, Y., Yasuda, Y., Tochikubo, K., and Hachisuka, Y. 1974. L-Amino acid dehydrogenases in *Bacillus subtilis* cells. *J. Bacteriol.* 117: 588–592.
- Ohshima, T., and Soda, K. 1979. Purification and properties of alanine dehydrogenase from *Bacillus sphaericus*. *Eur. J. Biochem.* 100: 29–39.

- Ohshima, T., and Soda, K. 1990. Biochemistry and biotechnology of amino acid dehydrogenases. *Adv. Biochem. Eng. Biotechnol.* 42: 187–209.
- Ohshima, T., Wandrey, C., and Conrad, D. 1989. Continuous production of 3-fluoro-L-alanine dehydrogenase. *Biotechnol. Bioeng.* 34: 394–397.
- Ohshima, T., Wandrey, C., Kula, M-R. and Soda, K. 1985. Improvement of L-leucine production in a continuously operated enzyme membrane reactor. *Biotechnol. Bioeng.* 27: 1616–1618.
- Ohyama, T., and Yamazaki, I. 1974. Purification and some properties of formate dehydrogenase. *J. Biochem.* 75: 1257–1263.
- Olson, B. J., Skavdahl, M., Ramberg, H., Osterman, J. C., and Markwell, J. 2000. Formate dehydrogenase in *Arabidopsis thaliana*: Characterization and possible targeting to the chloroplast. *Plant Sci.* 159: 205–212.
- Peacock, D., and Boulter, D. 1970. Kinetic studies of formate dehydrogenase. *Biochem. J.* 120: 763–769.
- Peters, J. 1998. Dehydrogenases: Characteristics, design of reaction conditions, and applications. In: Rehm, H-J. Reed, G. (ed.), *Biotechnology*, 2nd edition, Vol. 8a. pp 393-474. Weinheim, Germany: Wiley-VCH.
- Phungsangtham, P. 1997. Screening of pyridine nucleotide-dependent L-alanine dehydrogenase production of the enzyme. Master's Thesis, Department of Biochemistry, Faculty of Science, Chulalongkorn University.
- Poomipark, N. 2000. Nucleotide sequencing and cloning of alanine dehydrogenase gene from *Aeromonas hydrophila*. Master's Thesis, Department of Biochemistry, Faculty of Science, Chulalongkorn University.
- Popov, V. O., and Lamzin, V. S. 1994. NAD⁺ dependent formate dehydrogenase. *Biochem. J.* 301: 625–643.
- Popov, V. O., and Tishkov, V. I., 2003. NAD⁺-dependent formate dehydrogenase. From a model enzyme to a versatile biocatalyst. In: Uversky, V.N. (ed.), *Protein Structures: Kaleidoscope of Structural Properties and Functions Research*. pp. 441–473. Singapore: Signpost, Kerala.
- Porumb, H., Vancea, D., Muresan, L., Presecan, E., Lascu, I., Petrescu, I., Porumb, T., Pop, R., and Barzu, O. 1987. Structural and catalytic properties of L-alanine dehydrogenase from *Bacillus cereus*. *J. Biol. Chem.* 262: 4610–4615.

- Rissom, S., Schwarz-Linek, U., Vogel, M., Tishkov, V. I., and Kragl, U. 1997. Synthesis of chiral epsilon-lactones in a two-enzyme system of cyclohexanone mono-oxygenase and formate dehydrogenase with integrated bubble free aeration. *Tetrahedron-Asymmetry*. 8: 2523–2526.
- Roger, C. H. K., Phoebe, Y. T. H., and Reinhard, R. 2004. Amperometric biosensor for rapid determination of alanine. *Analytica Chimica Acta*. 523: 81–88.
- Rowell, P., and Stewart, W. D. P. 1976. Alanine dehydrogenase of the N₂-fixing blue-green alga, *Anabaena cylindrica*. *Arch. Microbiol.* 107: 115–124.
- Rozzell, J. D., Hua, L., Mayhew, M., and Novick, S. 2004. Mutants of enzymes and methods for their use. US Patent Application Publication US2004/0115691, 17.06.2004.
- Sakai, Y., Murdanoto, A. P., Konishi, T., Iwamatsu, A., and Kato, N. 1997. Regulation of the formate dehydrogenase gene, FDHI, in the methylotrophic yeast *Candida boidinii* and growth characteristics of an FDHI-disrupted strain on methanal, methylamine and choline. *J. Bacteriol.* 179: 4480–4485.
- Sakamoto, Y., Nagata, S., Esaki, N., Tanaka, H., and Soda, K. 1990. Gene cloning, purification and characterization of thermostable alanine dehydrogenase of *Bacillus stearothermophilus*. *J. Ferment. Bioeng.* 69: 154–158.
- Saleeba, J. A., Cobbett, C. S., and Hynes, M. J. 1992. Characterization of the *amd* A-regulated *aciA* gene of *Aspergillus nidulans*. *Mol. Gen. Genet.* 235: 349–358.
- Sambrook, J., Fritsch, E. F., and Maniatis, T. 2000. Molecular Cloning-A Laboratory Manual, 2nd Edn.; Cold Spring Harbor Laboratory Press: USA.
- Sawa, Y., Tani, M., Murata, K., Shibata, H., and Ochiai, H. 1994. Purification and characterization of alanine dehydrogenase from a cyanobacterium, *phormidium lapidium*. *J. Biochem.* 116: 995–1000.
- Schmidt, E., Vasic-Racki, D., and Wandrey, C. 1987. Enzymatic production of L-phenylalanine out of the racemic mixture of D, L-phenylactate. *Appl. Microbiol. Biotechnol.* 26: 42–48.
- Schutte, H., Flossdorf, J., Sahn, H., and Kula, M. R. 1976. Purification and properties of formaldehyde dehydrogenase and formate dehydrogenase from *Candida boidinii*. *Eur. J. Biochem.* 62: 151–160.

- Schwarz-Linek, U., Krodel, A., Ludwig, F. A., Schulze, A., Rissom, S., Kragl, U., Tishkov, V. I., and Vogel, M. 2001. Synthesis of natural product precursors by Baeyer-Villiger oxidation with cyclohexanone monooxygenase from *Acinetobacter*. *Synthesis-Stuttgart*. 33: 947–951.
- Seelbach, K., Riebel, B., Hummel, W., Kula, M. R., Tishkov, V. I., Egorov, A. M., Wandrey, C., and Kragl, U. 1996. A novel, efficient regenerating method of NADPH using a new formate dehydrogenase. *Tetrahedron Lett.* 37: 1377–1380.
- Serov, A. E., Popova, A. S., Fedorchuk, V. V., and Tishkov, V. I. 2002. Engineering of coenzyme specificity of formate dehydrogenase from *Saccharomyces cerevisiae*. *Biochem. J.* 367: 841–847.
- Shaked, Z., and Whitesides, G. M. 1980. Enzyme-catalyzed organic synthesis: NADH regeneration by using formate dehydrogenase. *J. Am. Chem. Soc.* 102: 7104–7105.
- Smith, M. T., and Emerich, D. W. 1993. Alanine dehydrogenase from soybean nodule bacteroids: Purification and properties. *Arch. Biochem. Biophys.* 304: 379–385.
- Suye, S. I., Kawagoe, M., and Inuta, S. 1992. Enzymatic production of L-alanine malic acid with malic enzyme and alanine dehydrogenase with coenzyme regeneration. *Can. J. Biochem. Eng.* 34: 306–312.
- Takamatsu, S., Yamamoto, K., Tosa, T., and Chibata, I. 1981. Stabilization of L-aspartate β -decarboxylase activity of *Pseudomonas dacunhae* immobilized carrageenan. *J. Ferment. Technol.* 59: 489–493.
- Tamura, K., Dudley, J., Nei, M., and Kumar, S. 2007. MEGA4: Molecular evolutionary genetics analysis (MEGA) software version 4.0. *Mol. Biol. Evol.* 24: 1596–1599.
- Tishkov, V. I., and Popov, V. O. 2004. Catalytic mechanism and application of formate dehydrogenase. *Biochemistry (Mosc.)*. 69: 1252–1267.
- Tishkov, V. I., and Popov, V. O. 2006. Protein engineering of formate dehydrogenase. *Biomol. Eng.* 23: 89–110.
- Tishkov, V. I., Galkin, A. G., Marchenko, G. N., Tsygankov, Y. D., and Egorov, A. M. 1993. Formate dehydrogenase from methylotrophic bacterium *Pseudomonas* sp. 101: Gene cloning and expression in *Escherichia coli*. *Biotechnol. Appl. Biochem.* 18: 201–207.

- Tishkov, V. I., Galkin, A. G., and Egorov, A. M., 1991. NAD-dependent formate dehydrogenase of methylotrophic bacteria *Pseudomonas* sp.101: Cloning, expression, and study of the gene structure. *Dokl. Akad. Nauk SSSR*. 317: 745–748.
- Tolxdorff-Neutzling, R., and Klemme, J. H. 1982. Metabolic role and regulation of L-alanine dehydrogenase in *Rhodopseudomonas capsulate*. *FEMS Microbiol. Lett.* 13: 155–159.
- Uotila, L., and Koivusalo, M. 1979. Purification of formaldehyde and formate dehydrogenases from pea seeds by affinity chromatography and S-formylglutathione as the intermediate of formaldehyde metabolism. *Arch. Biochem. Biophys.* 196: 33–45.
- Vali, Z., Kilar, F., Lakatos, S., Venyaminov, S. A., and Zavodszky, P. 1980. L-alanine dehydrogenase from *Thermus thermophilus*. *Biochim. Biophys. Acta.* 615: 34–47.
- Van Dijken, J. P., Oostra-Demkes, G. J. Otto, R., and Harder, W. 1976. S-formylglutathione: The substrate for formate dehydrogenase in methanol-utilizing yeast. *Arch. Microbiol.* 111: 77–83.
- Vancura, A., Vancorova, I., Volc, J., Ones, S. K. T., and Flieger, M. 1989. Alanine dehydrogenase from *Streptomyces fradiae*; purification and properties. *Eur. J. Biochem.* 179: 221–227.
- Vandamme, P., Henry, D., Coenye, T., Nzula, S., Vancanneyt, M., LiPuma, J. J., Speert, D. P., Govan, J. R., and Mahenthiralingam, E. 2002. *Burkholderia anthina* sp. nov. and *Burkholderia pyrrocinia*, two additional *Burkholderia cepacia* complex bacteria, may confound results of new molecular diagnostic tools. *FEMS Immunol. Med. Microbiol.* 33: 143–149.
- Vinals, C. Depiereux, E., and Feytmans, E. 1993. Prediction of structurally conserved regions of D-specific hydroxyl acid dehydrogenases by multiple alignments with formate dehydrogenase. *Biochem. Biophys. Res. Commun.* 192: 182–188.
- Wandrey, C., Fiolitakis, E., Wichmann, U., and Kula, M. R. 1984. L-amino acid from a racemic mixture of α -hydroxy acids. *Ann. N.Y. acad. Sci.* 434: 91–94.
- Whalen, W. A., and Berg, C. M. 1982. Analysis of an *avtA::Mu d1(Ap lac)* mutant: Metabolic role of transaminase C. *J. Bacteriol.* 150: 739–746.

- Wiame, J., and Pierard, A. 1955. Occurrence of an L(+)-alanine-dehydrogenase in *Bacillus subtilis*. *Nature (London)*. 176: 1073–1075.
- Wichmann, R., and Vasic-Racki, D. 2005. Cofactor regeneration at the lab scale. *Adv. Biochem Eng/Biotechnol.* 92: 225–260.
- Wichmann, R., Wandrey, C., Buckmann, A. F., and Kula, M. R. 1981. Continuous enzymatic transformation in an enzyme membrane reactor with simultaneous NAD(H) regeneration. *Biotechnol. Bioeng.* 23: 2789–2802.
- Wierenga, R. K., Terpstra, P., and Hol, W. G. J. 1986. Prediction of the occurrence of the ADP-binding beta alpha beta-fold in proteins, using an amino acid sequence fingerprint. *J. Mol. Biol.* 187: 101–107.
- Wong, C.-H., and Whitesides, G. 1982. Enzyme-catalyzed organic synthesis: NAD(P)H cofactor regeneration using ethanol-alcohol dehydrogenase-aldehyde dehydrogenase and methanol-alcohol dehydrogenase-aldehyde dehydrogenase-formate dehydrogenase. *J. Org. Chem.* 47: 2861–2818.
- Wong, C.-H., and Whitesides, G. M. 1981. Enzyme-catalyzed organic synthesis: NAD(P)H cofactor regeneration by using glucose 6-phosphate and the glucose-6-phosphate dehydrogenase from *Leuconostoc mesenteroides*. *J. Am. Chem. Soc.* 103: 4890–4899.
- Yamamoto, K., Tosa, T., and Chibata, I. 1980. Continuous production of L-alanine using *Pseudomonas dacungae* immobilization carrageenan. *Biotech. Bioeng.* 22: 2045–2054.
- Yoshida, A., and Freese, E. 1964. Purification and chemical characterization of alanine dehydrogenase of *Bacillus subtilis*. *Biochim. Biophys. Acta. (BBA) Specialized Section on Enzymological Subjects.* 92: 33–43.
- Yoshida, A., and Freese, E. 1965. Enzymic properties of alanine dehydrogenase of *Bacillus subtilis*. *Biochim. Biophys. Acta.* 96: 248–262.
- Zello, G. A., Wykes, L. J., Ball, R. O., and Pencharz, P. B. 1995. Recent advances in methods of assessing dietary amino acid requirements for adult humans. *J. Nutr.* 125: 2907–2915.



APPENDICES

สถาบันวิทยบริการ
จุฬาลงกรณ์มหาวิทยาลัย

APPENDIX B**Preparation for protein determination**

Reagent for determination of protein concentration (modified from Lowry, *et al.*, 1951)

Solution A (0.5% copper sulfate and 1% potassium tartate, pH 7.0)

Potassium tartate	1	g
Copper sulfate	0.5	g

Adjusted pH to 7.0 and adjust the solution volume to 100 ml.

Solution B (2% sodium carbonate and 1 N sodium hydroxide)

Sodium carbonate	20	g
Sodium hydroxide	4	g

Dissolved in distilled water to 1 liter.

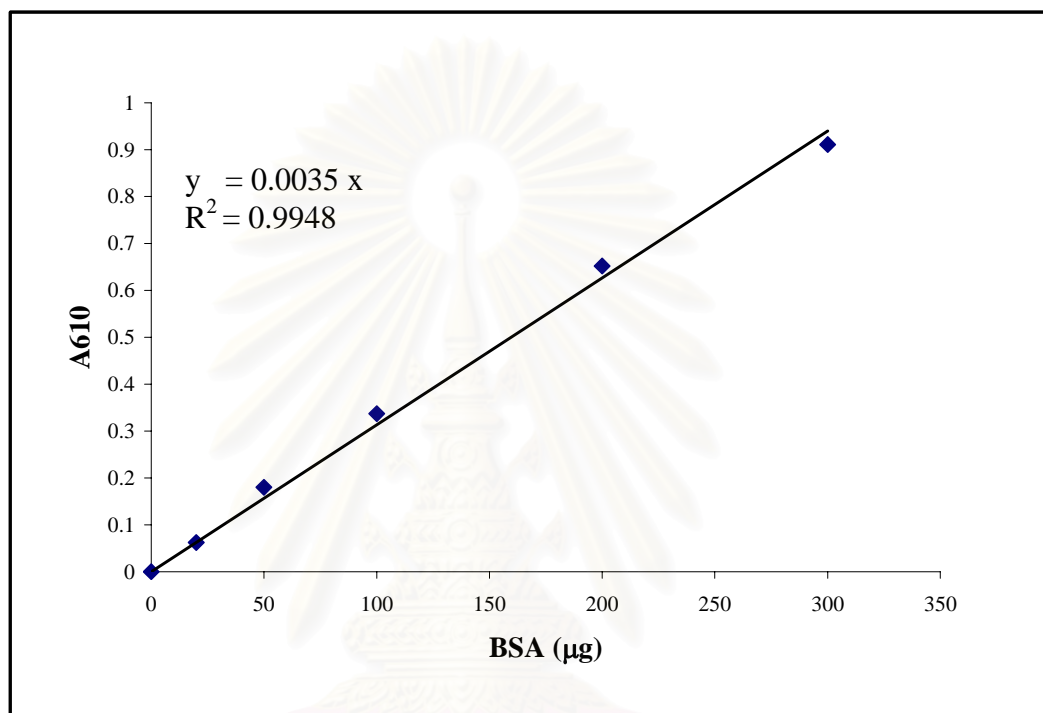
Solution C (phenol reagent)

Folin-Ciocalteu phenol reagent used in this work was reagent grade.

สถาบันวิทยบริการ
จุฬาลงกรณ์มหาวิทยาลัย

APPENDIX C

Standard curve for protein determination by Lowry's Method (1951)



สถาบันวิทยบริการ
จุฬาลงกรณ์มหาวิทยาลัย

APPENDIX E

Preparation for denaturing polyacrylamide gel electrophoresis

1. stock solutions

2 M Tris-HCl pH 8.8

Tris (hydroxymethyl)-aminomethane 24.2 g

Adjusted pH to 8.8 with 1 M HCl and adjusted volume to 100 ml with distilled water.

1 M Tris-HCl pH 6.8

Tris (hydroxymethyl)-aminomethane 12.1 g

Adjusted pH to 6.8 with 1 M HCl and adjusted volume to 100 ml with distilled water.

10 % SDS (W/V)

Sodium dodecyl sulfate (SDS) 10 g

Added distilled water to a total volume of 100 ml.

50 % Glycerol (W/V)

100 % Glycerol 50 ml

Added 50 ml of distilled water.

1 % Bromophenol blue (W/V)

Bromophenol blue 100 ml

Brought to 10 ml with distilled water and stirred until dissolved.

Filtration will remove aggregated dye.

2. Working solutions

Solution A (30 % (W/V) acrylamide, 0.8 % (W/V) bis-acrylamide)

Acrylamide 29.2 g

N, N'-methylene-bis-acrylamide 0.8 g

Adjusted volume to 100 ml with distilled water and stirred until completely dissolved.

APPENDIX E (continued)**Solution B (1.5 M Tris-HCl pH 8.8, 0.4 % SDS)**

2 M Tris-HCl (pH 8.8)	75 ml
10 % SDS	4 ml
Distilled water	21 ml

Solution C (0.5 M Tris-HCl pH 6.8, 0.4 % SDS)

1 M Tris-HCl pH 8.8	50 ml
10 % SDS	4 ml
Distilled water	46 ml

10 % Ammonium persulfate

Ammonium persulfate	0.5 g
Distilled water	5 ml

Electrophoresis buffer (25 mM Tris, 192 mM glycine, 0.1 % SDS

Tris (hydroxymethyl)-aminomethane	3.0 g
Glycine	14.4 g
SDS	1.0 g

Adjusted volume to 1 litre with distilled water (pH should be approximately 8.3).

5 x Sample buffer (60 mM Tris-HCL pH 6.8, 25 % glycerol, 2 % SDS, 0.1% bromophenol blue, 14.4 mM 2-mercaptoethanol)

1 M Tris-HCl pH 6.8	0.6 ml
50 % Glycerol	5.0 ml
10 % SDS	2.0 ml
2-Mercaptoethanol	0.5 ml
1 % Bromophenol blue	1.0 ml
Distilled water	0.9 ml

APPENDIX E (continued)

3. SDS-PAGE

10 % Separating gel

Solution A	3.3 ml
Solution B	2.5 ml
Distilled water	4.2 ml
10 % Ammonium persulfate	50 μ l
TEMED	5 μ l

5.0 % Stacking gel

Solution A	0.67 ml
Solution C	1.0 ml
Distilled water	2.3 ml
10 % Ammonium persulfate	30 μ l
TEMED	5 μ l

4. Protein staining solution

Staining solution, 1 litre

Coomassie brilliant blue R-250	1.0 g
Methanol	450 ml
H ₂ O	450 ml
Glacial acetic acid	100 ml

Destaining solution, 1 litre

Methanol	100 ml
Glacial acetic acid	100 ml
H ₂ O	800 ml

APPENDIX F

Preparation for non-denaturing polyacrylamide gel electrophoresis (Native-PAGE)

1. Stock solutions

2 M Tris-HCl (pH 8.8)

Tris (hydroxymethyl)-aminomethane 24.2 g

Adjusted pH to 8.8 with 1 N HCl and adjusted volume to 100 ml with distilled water.

1 M Tris-HCl (pH 6.8)

Tris (hydroxymethyl)-aminomethane 12.1 g

Adjusted pH to 6.8 with 1 N HCl and adjusted volume to 100 ml with distilled water.

1% (w/v) Bromophenol blue

Bromophenol blue 100 mg

Brought to 10 ml with distilled water and stirred until dissolved.

The aggregated dye was removed by filtration.

2. Working solutions

Solution A (30% (w/v) acrylamide, 0.8% (w/v) bis-acrylamide)

Acrylamide 29.2 g

N, N'-methylene-bis-acrylamide 0.8 g

Adjusted volume to 100 ml with distilled water.

Solution B (1.5 M Tris-HCl, pH 8.8)

2 M Tris-HCl (pH 8.8) 75 ml

Distilled water 25 ml

Solution C (0.5 M Tris-HCl, pH 6.8)

1 M Tris-HCl (pH 6.8) 50 ml

Distilled water 50 ml

APPENDIX F (continued)**10% (w/v) Ammonium persulfate**

Ammonium persulfate	0.5	g
Distilled water	5.0	ml

Electrophoresis buffer (25 mM Tris, 192 mM glycine)

Tris (hydroxymethyl)-aminomethane	3.0	g
Glycine	14.4	ml

Dissolved and adjusted to total volume 1 liter with distilled water
(final pH should be approximately 8.3)

5x Sample buffer (312.5 mM Tris-HCl pH 6.8, 50% (v/v) glycerol, 1% (v/v) bromophenol blue)

1 M Tris-HCl (pH 6.8)	0.6	ml
Glycerol	5.0	ml
1% Bromophenol blue	0.5	ml
Distilled water	1.4	ml

3. Native-PAGE**7.7% Separating gel**

Solution A	2.6	ml
Solution B	2.5	ml
Distilled water	4.9	ml
10% (w/v) Ammonium persulfate	50	μ l
TEMED	5.0	μ l

5.0% Stacking gel

Solution A	0.67	ml
Solution C	1.0	ml
Distilled water	2.3	ml
10% (w/v) Ammonium persulfate	30	μ l
TEMED	5.0	μ l

APPENDIX F (continued)**4. Protein staining solution****Staining solution, 1 liter**

Coomassie brilliant blue R-250	1.0	g
Glacial acetic acid	100	ml
Methanol	450	ml
Distilled water	450	ml

Destaining solution, 1 liter

Methanol	100	ml
Glacial acetic acid	100	ml
Distilled water	800	ml

5. Enzyme activity staining solution**1 M Tris-HCl, pH 8.5**

Tris (hydroxymethyl)-aminomethane 6.06 g

Adjusted to pH 8.5 with 1 N HCl and made up volume to 100 ml with distilled water

40 mM L-phenylalanine

L-phenylalanine 0.066 g

Dissolved with 10 ml distilled water

50 mM NAD⁺

NAD⁺ 0.359 g

Dissolved with 10 ml distilled water

0.25 mg/ml phenazine methosulfate

Phenazine methosulfate 0.0025 g

Dissolved with 10 ml distilled water

2.5 mg/ml nitroblue tetrazolium

Nitroblue tetrazolium 0.025 g

Dissolved with 10 ml distilled water

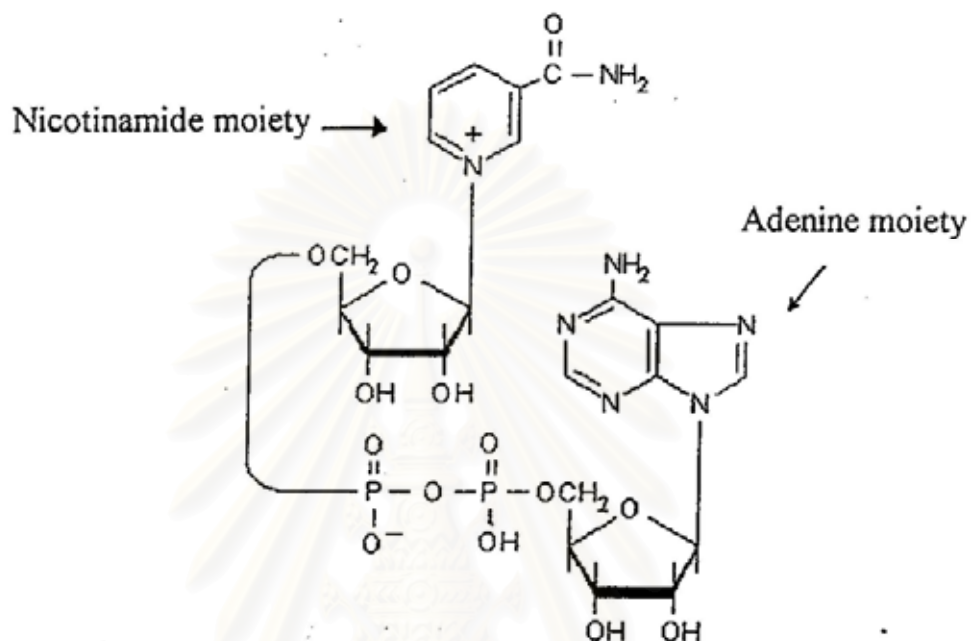
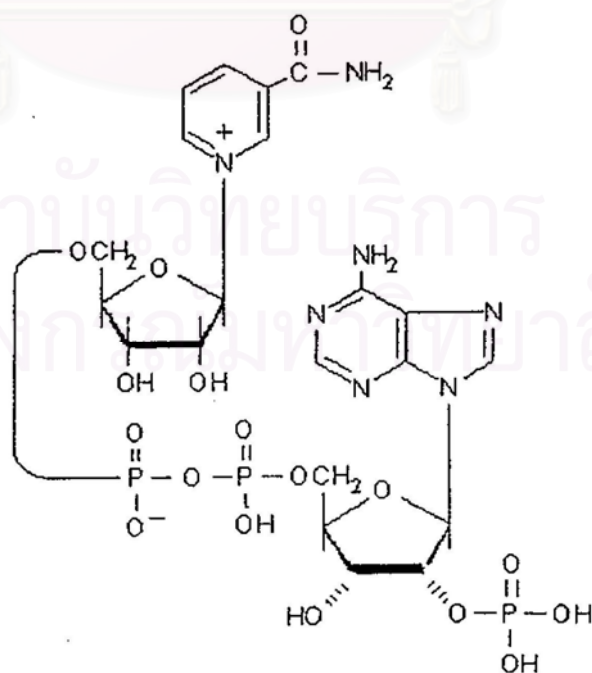
Activity staining solution (4.25 mM Tris-HCl, pH 8.5, 40 μ M L-phenylalanine 50 μ M NAD⁺, 250 μ g phenazine methosulfate and 2.5 mg nitroblue tetrazolium)

1 M Tris-HCl, pH 8.5	4.25	ml
40 mM L-phenylalanine	1.0	ml
50 mM NAD ⁺	1.0	ml
0.25 mg/ml phenazine methosulfate	1.0	ml
2.5 mg/ml nitroblue tetrazolium	1.0	ml
Distilled water	1.75	ml



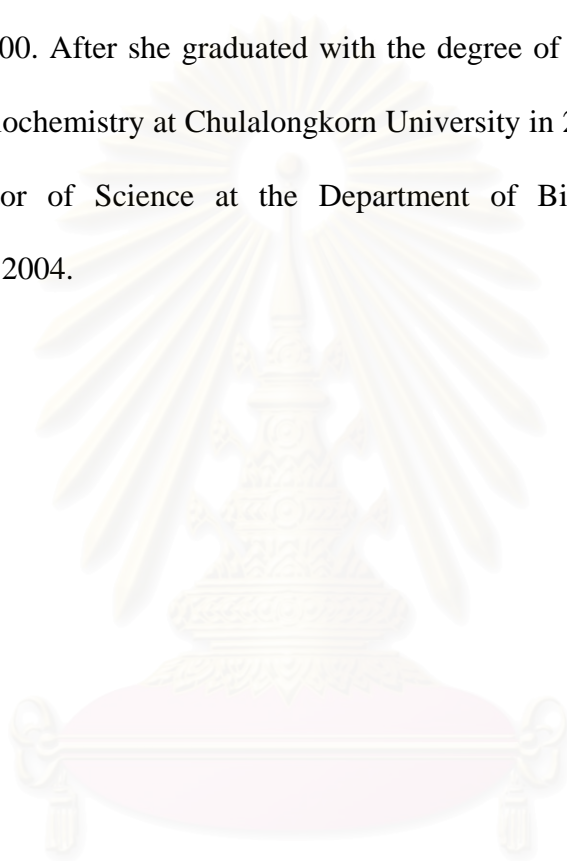
สถาบันวิทยบริการ
จุฬาลงกรณ์มหาวิทยาลัย

APPENDIX G

NAD⁺ and NADP⁺Nicotinamide adenine dinucleotide (NAD⁺)Nicotinamide adenine dinucleotide phosphate (NADP⁺)

BIOGRAPHY

Miss Rujirat Hatrongjit was born on July 25, 1979 in Udonthani. She graduated with the degree of Bachelor of Science from the department of Biochemistry at Kasetsart University in 2000. After she graduated with the degree of Master of Science from the department of Biochemistry at Chulalongkorn University in 2004, she has studied for the degree of Doctor of Science at the Department of Biochemistry, Chulalongkorn University since 2004.



สถาบันวิทยบริการ
จุฬาลงกรณ์มหาวิทยาลัย